The effect of inhibition of nucleotide synthesis on ribosome biogenesis and the induction of p53

Ferran Riaño Canalias

The effect of inhibition of nucleotide synthesis on ribosome biogenesis and the induction of p53

Doctoral thesis manuscript presented by

Ferran Riaño Canalias.

This work has been performed under the direction of

Drs. Antonio Gentilella and George Thomas at

Institut d'Investigació Biomèdica de Bellvitge (IDIBELL).

Programa de Doctorat en Biomedicina

Facultat de Farmàcia i Ciències de l'Alimentació

Universitat de Barcelona

L'Hospitalet de Llobregat 2017

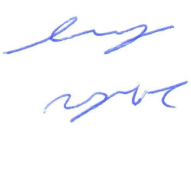

Albert Tauler Girona	**Antonio Gentilella**	**George Thomas**	**Ferran Riaño Canalias**
Tutor	Co-director	Co-director	PhD student

Als meus pares

A la Madrona

CONTENTS

ACKNOWLEDGEMENTS

First, I would like to thank my collaborators, Dr. Óscar Yanes and Dr. Sara Samino, who performed the LC-MS experiments in measuring nucleotide levels. I would also like to thank the laboratory of Dr. Neus Agell for their kind assistance and support in carrying out DNA fiber assay experiments. Finally, I would like to express my gratitude to Dr. Alberto Villanueva for his assistance during *in vivo* experiments.

My sincere thanks go as well to all my fellow lab mates Eugènia Almacellas, Dr. Constanza Cortés, Dr. Giulio Donati, Ana Fernández, Pedro Fuentes, Marta García, Dr. Xuemei Ge, Dr. Caroline Mauvezin, Dr. Cristina Mayordomo, Dr. Nathalie Meo Evoli, Carmen Morcelle, Francisco Morón, Dr. Mariona Pujol, Dr. Sónia Veiga, Dr. Guilherme Zweig and my PhD tutor, Dr. Albert Tauler. Thank you all for the wonderful work environment.

I would like to thank also Dr. Sara Kozma for reviewing this thesis.

Thanks to Dr. Mercè Juliachs for helping me with the figures.

I wish to express my gratitude to Marta Ruiz for her patience and technical support in conducting *in vivo* experiments.

I would like to thank Dr. Sandra Menoyo, who together with Dr. Antonio Gentilella developed the RPL11-Venus HCT116 cell line and kindly performed some of the immunoprecipitations included in this work.

My sincere gratitude also goes to Dr. Joffrey Pelletier, who performed some of the experiments presented in this thesis and with whom I have worked with in this project. Thank you for the challenge, it has allowed me to develop professionally as a scientist.

I would like to sincerely thank Dr. Antonio Gentilella for designing the RPL11-Venus HCT116, and for answering every question and in training me in molecular biology techniques. Thank you for the constructive discussions and the excitement after every

new result.

And last, but not least, I would like to thank Dr. George Thomas for giving me the opportunity to learn about science in such a remarkable laboratory. Thanks for the guidance and the adventure.

He d'agrair a la meva germana i als meus nebots el meravellós disseny de la portada d'aquesta tesi.

No voldria acabar sense recordar afectuosament i agrair profundament als meus avis i pares l'haver fet de mi el que sóc.

Per últim, he d'agrair a la Mercè la sensació que això no ha fet res més que començar.

ABBREVIATIONS

4E-BP1	Eukaryotic translation initiation factor 4E-binding protein 1
5'TOP	5'-Track of polypyrimidine
5-FU	5-fluorouracil
ACC	Acetyl-CoA carboxylase
ActD	Actinomycin D
AMP	Adenosine monophosphate
AMPK	5' AMP-activated protein kinase
ARF	Alternate reading frame
ARF-BP1/Mule	ARF-binding protein1/Mcl1-ubiquitin ligase E3
ATG7	Autophagy-related protein 7
ATM	Ataxia telangiectasia mutated
ATR	Ataxia telangiectasia and Rad-3 related
BAX	Bcl-2-associated X protein
BTG2	BTG anti-proliferation 2
BXDC1	Brix domain-containing protein
CBP	CREB-binding protein
CDK	Cyclin dependent kinase
Chk1	Checkpoint kinase 1
Chk2	Checkpoint kinase 2
COPI	Coat complex protein I
CRC	Colorectal Cancer
DBA	Diamond-Blackfan Anemia
DDR	DNA damage response
DNA	Deoxyribonucleic Acid
DNAPK	DNA-dependent protein kinase
DUB	Deubiquitinating enzyme
E2F	E2 Factor
ERK	Extracellular signal-regulated kinase
ETS	External transcribed spacer
FDA	Food and Drug Administration
GMP	Guanosine monophosphate
GMPS	Guanosine monophosphate synthase
HDM2	Human double minute 2
hRRS1	Human ribosome biogenesis regulator homolog
IMP	Inosine monophosphate
IMPDH	Inosine-5'-Monophosphate Dehydrogenase
INK4	Inhibitors of CDK4

ITS	Internal transcribed spacer
MCL1	Induced myeloid leukemia cell differentiation protein
MDM2	Murine double minute 2
MPA	Mycophenolic Acid
mRNA	Messenger RNA
mTOR	Mammalian target of Rapamycin
p300	E1A binding protein p300
PAI-1	Plasminogen activator inhibitor-1
PIRH2	p53-induced protein with RING-H2 domain
pRB	Retinoblastoma protein
PUMA	p53-upregulated modulator of apoptosis
RING	Really interesting new gene
RNA	Ribonucleic Acid
RNA Pol I/II/III	RNA Polymerase I/II/III
ROS	Reactive oxygen species
RP	Ribosomal protein
RPLx	Ribosomal protein Large
RPSx	Ribosomal protein Small
rRNA	Ribosomal RNA
SL1	Selectivity factor complex
snoRNP	Small nucleolar Ribonucleoprotein
TFIA	Transcription factor IA
TFIIIA/B/C	Transcription factor IIIA/B/C
TMP	Thymidine monophosphate
TP53I3	Tumour protein p53 inducible protein 3
tRNA	Transfer RNA
UBF	Upstream binding factor
ULK1	Unc-51 like autophagy activating kinase 1
USP10	Ubiquitin specific peptidase 10
USP7	Ubiquitin-specific-processing protease 7
WT	Wild-type
XMP	Xanthosine monophosphate

INTRODUCTION

1. The tumour suppressor p53

The studies described in this thesis center around the role of tumour suppressor p53, in sensing impaired ribosome biogenesis induced by inhibition of nucleotide synthesis. The discovery of p53 was made in 1979 by four different groups (Lane & Crawford, 1979; Linzer & Levine, 1979; DeLeo et al., 1979; Kress et al., 1979). It was first described as a potential oncogene and a positive effector of cell proliferation due to the high p53 levels in transformed cells (Lane & Crawford 1979; Sarnow et al. 1982; Reich & Levine 1984; Mercer et al. 1984). Furthermore, the transfection of p53 cDNA clones, combined with *RAS,* cooperate to transform primary cells in culture (Jenkins et al. 1984; Eliyahu et al. 1984; Parada et al. 1984). However, later studies revealed that the p53 clones used in previous studies were actually mutated (Eliyahu et al. 1988). In addition, co-transfection of wild-type (WT) p53 clones blocked transformation of rat fibroblasts (Finlay et al. 1989). These findings together with the fact that a high proportion of neoplasias have mutations in p53 (Takahashi et al. 1989; Gresch 1989), suggested that p53 was instead a negative regulator of cell proliferation.

Presently, it is widely accepted that p53, also known as “the guardian of the genome” or “the cellular gatekeeper”, is a tumour suppressor which plays a pivotal role in the regulation of cell cycle progression and apoptosis, acting to prevent genome instability and DNA damage (Levine 1997; Vogelstein et al. 2000; Ananiev et al. 2011). In fact, p53 functions as a cellular node where distinct pathways, elicited by several cellular insults, converge. Once activated, p53 mediates an intrinsic cellular response whose ultimate role is to preserve genome integrity (Vousden & Lu 2002). Although discovered over 35 years ago, p53 is still under intense study because of its central role in regulating cell cycle progression and apoptosis. Moreover, it has become evident that p53 is involved in the regulation of other important cellular processes such as DNA repair, senescence, metabolism, hypoxia and autophagy (Reinhardt & Schumacher 2012; Kruiswijk et al. 2015).

1.1. Structure and general function of p53

Human p53 is a 393 amino acid protein encoded by the *TP53* gene, composed of 11 exons. Five distinct domains have been identified in the p53 human protein: the N-terminal transactivation domain (TAD), the proline-rich domain (PRD), the central DNA binding domain (DBD), the tetramerization domain (TD) and the C-terminal basic domain (BD) (Joerger & Fersht 2008) (**Figure I-1**). The TAD plays a key role in controlling p53 transcriptional activity, stability and interaction with specific protein partners including the E_3-ubiquitin ligase human double minute 2 (HDM2) (Kussie et al. 1996; Schon et al. 2002), specific transcription factors (Lu & Levine 1995; Thut et al. 1995; Di Lello et al. 2006) as well as the acetyltransferase CREB binding protein/E1A binding protein p300 (CBP/p300) (Gu et al. 1997; Teufel et al. 2007). Moreover, it is subjected to a number of post-translational modifications that alter the affinity for protein binding partners that compete for binding to the TAD (Toledo & Wahl 2006; Bode & Dong 2004).

The PRD contains five repeats of the PXXP motif (where P represents proline and X represents any amino acid) and it has been shown necessary for p53 pro-apoptotic activity, but is dispensable for other functions such as cell cycle arrest (Walker & Levine 1996; Sakamuro et al. 1997; Venot et al. 1998; Baptiste et al. 2002). The TD mediates the formation of p53 homo-tetramers, an essential process for p53's

Figure I-1. Scheme of human protein p53 domains. Five different domains are described among the 393-aminoacid human p53 protein sequence. TAD: transactivation domain; PRD: proline-rich domain; DBD: DNA-binding domain; TD: tetramerization domain and BD (or CRD): C-terminal basic domain. Modified from Kamada et al. 2015.

transcription factor activity (Kamada et al. 2015; Kitayner et al. 2006; Balagurumoorthy et al. 1995). The DBD allows p53 protein tetramers to bind to the DNA p53 response element (RE) of its target genes and promote mRNA transcription (el-Deiry et al. 1992). In many organisms, the p53 RE is composed of two half sites with the sequence 5'-RRRCWWGYYY-3' (R corresponds to a purine, Y to a pyrimidine, W can be either adenine or thymine, C corresponds to cytosine and G to guanine) followed by 0 to 21 bases of spacer (el-Deiry et al. 1992; Riley et al. 2008). However, some of p53 REs present more than two half-sites. It has been shown that the affinity of p53 for its REs increases proportionally to the number of adjacent half-sites, as does the transcription level of a given target gene after p53 activation (Kern et al. 1992; Bourdon et al. 1997). *In vitro* studies showed that p53 binds with higher affinity to genes regulating cell cycle and growth arrest than to those involved in apoptosis (Weinberg et al. 2005).

Apart from genes related to cell cycle arrest (e.g. p21) and apoptosis (e.g. PUMA, NOXA, BAX), other p53 targets are genes coding for proteins related to senescence (e.g. PAI-1), p53 stabilization (e.g. HDM2), autophagy (e.g. ATG7, ULK1) (Kenzelmann Broz et al. 2013; Beckerman & Prives 2010) and DNA repair (Morris et al. 1996; Tanaka et al. 2000). The role in regulating DNA damage repair underscores the importance of p53 in acting as a guardian for genome integrity. In adverse conditions, p53 is able to elicit cell cycle arrest in order to allow repair of potential damage. If unrepaired, then other p53 target genes will lead the cell either to apoptosis or senescence. Despite the fact that other regulatory mechanisms, such as co-transcriptional factors and post-translational modifications of p53, are known to affect p53 transcriptional response, the mechanisms by which p53 directs its activity towards a given set of genes is still not completely understood (Riley et al. 2008) (**Figure I-2**).

p53 regulates also numerous cellular processes independently of its transcription factor function. For example, c-Myc overexpression sensitized fibroblasts to apoptosis in a p53 dependent-manner without induction of p53 transcriptional

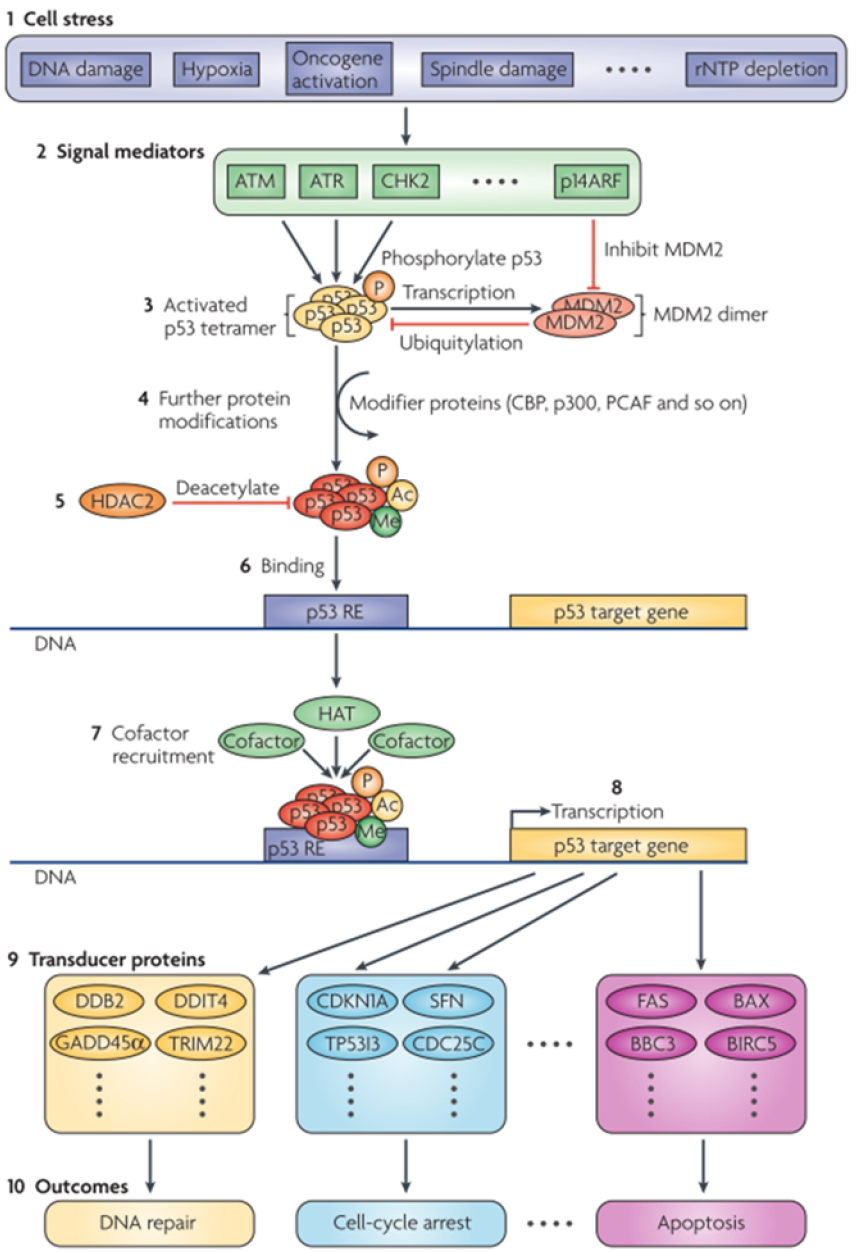

Figure I-2. p53 plays a key role in regulating cell response to many different stimuli. Harmful stimuli for the cell, including DNA damage or oncogene activation among others (1), can trigger the p53 response by activating signal mediators (2), which can induce p53 tetramerization, post-translational modifications like phosphorylation or they can alter p53 regulators such as HDM2 (3,4,5). p53 binds to the REs present in DNA sequence and together with other cofactors will stimulate the transcription of its targets genes (6, 7, 8). Those genes activated by p53 will lead to the translation of proteins that will execute the final output in terms of cell response (DNA repair, cell cycle arrest or apoptosis) (9, 10). From Riley et al. 2008.

targets, suggesting that p53-induced apoptosis was independent of its transcriptional activity (Wagner et al. 1994). Moreover, later studies showed that p53 mutants lacking the TAD and part of the DBD, which are unable bind to DNA, were able to trigger apoptosis without inducing expression of p53 target genes (Haupt 1995; Kakudo et al. 2005). Also, the translocation of p53 to the mitochondria and its role in mitochondrial membrane permeabilization and apoptosis was demonstrated both *in vitro* and *in vivo* independent of transcription (Mihara et al. 2003; Erster et al. 2004).

In addition to apoptosis and mitochondrial membrane permeability, which have been shown to be affected independently of p53 transcriptional activity, inhibition of p53 in enucleated cells leads to the activation of autophagy (Tasdemir et al. 2008). Consistent with this finding, expression of cytoplasmic p53 in p53-null cells was shown to decrease autophagy and was not recapitulated by expression of nuclear p53 (Tasdemir et al. 2008), suggesting an anti-autophagic role of cytoplasmic p53. These transcription-independent functions of p53 act together with its transcription-dependent activity in order to regulate the cell responses to specific stresses, especially those affecting genome stability.

1.2. p53 regulation

Cellular responses mediated by p53 can be triggered by many different stress stimuli including DNA damage (Lakin & Jackson 1999; Reinhardt & Schumacher 2012), oncogene activation, nutrient deprivation and metabolic stress (Kruiswijk et al. 2015) as well as impairment of ribosome biogenesis (Horn & Vousden 2007), a critical response in the studies described here. Once p53 is activated, it stimulates the transcription of those genes implicated in specific cellular responses, including cell cycle arrest, apoptosis and senescence. Therefore, this classical model of p53 activation consists in three basic steps: (I) p53 activation by transactivation domain phosphorylation, which disrupts HDM2-p53 interaction; (II) p53 binding on specific sequences of DNA and (III) recruiting the transcriptional machinery followed by the

transcription of target genes (Kruse et al. 2009).

The process of p53 activation is highly regulated by different mechanisms that will eventually affect the output of p53 response. One of these mechanisms is the post-translational modification of p53 by several enzymes. Other mechanisms include regulator proteins that act on p53. Among these there is HDM2, which plays an essential role in promoting p53 degradation and is thought to act as the main negative effector of p53 stability (Honda et al. 1997; Haupt et al. 1997; Kubbutat et al. 1997).

1.2.1. Post-translational modifications of p53

p53 protein can be post-translationally modified by different covalent regulators that bind to many conserved sites. These modifications include: phosphorylation, acetylation, methylation, sumoylation, neddylation and ubiquitination (**Figure I-3**) (Watson & Irwin 2006; Kruse & Gu 2008; Meek & Anderson 2009). In this thesis I will focus on phosphorylation and ubiquitination due to their importance to my studies.

1.2.1.1. Phosphorylation

p53 protein contains several serine and threonine residues, which can be phosphorylated depending on the cellular insult (Meek & Anderson 2009). The majority of these residues are located in the N-terminal TAD and in the regulatory CTD. Some of the N-terminal phosphorylation sites are utilized by different kinases, which can phosphorylate p53 at the same residue. For example, the ataxia telangiectasia mutated (ATM) and ataxia telangiectasia and Rad-3 related (ATR) protein kinases are known to phosphorylate p53 at residue serine 15 (numbering using human-sequence) following DNA damage (Banin et al. 1998; Canman et al. 1998; Lakin & Jackson 1999; Tibbetts et al. 1999). Serine 15 can also be phosphorylated by other protein kinases such as DNA-dependent protein kinase (DNAPK) or extracellular signal-regulated kinase (ERK) (Lees-Miller et al. 1992; She et al. 2000). p53 serine 20 is

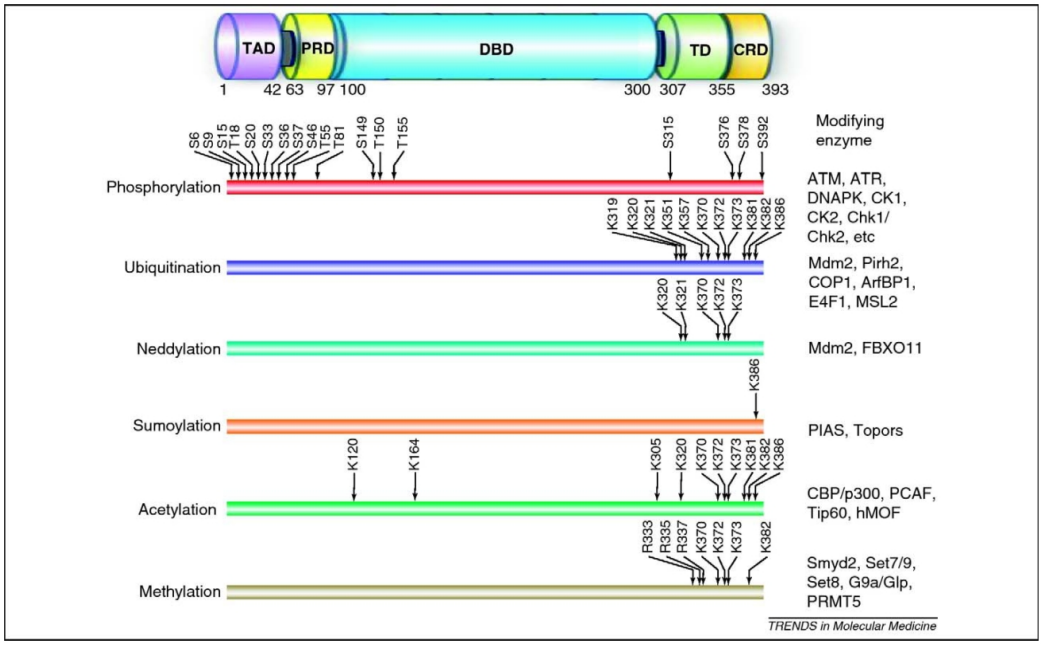

Figure I-3. Scheme showing post translational modifications of p53 and major sites of phosphorylation, ubiquitination, neddylation, sumoylation, acetylation and methylation. The enzymes responsible of each type of modification are listed on the right. From Dai & Gu 2010.

phosphorylated by protein kinases involved in the DNA Damage Response (DDR) such as checkpoint kinase 1 (Chk1) and checkpoint kinase 2 (Chk2) (Shieh et al. 2000). On the other hand, AMP kinase (AMPK) is known to phosphorylate serine 15 under glucose deprivation conditions (Jones et al. 2005). Phosphorylation at both serine residues 15 and 20 are known to interfere with p53-HDM2 interaction, leading to p53 stabilization (Shieh et al. 1997). However, other studies have revealed that mice bearing a mutation in serine 18 (homologous to human serine 15), although displaying a defective induction of apoptosis, exhibit the same stabilization of p53 protein and no difference in terms of spontaneous tumorigenesis when compared to p53 WT animals (Chao et al. 2003; Sluss et al. 2004), suggesting a more complex regulation of p53 activation. In addition, when mutations in serine 18 are combined with mutations in serine 23 (homologous to human serine 20) the animals develop spontaneous tumours like p53 knock-out animals, but in a tissue dependent manner (Chao et al. 2006). Taken together, these studies underscore the complexity of p53 regulation,

with many players and mechanisms acting at the same time, sometimes redundantly, depending on the cell and tissue context.

1.2.1.2. Ubiquitination

Ubiquitin is a small protein (76 amino acids), which can be covalently attached to lysine residues of a large number of proteins by a three-enzyme signalling cascade: the E_1, E_2 and E_3 enzymes. Ubiquitin can be attached as a single protein or to a previously attached ubiquitin, thus forming polyubiquitin chains bound to a specific lysine residue of the target protein (Berndsen & Wolberger 2014). Ubiquitination plays many regulatory roles in eukaryotic cells, the most important being protein degradation. Ubiquitin selectively "tags" specific proteins for degradation, mainly through the 26S proteasome, the cellular machinery with proteolytic activity and in charge of protein clearance and housekeeping (Ravid & Hochstrasser 2008).

With a half-life of approximately 30 minutes in non-transformed cells (Oren et al. 1981), p53 protein levels are under intense monitoring, with its levels relatively low in normal conditions, whereas they can be rapidly stabilized in stress conditions by inhibiting its degradation. This makes ubiquitination and degradation primary p53 regulatory mechanisms. Apart from targeting p53 for degradation, ubiquitination plays additional roles in p53 regulation. It has been reported that p53 can be either monoubiquitinated or polyubiquitinated. Monoubiquitination of p53 leads to nuclear export of the protein, whereas polyubiquinitation triggers p53 degradation (Li et al. 2003).

A large number of E_3-ubiquitin ligases have been described to ubiquitinate p53 including HDM2, p53-induced protein with RING-H2 domain (PIRH2) and Coat complex protein I (COP1). Most of them promote p53 degradation, but other functions such as mediating p53 nuclear export or transcriptional inactivation have been described for the E_3-ubiquitin ligases (Jain & Barton 2010). As mentioned above, among the E_3-ubiquitin ligases, HDM2 stands out as the main p53 regulator, negatively acting on p53

by promoting its degradation (Honda et al. 1997; Haupt et al. 1997; Kubbutat et al. 1997).

1.2.2. HDM2 – p53 regulation

HDM2 is a RING finger domain protein that was first described as a p53-interacting protein and a negative effector of p53 stability (Momand et al. 1992). HDM2 binds to the TAD of p53 and prevents its transcriptional activation (Kussie et al. 1996). It has been shown that the p53 and HDM2 interaction is impaired when the TAD of p53 is phosphorylated in response to DNA damage (Shieh et al. 1997). HDM2 negatively regulates p53 stability by ubiquitinating several lysine residues in the BD, leading to its proteasomal degradation (Rodriguez et al. 2000).

The importance of HDM2 in regulating p53 activity was underscored by studies carried out in mice, in which *Mdm2* (mouse orthologous gene of HDM2) knock-out was shown to be lethal due to exacerbated p53 activity (de Rozieres et al. 2000). The lethal phenotype observed in *Mdm2*-null animals was rescued by co-deletion of p53 (Jones et al. 1995; Montes de Oca Luna et al. 1995). HDM2 expression has been found to be altered in human cancer. For example, HDM2 gene was shown to be amplified in several sarcoma types (Oliner et al. 1992) and malignant gliomas (Liu et al. 1993). Heterozygous deletion of *Mdm2* in mice inhibits lymphomagenesis in *Eμ-myc* mice (Alt et al. 2003), an animal model of high c-Myc expression which is characterized by a high incidence of lymphomas (Harris et al. 1988). It also reduces colon cancer incidence in Apc^{min} mice, a model of increased intestinal adenoma formation (Moser et al. 1995), without affecting aging or lifespan (Mendrysa et al. 2006). Together these studies highlight the role of HDM2 in inhibiting p53 activity, thus acting as a negative regulator of p53, and the implications that this interaction has in cell proliferation and cancer.

HDM2 and p53 constitute an auto-regulated negative feedback loop. HDM2 is a transcriptional target of p53 (Barak et al. 1993; Perry et al. 1993) that at the same

time negatively regulates p53 (Momand et al. 1992), keeping its levels low in non-stressed cells. HDM2 regulates p53 at the level of stability, function and subcellular localization. Transgenic mice bearing a mutation of *Mdm2* (C462A), which abolishes its ubiquitin ligase activity while it has no effect on MDM2-p53 interaction, show a phenotype similar to the *Mdm2*-null animals (Itahana et al. 2007), suggesting that MDM2 regulates p53 activity through promoting its degradation. However, p53 is still subject to degradation in *Mdm2*-null mice (Ringshausen et al. 2006), consistent with the existence of additional E_3-ubiquitin ligases implicated in modulating p53 stability, and therefore its activity (**Figure I-4**). Regarding subcellular localization of p53, low levels of HDM2 inducing monoubiquitination of p53 promote its nuclear export (Li et al. 2003).

Other players have been described to modulate the HDM2-p53 regulatory feedback loop. For instance, HDMX (MDMX in the case of the mouse ortholog) is a protein highly homologous to HDM2 (Shvarts et al. 1996) that has been described to

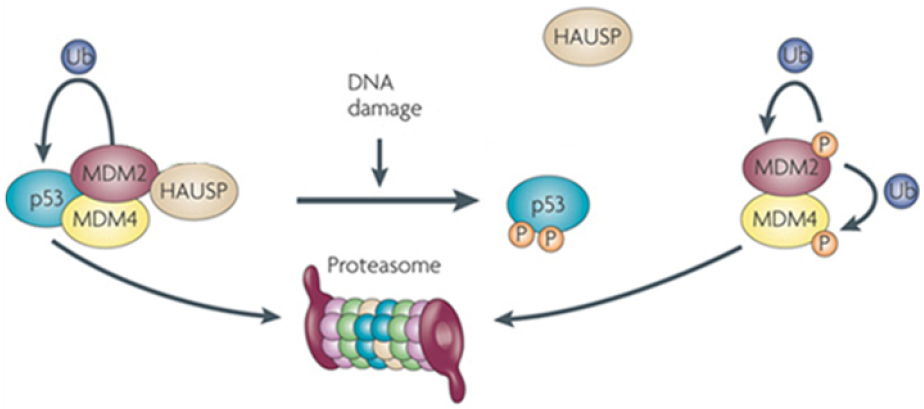

Figure I-4. **Regulation of p53 by ubiquitination**. Under physiological conditions the hetero-dimer of HDM2 (MDM2 in the figure) and HDMX (MDM4 in the figure) ubiquitinates p53, thus promoting its proteasomal degradation. After a cell stress or insult like DNA damage, p53 gets phosphorylated so HDM2 and HDMX are not able to perform their ubiquitination functions on p53, which is then stabilized. HDM2 and HDMX are then degraded because of ubiquitination activity of HDM2 on HDMX and itself. DUBs like USP7 (HAUSP in the figure) participate as well in the regulation of p53 through its deubiquinitation activity. Under physiological conditions USP7 can deubiquitinate HDM2 in order to keep its ubiquitine-ligase activity towards p53. Modified from Meek 2009.

form hetero-dimers with HDM2. The HDMX/HDM2 hetero-dimerization may act as a more effective driver of p53 ubiquitination (Wade et al. 2013). On the other hand, the alternate reading frame tumour suppressor protein, also known as $p14^{ARF}$ in human and $p19^{ARF}$ in mouse, acts as a positive effector of p53 induction after oncogenic stress (Lowe & Sherr 2003). $p14^{ARF}$ antagonizes the inhibitory effect of HDM2 on p53 by binding to the C-terminus end of HDM2 and disrupting the physical interaction between HDM2 and p53 (Pomerantz et al. 1998; Sherr 2006).

1.3. Role of p53 in cell cycle progression

The term "cell cycle" refers to the set of events that brings a cell to become two daughter cells. It basically consists in cell growth, genome duplication and mitosis. Classically, the cell cycle is divided in two main phases or stages: (I) mitosis or M phase, in which cells divide and generate two daughter cells; and (II) interphase, in which cells grow and replicate their genome. Interphase can be further divided into three different phases: G_1 phase, S phase, and G_2 phase. The S phase or synthesis phase is when DNA replication takes place. The two different phases before and after S phase are termed Gap_1 (G_1) and G_2. During these two phases, cells increase their biomass, but they also ensure that internal and external conditions are suitable for cell division and that the DNA is properly replicated and potentially repaired (**Figure I-5**). G_1 occurs before S-phase, that is, before DNA replication, and enables cells to ascertain whether it is feasible to replicate their DNA. This is

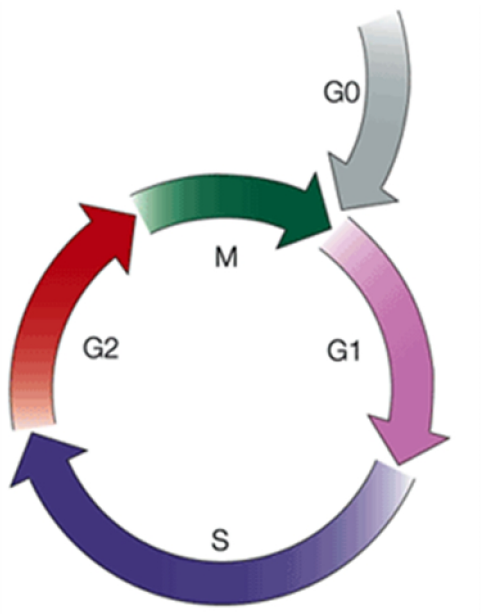

Figure I-5. Schematic representation of cell cycle. Modified from Coleman et al. 2004.

particularly important since any impediment during DNA replication could lead to genomic instability. Several pathways and cellular checkpoints converge during G_1 in order to prevent DNA instability and the final outcome will dictate cellular fate: to continue cycling, stop or die (Massagué 2004; Alberts et al 2007). Cells in G_1 phase can exit the cell cycle and stop dividing by entering into quiescent state, also termed G_0 phase, where they stop proliferating (Cheung & Rando 2013) (**Figure I-5**). Once committed to cell division, cells enter S phase and start DNA replication. G_2 takes places after S phase, when DNA has been completely replicated and before mitosis or cell division. G_2 permits cells to repair potential DNA damage or replication errors, apart from assuring that cell division can be executed correctly. Finally, cell division occurs in M phase or mitosis.

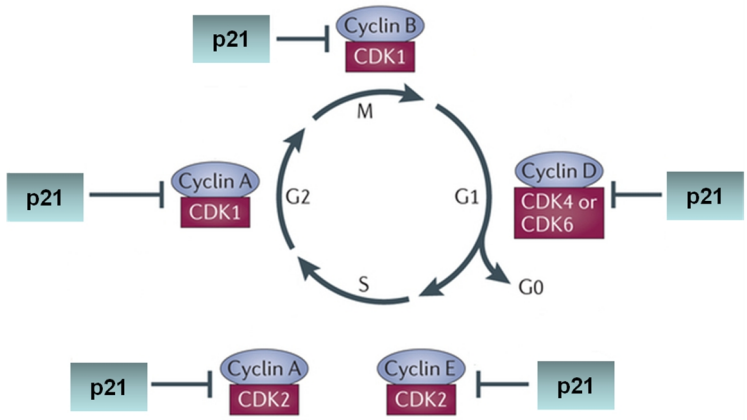

Figure I-6. Schematic representation of cell cycle regulation by cyclins and CDKs. Each cyclin-CDK complex is represented in the phase of the cell cycle where it is expressed and it regulates and facilitates progression through the cell cycle. The p53 transctiptional target p21 acts as one of the main negative regulators of cyclin-CDK complexes thus negatively regulating cell cycle progression. Modified from Yang 2009.

The cell cycle is mainly regulated by different holoenzymes formed by regulatory subunits called cyclins and a catalytic subunits called cyclin-dependent kinases (CDKs). Exogenous mitogenic signals, such as nutrient availability or growth factor stimulation

initiate a signalling cascade that ends with the expression and assembly of the cyclins and CDKs. These different complexes are sequentially activated at different stages of-, and required for progression through- the cell cycle (Graña & Reddy 1995) (**Figure I-6**). For example, one of the main substrates of the CDKs is the RB protein, which is sequentially phosphorylated by cyclin D/CDK4, cyclin E/CDK2 and cyclin A/CDK2 complexes. This leads to the activation of E2F transcription factors family members, which promote the expression of genes required for DNA replication (Sherr 1994; Graña & Reddy 1995; Dyson 1998) (**Figure I-7**). p53 plays a central role in regulating cell cycle progression. Mainly through its transcriptional activity, p53 is able to stop cell cycle and arrest cell growth during G_1 and G_2 cellular checkpoints (Giono & Manfredi 2006). For example, conditional expression of WT p53 in glioblastoma cells is sufficient to cause cellular arrest in G_1 (Lin et al. 1992). On the other hand, p53 knock-out progenitor hematopoietic-cells fail to arrest cell cycle in G_1 following DNA damage (Kastan et al. 1991).

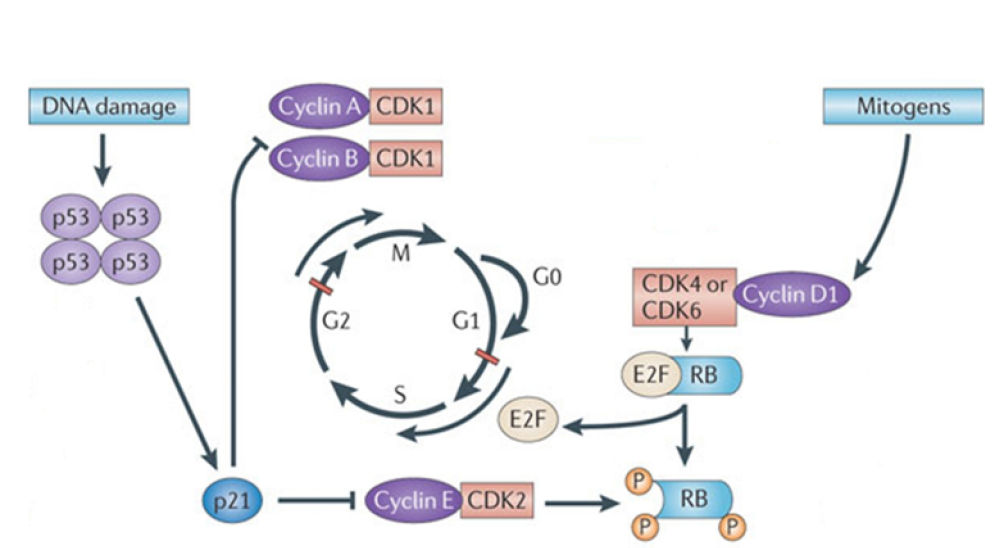

Figure I-7. p21 plays a key role in G_1 arrest regulation. During normal cell cycle the mitogenic signalling promotes cyclin D1 binding to CDK4 or CDK6. This leads to the phosphorylation of RB protein and the release of E2F transcription factor family, which induces DNA replication. In an stress situation like DNA damage, p53 activates p21, which inhibits kinase activity of CDK2 thus inducing cell cycle arrest. Modified from René Leemans et al. 2011.

1.3.1. The CDK inhibitor p21

Among p53 transcriptional targets, the 165-aminoacid CDK inhibitor p21 is one of the main negative-regulators of cell cycle progression and it exerts its activity by binding to-, and inhibiting the kinase activity of-, CDK1 and CDK2 (Abbas & Dutta 2009) (**Figure I-6**). p21 knock-out mice have been reported to show defective G_1 checkpoint-execution after DNA damage or nucleotide pool perturbation (Deng et al. 1995; Brugarolas et al. 1995). In addition, expression of different mutants of p21 reduces the ability of the cells to halt cell cycle progression and inhibit DNA synthesis (Rousseau et al. 1999). Together, these studies demonstrate the central role of the p53-p21 axis in arresting cell cycle during G_1 and G_2 phases. Moreover, it underlines the importance of p53 in preventing genomic instability by halting cell cycle progression before the DNA replication is initiated in S phase. In this sense, G_1 phase plays a key role in preventing potential DNA damage since it is during G_1 that cells become committed to DNA replication or cell cycle arrest (Massagué 2004). Several signaling pathways converge during G_1 phase in order to transduce both intracellular and extracellular inputs, such as oncogenic activation or nutrient availability, in order to influence G_1 progression through the activation of different cellular checkpoints (Massagué 2004). Among them, as previously mentioned, the CDK inhibitor p21 is one of the main regulators of G_1 cell cycle arrest (**Figure I-8**). Ribosome biogenesis impairment has been shown to stabilize p53 and induce cell cycle arrest (Teng et al. 2013). Our studies are focused on characterizing the effects of ribosome biogenesis impairment and nucleotide synthesis inhibition in the stabilization of p53, as well as the impact on cell cycle.

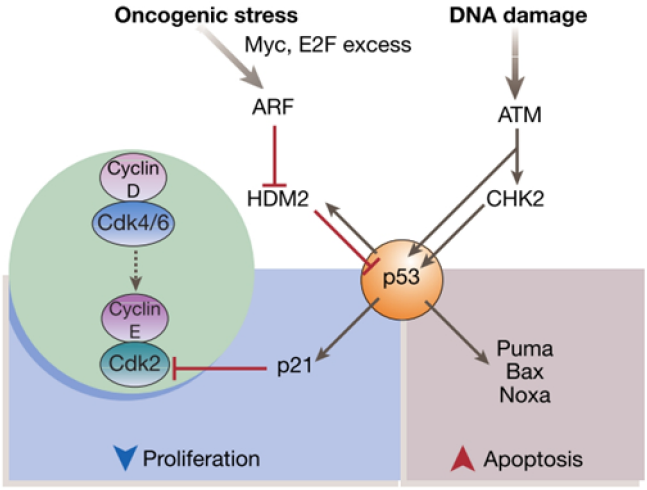

Figure I-8. The p53 node as genomic instability preventor and its role in cell cycle regulation. Modified from Massagué 2004

2. Ribosome Biogenesis

The eukaryotic ribosome is the main component of translational machinery of the cell and it is formed by two different subunits: (I) the 40S or small subunit, which comprises the 18S ribosomal RNA (rRNA) and 33 distinct ribosomal proteins (RPs); and (II) the 60S or large subunit, formed by 28S, 5.8S and 5S rRNA species together with 47 RPs (Henras et al. 2015). In eukaryotes, ribosome biogenesis is one of the most energy consuming biological processes that cells must fulfill in order to achieve the levels of protein synthesis required for growth and proliferation. As an example, yeast cells generate 2,000 new ribosomes per minute. Regarding rRNA, in yeast it represents 80% of the total cellular RNA and its transcription by RNA Pol I stands for 60% of total cellular transcription. On the other hand, it is estimated that 50% of RNA Pol II transcription activity is confined to RP mRNAs (Warner 1999). In addition, apart from rRNA and RPs, more than 200 proteins and non-coding RNAs participate in the processing, assembling and transport of pre-ribosomal components from the nucleus to the cytoplasm and *vice versa* (Henras et al. 2008; Lempiäinen & Shore 2009). In total, 80% of the total energy consumed by the yeast cell is invested in ribosome biogenesis (Schmidt 1999). Taking into account the large amount of molecules involved, the energetic cost of the biological process and the crucial role of ribosomes in driving protein synthesis, it is not unexpected that ribosome biogenesis is a highly regulated cellular event.

2.1. rRNA processing and ribosome assembly

Ribosome biogenesis takes place mainly in the nucleolus, a nucleoplasmic structure, whose function has been attributed for “the act of building ribosomes” (Mélèse & Xue 1995). The size of nucleolus varies in accordance to levels of ribosome synthesis. The observation that cancer cells present larger nucleoli was made in 1896 by Pianese et al. In fact, the size of the nucleolus has been used as a marker of high-proliferation in cancer cells (Montanaro et al. 2008; Hernandez-Verdun et al. 2010).

Importantly, nucleolar function has been related to several cellular responses apart from ribosome biogenesis, such as cell cycle progression or DDR. Therefore, the nucleolus integrity and proper functioning has been postulated to be a barrier against cancer development (Orsolic et al. 2016). On the other hand, several human genetic disorders have been linked to mutations in genes encoding for proteins interacting with nucleoli, such as Werner syndrome (Brosh et al. 2001) . Moreover, some of these diseases have been reported to involve an increased susceptibility to cancer development, suggesting a role of the nucleolus in protecting DNA integrity (Boisvert et al. 2007).

Three essential steps of ribosome biogenesis are executed in the nucleolus: (I) rRNA gene transcription, (II) rRNA processing and (III) rRNA assembling with RPs (Boisvert et al. 2007). Transcription of rRNA is performed by two different RNA polymerases: RNA Pol I and RNA Pol III. RNA Pol I transcribes the rRNA precursor or pre-RNA 47S, which after several modifications and cleavages will be processed into the mature forms 28S, 18S and 5.8S rRNAs (**Figure I-9**). To do so, RNA Pol I associates with three other transcriptional factors: transcription factor 1A (TFIA), selectivity factor complex (SL1) and upstream binding factor (UBF). On the other hand, 5S rRNA is transcribed by RNA Pol III in the nucleus, and is the only rRNA molecule whose transcription occurs out of the nucleolus (Fedoriw et al. 2012). Finally, RNA Pol II does

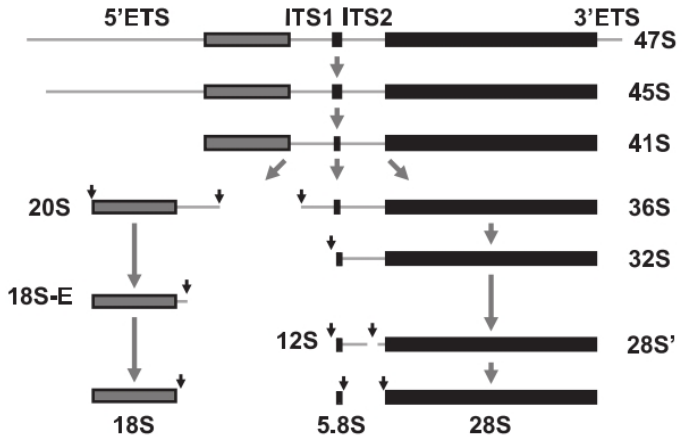

Figure I-9. Schematic view of rRNA processing. Precursor 47S rRNA is flanked by 5'ETS and 3'ETS. The sequences of mature rRNA 28S, 18S and 5.8S are separated by ITS1 and ITS2. After several cleavages, folding and modifications, it gives raise to the mature forms of rRNA, which are assemblend into the mature ribosome. From Donati et al. 2013.

not participate in rRNA transcription. However, its role is essential for ribosome biogenesis since it is the enzyme required for RP mRNA transcription, as well as proteins involved in rRNA processing (Sainsbury et al. 2015).

Nucleoli are situated around nucleolar organizer regions (NORs), clusters of tandem repeats of 47S rRNA gene that are located in all acrocentric chromosomes. Pre-rRNA 47S gene contains external transcribed spacers (5' ETS and 3' ETS) at both ends. The 28S, 18S and 5.8S rRNA sequences located within the sequence of the precursor 47S rRNA are separated by the internal transcribed spacers, ITS1 and ITS2, sequences (**Figure I-9**). For pre-rRNA processing into mature rRNA, the nascent transcripts associate co-transcriptionally with non-ribosomal factors and small nucleolar RNAs (snoRNAs) to form large ribonucleoproteins (RNPs) complexes in which pre-RNA is modified and folded (Hernandez-Verdun et al. 2010). For instance, in yeast cells the association of U3 snoRNP to the nascent pre-rRNA is essential for later pre-rRNA cleavages and 40S subunit maturation (Venema & Tollervey 1999). The main function of the snoRNPs is to modify pre-RNA nucleotides through methylation and pseudouridylation (Kressler et al. 2010). In addition, the rRNA precursors are also

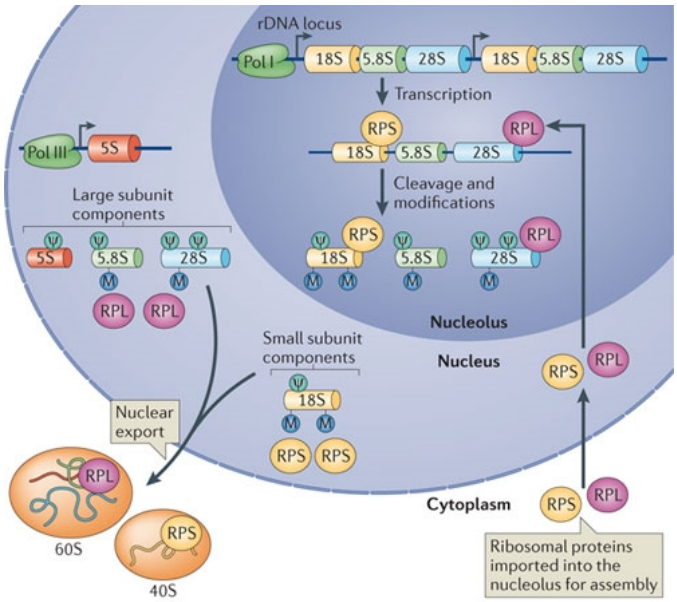

Figure I-10. Schematic view of ribosome biogenesis. RNA Pol I transcribes the rDNA to generate the precursor 47S rRNA, which is modified and cleaved in order to generate the mature forms 28S, 18S and 5.8S rRNA. During this process they are assembled with ribosomal proteins. On the other hand, RNA Pol III synthesizes 5S rRNA in the nucleoplasm. Finally, the 40S and 60S subunits formed by RPs and the 4 rRNA species are exported to the cytoplasm. Modified from Xue & Barna 2012.

assembled with RPs, which have been previously translated in the cytoplasm by mature ribosomes and imported into the nucleus. Distinct RPs are necessary for the last steps of pre-rRNA maturation in the cytoplasm. During this process of maturation and assembly, different endo- and exoribonucleases cleave the pre-rRNA at ETS and ITS sequences (Henras et al. 2015). After rRNA processing and maturation, pre-ribosomal subunits 40S and 60S are independently exported to the cytoplasm where they undergo the last steps of maturation before they become translationally competent (Tschochner & Hurt 2003) (**Figure I-10**).

2.1.1. The 5S rRNA

5S rRNA is a small RNA with a molecular mass of 40 kDa and 120 nucleotides in length. In mammals, there are a variable number of genes encoding for 5S rRNA in clusters of tandem repeats usually located on chromosome 1 in humans. In the case of yeast, 5S rDNA is located between other rRNA genes (Ciganda & Williams 2011). The secondary structure of 5S rRNA comprises five helices or stems (designed by Roman letters I-V) and five inner and external loops (designed by Latin letters A-E), which form the three different domains of the 5S rRNA (designated by Greek letters α, β and γ) (Smirnov et al. 2008) (**Figure I-11**). This three-domain structure gives the 5S rRNA molecule a tridimensional "Y" shape, a conformation highly conserved along evolution

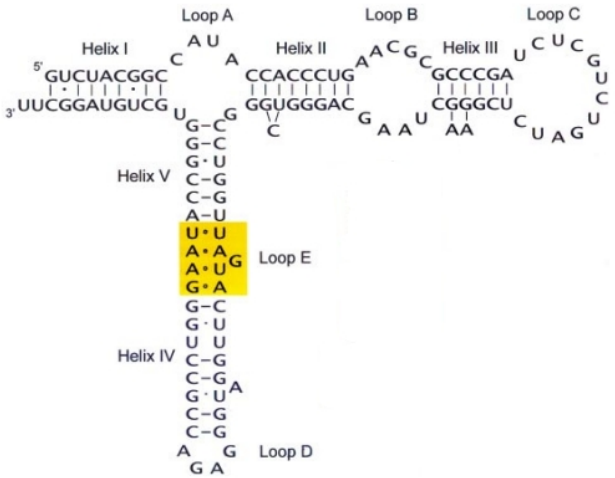

Figure I-11. Secondary structure of eukaryotic 5S rRNA. α-domain is formed by helix I; β-domain is formed by helix II and III and B and C loops; γ-domain includes helix IV and V and loops E and D. Figure taken from Szymański et al. 2003.

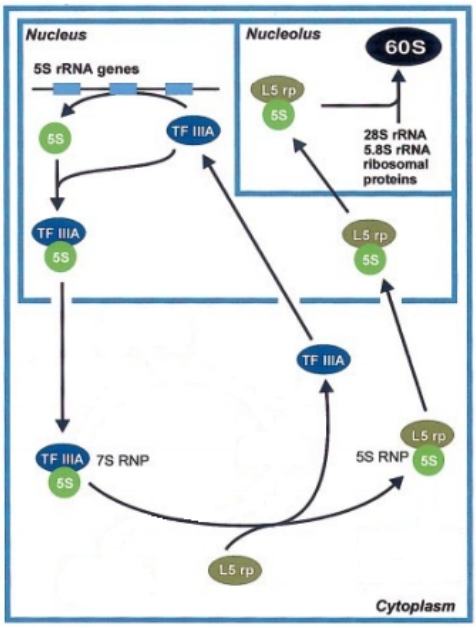

Figure I-12. 5S rRNA biosynthesis and interactions. 5S rRNA is exported from the nucleus bound to TFIIIA and it is imported back together with RPL5. Modified from Szymański et al. 2003.

that is common in *Archaeabacteria* and *Eubacteria* (Sun & Caetano-Anollés 2009). In fact, 5S rRNA sequence has initially used as a phylogenetic marker (Hunt et al. 1984).

As stated above, unlike the other rRNA molecules which are synthesized by RNA Pol I in the nucleolus, 5S rRNA is synthesized by RNA Pol III in the nucleoplasm (Ciganda & Williams 2011). Transcriptional co-factors such as transcription factors IIIA, IIIB and IIIC (TFIIIA, TFIIIB and TFIIIC), are necessary together with RNA Pol III for 5S rDNA transcription (Kassavetis et al. 1990). Among them, TFIIIA plays two critical roles in 5S rRNA biogenesis: (I) it is necessary for 5S rDNA transcription initiation and (II) it binds to the product of transcription, the 5S rRNA molecule and stabilizes it, forming the 7S RNP particle (Szymański et al. 2003). It has been reported that before its binding to TFIIIA, a small proportion of free 5S rRNA molecules interact with La protein transiently and it acts as a chaperone, stabilizing its RNA partners by modification and folding events (Wolin & Cedervall 2002; Ciganda & Williams 2011). The maturation process of 5S rRNA also includes nucleotide excision by enzymes with exonuclease activity (Lee & Nazar 1997; Yoo et al. 1997).

Once 5S rRNA binds to TFIIIA forming the 7S RNP, it is exported to the cytoplasm where it functions as a 5S rRNA cytoplasmic retention particle (Guddat et al. 1990; Rudt & Pieler 1996). In the cytoplasm, after the cleavage of 2 uridylates from the 3'-end, 5S rRNA binds to central region of the nascent polypeptidic chain of RPL5 (Lin et al. 2001). This means that 5S rRNA is the only rRNA molecule that interacts with RPs

before being assembled into the nascent ribosome. 5S rRNA has been used for years as a model for protein-RNA interaction studies (Szymański et al. 2003). The binding to RPL5 is essential for 5S rRNA import into the nucleolus, where it will be incorporated into the nascent 60S ribosome subunit (Steitz et al. 1988; Murdoch & Allison 1996) (**Figure I-12**). The reason why 5S rRNA is exported from the nucleus to the cytoplasm and then imported from the cytoplasm together with RPL5 is still unclear. Some studies have shown that the RPL5 yeast homologue contributes to stabilize 5S rRNA (Deshmukh et al. 1993). It is possible that both molecules are required for mutual stability and/or nuclear import. The fact that 5S rRNA-RPL5 interaction appeared relatively early in 5S rRNA evolution (Sun & Caetano-Anollés 2009) would support this idea.

The specific role of 5S rRNA in the mature ribosome is not clear. However, its structure and interactions with adjacent RPs could help to infer the general function of 5S rRNA in mature ribosomes and protein synthesis. Early studies of 5S rRNA sequence in prokaryotic cells led to hypothesize that it could interact with the common arm of the tRNAs, helping the ribosome to translocate along the mRNA (Fox & Woese 1975). Later studies confirmed the essential role of 5S rRNA ribosome biogenesis (Dohme & Nierhaus 1976). Partial deletion of 5S rRNA operons in *Escherichia coli* impaired the translational capacity and cell growth in a greater extent than partial deletion of other rRNA operons encoding 16S or 23S rRNA. All three rRNA species are essential for ribosome biogenesis, however partial deletion of 16S or 23S rRNA operons is compensated by increased transcription of the remaining operons, which does not occur in the case of 5S rRNA (Condon et al. 1993; Ammons et al. 1999). In eukaryotic cells, expression of mutated forms of 5S rRNA in the absence of the WT allele of 5S rRNA was shown to be inviable in yeast (Kiparisov et al. 2005). Moreover, 5S rRNA is essential for pre-rRNA maturation of ribosomal large subunit in yeast (Dechampesme et al. 1999). Importantly, studies from our laboratory demonstrated that depletion of 5S rRNA by TFIIIA knock-down in human cells abolished the formation of new 60S ribosomal subunits (Donati et al. 2013). Together these studies suggest that 5S rRNA is

an essential component of mature ribosome and it plays a central role during the process of ribosome biogenesis.

2.2. Ribosome biogenesis regulation: the transcription factor c-Myc

The family of Myc transcription factors includes c-Myc, L-Myc and N-Myc. They are basic proteins that act as a sequence-specific transcription factors. To do so they interact with the small protein Max, which binds to E-box sequence CACGTG (Eilers & Eisenman 2008). The Myc-Max interaction has been associated with increased expression of target genes but it can also drive gene repression under certain circumstances (Kleine-Kohlbrecher et al. 2006). c-Myc has been described to directly interact and regulate ~ 11% of the genome (Fernandez et al. 2003). In conditions of c-Myc overexpression or amplification, like oncogenic activation, c-Myc has been shown to bind and to enhance transcription of active genes sets (Lin et al. 2012; Nie et al. 2012). In general, c-Myc is considered a global regulator of different cellular processes such as transcription, DNA replication, translation and ribosome biogenesis, among others (van Riggelen et al. 2010). Importantly, c-Myc de-regulation has been associated to many types of cancers (Dang et al. 2006; Dang et al. 2012). For example, early studies reported that c-Myc overexpression transformed mouse fibroblasts in cooperation with *Ras* (Land et al. 1983). In addition, c-Myc has been reported to be amplified in many cancer types including colorectal cancer (CRC) (He 1998; Beroukhim et al. 2010). Consistent with an upregulation of ribosome biogenesis, c-Myc has been shown to increase cell growth and proliferation together with upregulation of protein synthesis (Iritani & Eisenman 1999; Johnston et al. 1999).

c-Myc upregulates ribosome biogenesis at different levels (van Riggelen et al. 2010) (**Figure I-13**). First, c-Myc promotes transcription of all the rRNA species present in the ribosome. c-Myc increases 28S, 18S and 5.8S rRNA synthesis by two mechanisms: (I) by regulating RNA Pol I-dependent transcription of pre-rRNA and (II) by promoting chromatin structure remodeling in order to interact with RNA Pol I

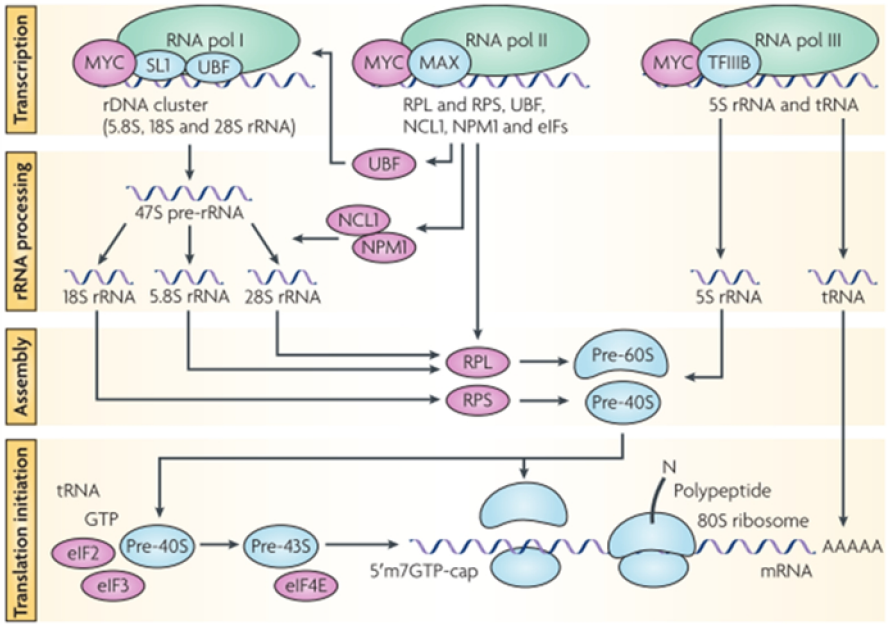

Figure I-13. Myc regulates ribosome biogenesis at different levels. The transcription factor c-Myc upregulates RNA Pol I, II and III. RNA Pol II increases the transcription of genes related to rRNA processing, ribosome assembly and translation initiation factors. From van Riggelen et al. 2010.

transcriptional co-factors (Arabi et al. 2005; Grandori et al. 2005). Moreover, c-Myc binds directly to TFIIIB, a co-transcriptional factor of RNA Pol III, and enhances 5S rRNA synthesis (Gomez-Roman et al. 2003). In fact, overexpression of c-Myc in *Drosophila melanogaster* and human fibroblasts has been shown to increase rRNA synthesis (Grewal et al. 2005). On the other hand, c-Myc-null rat fibroblasts showed decreased levels of rRNA (Mateyak et al. 1997). These studies suggest a direct correlation between levels of rRNA and c-Myc expression and are consistent with the direct regulation of RNA Pol I and III by c-Myc. Second, c-Myc enhances the synthesis of RPs transcriptionally but also at the translational level by promoting eukaryotic translation initiation factor 4E-binding protein 1 (4E-BP1) phosphorylation in a mammalian target of rapamycin (mTOR)-dependent manner, thus enhancing the translation of 5'TOP mRNAs, including RPs mRNAs (Pourdehnad et al. 2013; Gentilella et al. 2015). Third, c-Myc enhances the transcription of protein factors that are needed during rRNA processing and maturation such as nuclear transporters involved in the translocation

of ribosomal components (van Riggelen et al. 2010; Golomb et al. 2012).

The fact that c-Myc participates in ribosome biogenesis regulation and together with the high proportion of human cancers with c-Myc amplification suggests that ribosome biogenesis genes upregulation by c-Myc could have a role in cancer development and progression (Dang et al. 2012). Due to a deregulation of CAP-dependent mRNA translation throughout the cell cycle, *Eμ-myc* mice present genome instability and increased susceptibility to develop B-cell lymphoma. Significantly, crossing *Eμ-myc* mice with mice carrying haploinsufficiency of *Rpl24* rescues translational deregulation and increases disease-free survival (Barna et al. 2008). This study underscores the role of c-Myc in driving tumorigenesis and the potential use of ribosome biogenesis impairment to disrupt c-Myc-driven oncogenic malignancies. Thus, it is foreseeable that targeting ribosome biogenesis is increasingly being studied as an anti-cancer therapeutic strategy (Bywater et al. 2012; Devlin et al. 2016).

2.3. The Impaired Ribosome Biogenesis Checkpoint (IRBC)

Ribosome biogenesis disruption by different means leads to p53 stabilization (Teng et al. 2013; Bursac et al. 2014). We have recently termed this response the "impaired ribosome biogenesis checkpoint" (IRBC) (Gentilella et al. 2017). In brief, upon insults to ribosome biogenesis, a pre-ribosomal complex formed by RPL11, RPL5 and 5S rRNA is redirected from the assembly into nascent 60S subunits to the binding and inhibition of HDM2. The pre-ribosomal complex RPL11/RPL5/5S rRNA, or IRBC complex, inhibits HDM2 ubiquitin activity, allowing p53 stabilization (Donati et al. 2013; Sloan et al. 2013) (**Figure I-14**). However, the sequence of molecular events that regulate the transition of the pre-ribosomal complex RPL11/RPL5/5S rRNA complex upon impaired ribosome biogenesis into the IRBC complex is unknown.

Several RPs apart from RPL5 and RPL11 have been described to interact with HDM2 after ribosome biogenesis impairment: RPS3 (Yadavilli et al. 2009), RPS7 (Chen et al. 2007), RPS14 (Zhou et al. 2013), RPS15, RPS20, RPL37 (Daftuar et al. 2013),

RPS27, RPS27-like (Xiong et al. 2011), RPL4 (He et al. 2016), and RPL23 (Dai et al. 2004). However, the interaction of many of these RPs with HDM2 could be explained by their intrinsic basic properties, which might have non-specific higher affinity for acidic central domain of HDM2. On the other hand, depletion of a number of these RPs was shown to rescue p53 stabilization induced by actinomycin D (ActD) treatment. However, this appears to be attributed to a general decrease in protein synthesis capacity caused by RP depletion, combined with the short half-life of p53 (Fumagalli et al. 2012). Recent studies from our laboratory and others support the role of only RPL5 and RPL11 together with 5S rRNA as essential in driving the IRBC by binding to HDM2. First, the identification of the IRBC complex as a pre-ribosomal particle in yeast prior to its incorporation into the 60S subunit (Zhang et al. 2007) is in agreement with the extra-ribosomal function of the IRBC complex before it is assembled into the nascent ribosome. Second, p53 stabilization induced by ribosome biogenesis impairment can only be rescued by knocking down RPL11, RPL5 or TFIIIA (which decreases the levels of nascent 5S rRNA) and not by other RPs depletion (Fumagalli et al. 2012; Donati et al. 2013). Third, unlike other RPs, ribosomal-free RPL11 and RPL5 have been shown to accumulate after ribosome biogenesis disruption with actinomycin D, which does not block Pol III rRNA transcription (Bursac et al. 2012), supporting the selective role of the nascent RPL5/RPL11/5S rRNA complex in inhibiting HDM2, when ribosome biogenesis is compromised.

It was first argued that nucleolar disruption causes the passive release of RPs from the nucleolus to the nucleoplasm, where they are able to interact and inhibit HDM2 (Dai et al. 2004; Chen et al. 2007) and that insults in ribosome biogenesis affect nucleolar integrity to different extents (Boulon et al. 2010). However, later studies demonstrated that the IRBC complex could be bound to HDM2 after ribosome biogenesis impairment without detectable nucleolar disruption. Down regulation of ribosomal proteins RPS6, RPL7a or RPL23 does not disrupt nucleolar structure nor does it alter the synthesis of the other ribosomal subunit despite eliciting the IRBC (Fumagalli et al. 2009; Fumagalli et al. 2012). These results suggest that although

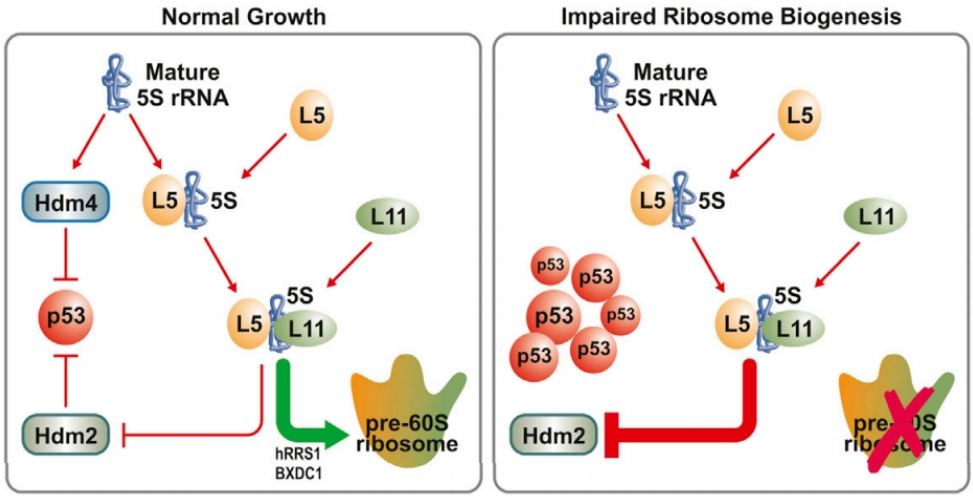

Figure I-14. The IRBC is executed upon ribosome biogenesis disruption. In normal growing conditions (left pannel), the IRBC complex is incorporated into the nascent 60S ribosomal subunit. When ribosome biogenesis is impaired, the IRBC complex is redirected to the binding and inhibition of HDM2, which leads to p53 stabilization. Modified from Donati et al. 2013.

nucleolar disruption may lead to ribosome biogenesis impairment, it is not necessary to elicit the IRBC. In this regard, the IRBC is argued to be a regulated response rather than a passive event induced by nucleolar disruption and the release of RPs from nucleolus, where they could bind and inhibit HDM2.

2.3.1. Ribosome biogenesis and IRBC in human disease: ribosomopathies

A number of human diseases, referred to as ribosomopathies, have been linked to alterations in ribosome biogenesis. Most are inherited diseases caused by haploinsuffiency of genes related to ribosome biogenesis. For instance, 25% of Diamond Blackfan Anemia (DBA) patients are haploinsufficient for *RP19*, whereas all *5q*$^{-}$ syndrome are thought to be due to a sporadic deletion of one allele of chromosome 5, which encompasses the *RPS14* gene (Narla & Ebert 2010; Teng et al. 2013). In this regard, we have recently identified the RNA-binding protein LARP-1 as a key factor in regulating RPs mRNA stability together with the 40S ribosomal subunit, thus describing a role of 40S ribosomal subunit in regulating 5'TOP mRNA stability. Critically, LARP-1 deletion in human hematopoietic stem cells leads to a reduction of

5'TOP mRNAs and the induction of p53, demonstrating the implication of this RNA-binding protein in RPs mRNA stability and *5q*$^{-}$ syndrome pathophysiology (Gentilella et al. 2017). Ribosomopathies like DBA and *5q*- syndrome share common symptoms, which include bone marrow failure, anemia and higher predisposition to cancer development (Narla & Ebert 2010; Teng et al. 2013). However, there are two major features of ribosomopathies that are not fully understood. First, the fact that ubiquitous haploinsufficiency of genes related to ribosome biogenesis only induces symptoms in specific tissues like bone marrow. Second, the increased possibility to develop cancer, although they display reduced ribosome biogenesis.

The stabilization of p53 induced upon ribosome biogenesis impairment is thought to promote the ribosomopathies. In the case of DBA and 5q- syndrome, several animal models of RPs haploinsufficiency, recapitulating the human anemia phenotype, have been developed in mouse and zebrafish: *Rps6* (Volarevic et al. 2000; Keel et al. 2012), *Rps14* (Schneider et al. 2016), and *Rps19* (Danilova et al. 2008; Devlin et al. 2010). A number of these models confirm that p53 stabilization induced by ribosome biogenesis impairment plays a key role in the pathophysiology of the disease since the symptoms remitted in a p53$^{-/-}$ background (McGowan et al. 2011; Schneider et al. 2016). Importantly, the anemic phenotype shown by *Rps19* haploinsufficient mice was partially rescued when crossed with MDM2^{C305F} mutant mice (Jaako et al. 2016), a mutation which disrupts RPL11 binding to MDM2 (Lindstrom et al. 2007). This finding implies an essential role of the IRBC complex in driving p53 stabilization upon ribosome biogenesis impairment. All these studies support the hypothesis of IRBC and p53 stabilization as the main drivers of the symptoms observed in ribosomopathies.

Recent studies suggest that the IRBC may also play a critical role in tumorigenesis. It was shown that MDM2^{C305F} mutant background increased tumorigenesis in *Eμ-myc* mice, leading the authors to suggest that the absence of RPL5 and RPL11 binding to MDM2 in a context of increased rates of ribosome biogenesis facilitates malignant development (Macias et al. 2010). Consistent with this interpretation, *APC*$^{+/min}$ mice, which have constitutive activation of c-Myc, when

crossed with MDM2^{C305F} mice showed earlier appearance of CRCs when compared to MDM2 WT animals (Liu et al. 2016). Importantly, *Rpl11* haploinsufficiency in mice has been shown to induce lymphomagenesis in addition to the anemic phenotype (Morgado-Palacin et al. 2015). Moreover, RPL5 and RPL11 have also been shown to inhibit c-Myc transcription and destabilize c-Myc mRNA (Dai et al. 2010; Challagundla et al. 2011; Liao et al. 2013), consistent with c-Myc levels elevated in *Rpl11*-heterozygous primary MEFs (Morgado-Palacin et al. 2015). However whether this response is mediated by the IRBC and constitutes a further barrier against c-Myc driven tumours is unknown. Therefore, the specific role of the IRBC in preventing c-Myc-driven malignancies needs to be elucidated in view of designing potential cancer therapies targeting ribosome biogenesis.

Some drugs used in CRC therapy that inhibit nucleotide synthesis, such as 5-FU, have been shown to elicit the IRBC (Sun et al. 2007). This is probably due to alterations in rRNA synthesis caused by nucleotide imbalance. The aim of this study is to evaluate the effects of nucleotide biosynthesis inhibition on ribosome biogenesis and IRBC activation.

3. Nucleotide metabolism

Nucleotides are essential cellular molecules required for a wide variety of anabolic processes. Indeed, nucleotides are the essential components of nucleic acids, that is, DNA and RNA. In addition, nucleotides like ATP or GTP play a central role in energy metabolism and they are indispensable co-factors of many cellular enzymatic reactions (Nelson et al. 2013).

3.1. Nucleotide structure

Nucleotides are made of three characteristic components: (I) a nitrogenous base, (II) a pentose and (III) a phosphate (**Figure I-15A**). Nucleotides without the phosphate group are termed nucleosides. There are two different groups of nucleotides in the cell, depending on the parental compound they are derived from: purines and pyrimidines (**Figure I-15B**). The two major purine bases present in both RNA and DNA are adenine (A) and guanine (G). In the case of pyrimidines, cytosine (C) is common to both DNA and RNA, whereas thymidine (T) is exclusively found in DNA and uracil (U) in RNA (**Figure I-15C**). Nucleotides contain one of two different kinds of pentose: 2'-deoxy-D-ribose (deoxynucleotides) defines DNA and D-ribose (ribonucleotides) defines RNA (Nelson et al. 2013).

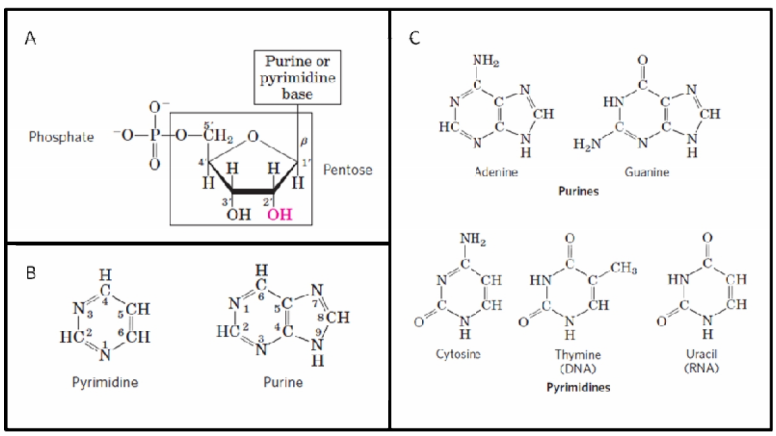

Figure I-15. Nucleotide structure. (A) General structure of a ribonucleotide. (B) Model of pyrimidine and purine rings with the numeration of the atoms. (C) Molecular structure of nucleosides present in nucleic acids. Figures taken from Lehninger 6th edition.

3.2. Nucleotide biosynthesis

Two different pathways are used for cellular nucleotide biosynthesis: the *de novo* biosynthesis pathway, which consists in synthesizing nucleotides from its precursors (amino acids, ribose 5-phosphate, CO_2 and NH_3); and the salvage pathway, which uses recycled bases and nucleosides released from nucleic acid breakdown (Nelson et al. 2013).

3.2.1. "De novo" nucleotide biosynthesis

Cellular nucleotide pools are relatively low in respect to the nucleotides required for DNA and RNA synthesis. It means that cells are required to generate continuously new nucleotides in order to reach demands for DNA and RNA synthesis (Nelson et al. 2013).

3.2.1.1. Purine synthesis

The *de novo* synthesis of purines starts from a PRPP molecule obtained from the pentose phosphate pathway (PPP), and needs glutamine, glycine, formate, aspartate and CO_2 (**Figure I-16**). The common precursor of purine nucleotides is inosine monophosphate (IMP), the first intermediate metabolite with a complete purine ring. The final nucleosides monophosphate obtained, adenosine monophosphate (AMP) and guanosine monophosphate (GMP), are converted in diphosphate (adenosine diphosphate [ADP], guanosine diphosphate [GDP]) and triphosphate (adenosine triphosphate [ATP],

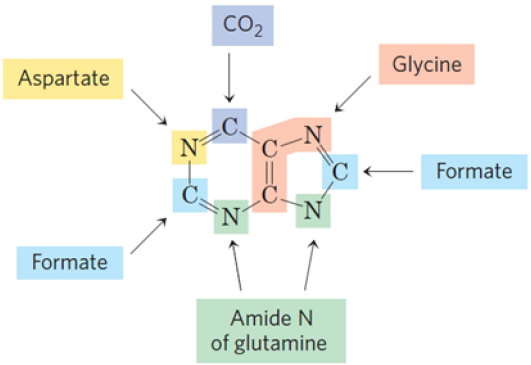

Figure I-16. The purine ring. This schematic view of the purine ring shows the origin of the atoms of the molecule. From Lehninger 6th edition.

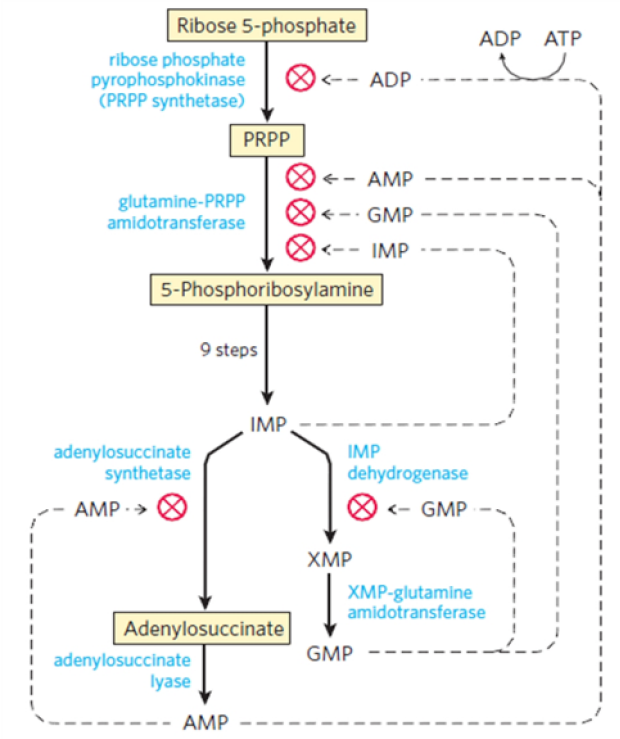

Figure I-17. Schematic view of purine synthesis and its negative regulatory feedbacks. The regulatory feedback loops of AMP, GMP and IMP affect the first step of the common pathway catalyzed by glutamine-PRPP amidotransferase. GMP and AMP also inhibit the first steps of their respectives pathways from IMP. From Lehninger 6th edition.

guanosine triphosphate [GTP]) forms by different nucleotide kinases. Regulation of purine biosynthesis occurs mainly at enzymatic level by allosteric interactions in negative feedback regulatory loops (**Figures I-17 and I-18**) (Nelson et al. 2013).

3.2.1.2. Pyrimidine synthesis

The pyrimidine ring is synthesized from the aminoacid aspartate and carbamoyl phosphate to form orotate. PRPP acts as a donor for the ribose that is attached to the orotate generated in the mitochondria from the aspartate (Lane & W-M Fan 2015). Regulation of pyrimidine synthesis is similar to that of purine synthesis, mainly regulated by negative feedback loops (Nelson et al. 2013).

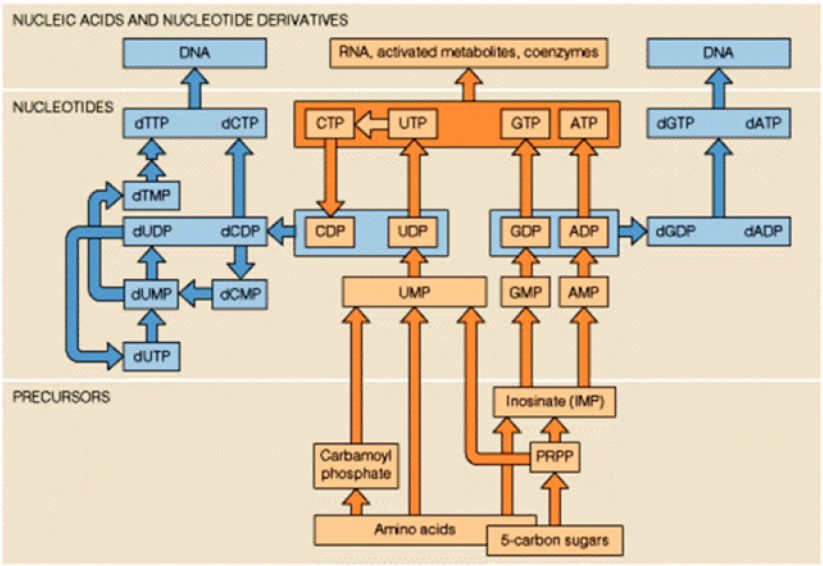

Figure I-18. Schematic view of de novo synthesis of nucleotides. The main procursors of *de novo* nucleotide synthesis are aminoacids and pentoses, coming from the pentose phosphate pathway. PRPP is an essential molecule of the nucleotide synthesis, since it participates in both the *de novo* and salvage pathways.

3.2.1.3. Deoxyribonucleotide synthesis

Synthesis of deoxyribonucleotides for DNA synthesis is catalyzed by a single enzyme that converts all the ribonucleotides in their deoxyribonucleotide counterparts (**Figure I-18**). This enzyme is called ribonucleotide reductase (RNR) and carries out the reduction of the 2'-carbon of the ribose directly on the nucleotide (**Figure I-18**) (Nelson et al. 2013).

3.2.2. The salvage pathway

Purines and pyrimidines can be recycled to generate new nucleotide molecules through the salvage pathway. Free nucleosides, purines and pyrimidines are constantly released in the cell from nucleic acid degradation, such as rRNA cleavage during its processing in the nucleolus. These free bases and nucleosides are used to generate new nucleotides in a much less complicated biochemical pathway than that

of their *de novo* synthesis. For purines and pyrimidines, PRPP molecules are used as the donors of ribose, which will be incorporated by the action of phosphoribosyltransferase enzymes into nitrogenous bases in order to generate new ribonucleotides. On the other hand, nucleosides can be also recycled by addition of a phosphate group by nucleotide kinases. The nucleotide salvage pathway is essential in some tissues, like the nervous system, and mutations in the enzymes involved in the pathway can cause diseases such as Lesch-Nyhan syndrome (Fasullo & Endres 2015). Computational analyses have reported a high reliance of CRC in both *de novo* nucleotide synthesis and salvage pathway, although no experimental confirmation has been provided at present (Qi & Voit 2014) (**Figure I-19**).

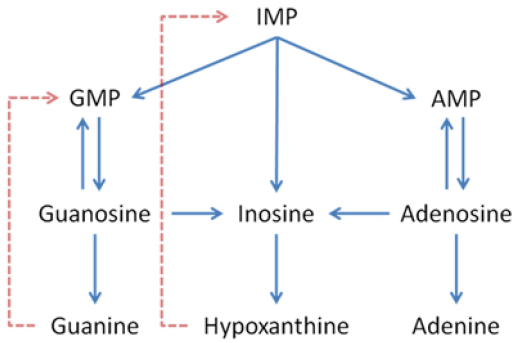

Figure I-19. Purine salvage pathway. Schematic view of the salvage pathway for purine synthesis. The red dotted arrows represent the reactions catalyzed by Hypoxanthine-guanine phosphoribosyl transferase (HGPRT).

3.3. Nucleotide synthesis in cancer

In general, cancer cells are characterized by high rates of growth and proliferation. In order to replicate their genome and generate new RNAs, cancer cells present high rates of nucleotide synthesis (Tong et al. 2009). One of the main regulators of nucleotide synthesis is the transcription factor c-Myc (Liu et al. 2008; Mannava et al. 2008), which is known to be amplified in many cancer types (Beroukhim et al. 2010). Many genes coding for nucleotide biosynthetic enzymes such as inosine 5'-monophosphate dehydrogenase (IMPDH) have been reported to be c-Myc transcriptional targets (Liu et al. 2008). As stated earlier, c-Myc is coordinating

several different cellular machineries to reach the high metabolic demands of proliferating cancer cells. In fact, c-Myc has been shown to regulate translation of PRPS2, the enzyme which catalyzes PRPP synthesis, therefore coupling protein synthesis with nucleotide biosynthesis (Cunningham et al. 2014).

Maintaining the appropriate levels of nucleotides is essential for the cell. *De novo* biosynthesis, salvaging and degradation of nucleotides must be balanced and coordinated in order to maintain homeostasis. Perturbations in the amounts of nucleotides result in DNA damage and genomic instability, which can lead to the development of malignancies (Meuth 1989; Chabosseau et al. 2011). It was shown that oncogenic activation of E2F or cyclin E in primary keratinocytes decreased the levels of nucleotides which led to replicative stress and tumorigenicity. These phenotypes were abolished by exogenous supply of nucleotides or by overexpression of nucleotide genes by c-Myc induction (Bester et al. 2011). On the other hand, it has been described that many CRCs have mutations in the SAM domain and HD domain-containing protein 1 (SAMHD1) gene, which encodes for an enzyme involved in dNTP degradation. The downregulation of SAMHD1 causes increased dNTP levels and genomic instability, which combined with defects in DNA repair machinery leads to higher rates of mutations (Rentoft et al. 2016). These studies underline the importance of the nucleotide levels regulation and the potential impact in DNA replication and repair.

3.3.1. Nucleotide synthesis inhibition in cancer treatment

Importantly, cancer cells present higher concentrations of deoxynucleotides compared to normal cells (Traut 1994). Because of their high demand of nucleotides, cancer cells are generally more sensitive to those drugs affecting nucleotide metabolism than normal growing cells (Cheung-Ong et al. 2013). Several anti-cancer drugs, currently used in the clinic, affect nucleotide metabolism. For example, methotrexate is a competitive inhibitor of dihydrofolate reductase, thus affecting the

synthesis of purines and thymidine nucleotides (Gorlick et al. 1996). Also, 5-FU acts as an inhibitor of thymidylate synthase limiting the biosynthesis of TMP, and it is widely used in CRC treatment (Longley, Harkin, Johnston, et al. 2003).

3.3.1.1. Mycophenolic Acid (MPA)

MPA is a FDA-approved potent and reversible inhibitor of inosine-5'-monophosphate dehydrogenase (IMPDH), the enzyme that catalyzes the convertion of inosine monophosphate (IMP) in xanthosine monophosphate (XMP) in the *de novo* GMP synthesis pathway (**Figure I-17**) (Allison & Eugui 2000). It has been widely used as an immunosuppressant to avoid rejection in transplantation patients, due to its anti-proliferative effects on B and T lymphocytes. It has been also used in the treatment of autoimmune diseases such as lupus nephritis, idiopathic thrombocytopenic purpura and scleroderma (Van Leuven et al. 2006; Zwerner & Fiorentino 2007).

Earlier studies also showed that MPA has anticancer properties (Williams et al. 1968). MPA affects the proliferation of different cell types (Floryk et al. 2006; Takebe et al. 2006). Although the mechanisms by which MPA exerts its anti-cancer are not clear they appear to be tissue-specific (Majd et al. 2014). Treatment with MPA showed anti-cancer efficacy in subcutaneous tumours generated by injecting athymic mice with several human cancer cell lines: A3.01 (T-lymphoblast), Molt-4 (T-cell leukaemia), CaPan-2 (pancreatic adenocarcinoma), CaLu-3 (non-small-cell lung adenocarcinoma), LS174T and T84 (colon adenocarcinoma), and Daudi (B-cell lymphoma). Moreover, it increased survival in a metastatic lymphoma *in vivo* murine model (Tressler et al. 1994).. Indeed, MPA and other IMPDH inhibitors have been tested in clinical trials of myeloma and pancreatic cancer patients (Majd et al. 2014).

By inhibiting IMPDH, MPA impairs the *de novo* synthesis of GMP and causes nucleotide depletion. This results in hindering the cells ability to synthesize RNA or replicate DNA. Consistent with this observation, MPA has been shown to inhibit rRNA synthesis and disrupt the nucleolus, suggesting that IMPDH inhibition leads to

ribosome biogenesis impairment (Huang et al. 2008). Moreover, MPA-induced stabilization of p53 has been argued to depend on RPL11 and RPL5, the two protein components of the IRBC complex (Sun et al. 2008).

3.3.2. Replicative stress and DNA damage

Nucleotide imbalance can lead to the triggering of replicative stress response or DDR (Zeman & Cimprich 2013). Drugs affecting nucleotide synthesis often cause replicative stress and/or DDR. Replicative stress occurs when the DNA replication fork is stalled for any reason. Some physiological reasons for stalled forks are accumulation of reactive oxygen species (ROS), stochastic misincorporation of nucleotides or topological impediment of polymerization. When this takes place, DNA polymerases stop the replication process and the fork is stalled. Thus, replicative stress response can be potentially elicited every time cells replicate DNA. In other words, external stimuli like UV radiation are not necessary to trigger the replicative stress response, which is considered one of the primary causes of genomic instability (Gaillard et al. 2015).

After fork arrest, a signaling pathway is activated in order to elicit the mechanisms needed for DNA repair to ensure accurate DNA replication. If the problem is repaired, replication re-starts. If not, the fork collapses and the replication machinery is released from the DNA strand. The exposed forks or strands often undergo DNA cleavage carried out by DNA endonucleases, which can lead to single-strand breaks or double-strand breaks. Fork arrest and single-strand breaks lead to the activation of the ATR kinase, which phosphorylate Chk1 and p53 (Dobbelstein & Sørensen 2015; Gaillard et al. 2015). On the other hand, double-strand breaks cause the activation of Chk2, and p53 (Zannini et al. 2014) (**Figure I-20**). These responses are elicited to suppress the cell cycle in order to repair potential DNA damage and continue with DNA replication once the threat is resolved. Importantly, GMP Synthetase (GMPS), the next enzyme in nucleotide synthesis downstream of IMPDHs

and last in the *de-novo* synthesis of GMP **(Fig. I-17)**, was shown to form a complex with the USP7 deubiquitinase, translocating to the nucleus, to stabilize p53 under conditions of MPA treatment (Reddy et al. 2014). It was suggested to be mediated by the activation of a DNA damage sensing kinase, such as ATM, through a GMPS/USP7 complex. The findings implicating the IRBC, through inhibition of HDM2, in stabilizing p53 (Sun et al. 2008) *versus* those arguing that this response was mediated by the GMPS/USP7 complex, appears incongruent. Therefore we set out to better understand the role of MPA in inducing the IRBC and p53 stabilization.

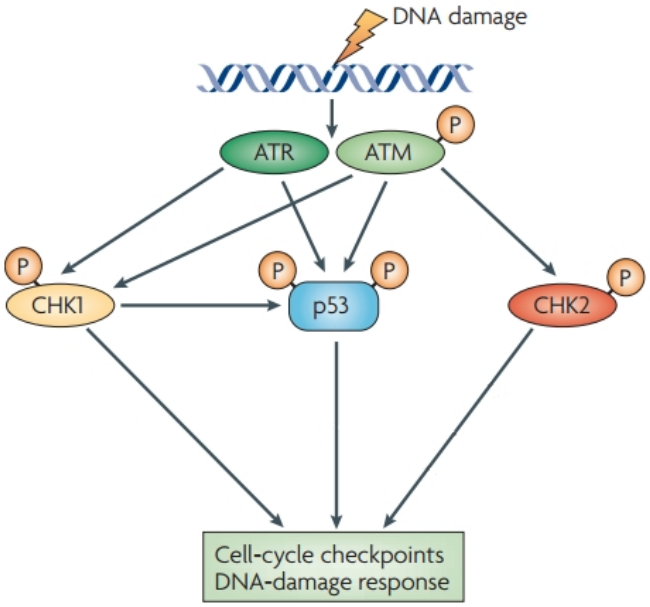

Figure I-20. Role of ATR/ATM pathway in p53 regulation. After DNA damage or replicative stress induced by oncogenic activation, the kinases ATM and ATR are activated. Usually, ATM activation is associated to double-strand break and ATR activation to single-strand break. ATR and ATM can phosphorylate p53 at serine 15. ATR activates Chk1 and ATM activates Chk1 and Chk2, which can phosphorylate p53 at serine 20. Moreover, the kinases Chk1 and Chk2 can phosphorylate other targets that control cell cycle, such as Cdc25. Modified from Moorhead et al. 2007.

4. RATIONALE OF THE STUDY

Ribosome biogenesis is a highly regulated and energy consuming cellular process that involves the synthesis and assembling of 79 RPs and 4 different non-coding rRNAs. The final outcome of ribosome biogenesis is the mature ribosome, the main molecular constituent of the translational machinery of the cell. As mature ribosomes are in charge of the synthesis of every structural and catalytic protein component of the cell, they play a key role in driving cell growth and proliferation. In order to give rise to newly synthesized ribosomes, cells must couple protein synthesis and nucleotide synthesis to generate the required RPs and rRNA species. One of the main regulators and positive effectors of these two biological processes is the transcription factor c-Myc (van Riggelen et al. 2010; Mcmahon 2011). When c-Myc becomes deregulated through overexpression or constitutive activation by an upstream signaling event, this results in upregulation of nucleotide synthesis and ribosome biogenesis, leading to rapid growth, proliferation and tumorigenesis. Nucleotide and protein synthesis are essential coupled events in c-Myc driven tumours. This was recently underscored by the observation that oncogenic c-Myc drives the selective translation of PRPS2 (Cunningham et al. 2014). PRPS1 and PPRS2 convert ribose 5-phosphate (R5P) into phosphoribosyl pyrophosphate (PRPP), required for both purine and pyrimidine synthesis. Importantly, deletion of PRPS2 selectively blocks c-Myc driven tumorigenesis in mice, demonstrating the close coupling of the nucleotide and protein synthesis (Cunningham et al. 2014).

The observations above are also supported by the fact that many drugs used in cancer therapy that target and impair nucleotide synthesis and/or ribosome biogenesis have demonstrated clinical efficacy (Burger et al. 2010), particularly in those tumours with overexpression or constitutive activation of c-Myc. For instance, 5-fluorouracil (5-FU) is a pyrimidine analogue that inhibits RNA and DNA synthesis by hindering the production of pyrimidines (Longley, Harkin & Johnston 2003); on the other hand, oxaliplatin has been recently shown to elicit p53 stabilization by inhibiting

ribosome biogenesis (Bruno et al. 2017). Both drugs are currently used in the treatment of sporadic CRC, which in almost all cases is characterized by c-Myc deregulation (Nesbit et al. 1999; The Cancer Genome Network Atlas 2012). Thus, inhibition of ribosome biogenesis is emerging as a critical target in cancer therapy and new inhibitors and combinations are being developed (Bywater et al. 2012; Devlin et al. 2016).

Our group (Donati et al. 2013) and others (Sloan et al. 2013) have recently shown that upon ribosome biogenesis impairment, a pre-ribosomal complex formed by RPL11 and RPL5 and noncoding 5S rRNA is re-directed from its assembly into the newly synthesized 60S ribosome to the binding and inhibition of HDM2, inducing p53 stabilization and cell cycle arrest (Teng, Mercer et al. 2013). Apparently, the IRBC complex is also involved in p53 stabilization following inhibition of nucleotide synthesis by MPA (Sun et al. 2008), an inhibitor of IMPDH, the rate-limiting enzyme in the *de novo* synthesis of GMP (Hedstrom 2009). In addition, 5-FU was reported to induce the binding of the IRBC to HDM2 (Sun et al. 2007; Donati et al. 2013). However, other studies have described other mechanisms involved in p53 stabilization induced by MPA, such as GMPS/USP7 complex (Reddy et al. 2014) or AMPK (Maddocks et al. 2013). In this study we set out to analyze the effect of nucleotide synthesis inhibition on ribosome biogenesis and address the molecular mechanism behind the crosstalk between nucleotide imbalance and rRNA synthesis.

OBJECTIVES

The specific scientific objectives of this study are:

1. To study, in CRC cell lines, the effects of impaired ribosome biogenesis induced by nucleotide imbalance on p53 stability, IRBC complex formation and cell cycle progression.
2. To evaluate the contribution of IRBC in preventing DNA replication upon nucleotide imbalance.

RESULTS

1. MPA treatment causes a drop in guanine nucleotides and stabilizes p53

Previous studies have shown that treatment of U2OS osteosarcoma cells with 10 µM MPA induces stabilization of p53, which can be rescued by depleting cells of RPL11 or RPL5 (Sun et al. 2008), suggesting a role of IRBC in this response. With the aim of elucidating whether the inhibition of the *de novo* nucleotide synthesis induced by MPA treatment is involved in the p53 response in c-Myc-driven CRC, HCT116 cells were treated with increasing concentrations of MPA. Consistent with previously published studies (Sun et al. 2008), p53 levels were higher in MPA treated cells in a time and dose dependent manner (**Figure R-1A**). To further characterize the MPA effects on HCT116 cells, nucleotide levels were measured after treatment with MPA 10 µM, the dose at which the highest levels of p53 protein stability were achieved (**Figure R-1A**). Levels of all the guanine nucleotides showed a significant drop after 6 hours of 10 µM MPA treatment (**Figure R-1B**) with no significant effect in adenine

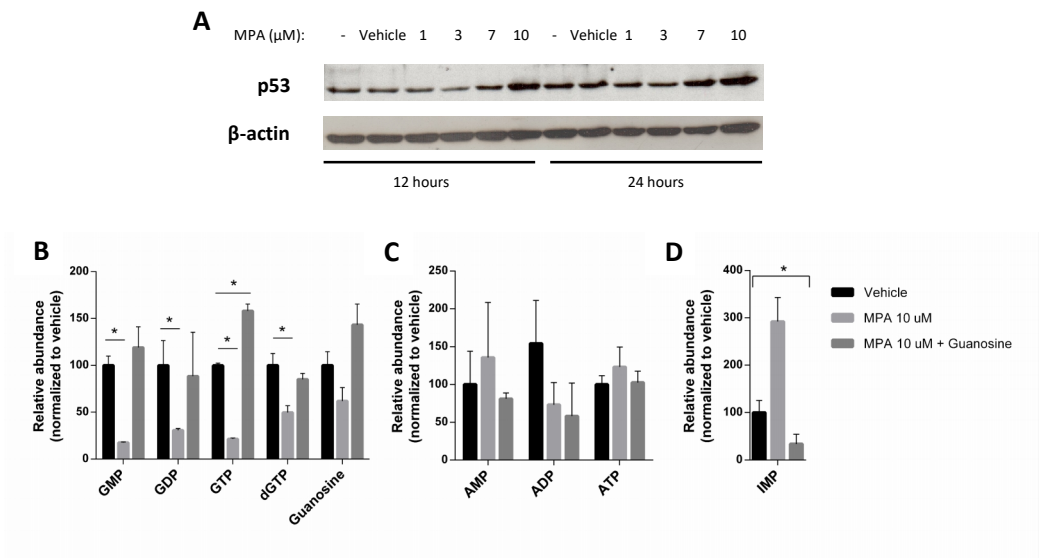

Figure R-1. MPA treatment induce nucleotide imbalance and stabilizes p53. (A) Immunoblot showing protein levels of p53 and loading control β-actin after MPA treatment at indicated concentrations for the specified time in HCT116 cells. (B, C, D) Histograms showing the relative levels of the indicated nucleotides as measured by LC-MS after 6 hours of specified treatment in HCT116 cells.

nucleotides (**Figure R-1C**), suggesting that the increase in p53 levels observed was due to a drop in the pool of guanine nucleotides. Moreover, consistent with IMPDH inhibition the precursor of GMP, IMP, showed an accumulation in MPA-treated cells with respect to the non-treated cells (**Figure R-1D**).

Cells obtain nucleotides by the *de novo* synthesis pathway or by taking advantage of already existing nucleotides through the salvage pathway (Berg et al. 2002). In order to confirm that the drop in guanine nucleotide levels induced by 10 µM MPA treatment was responsible for p53 stabilization, cells were treated with the exogenous nucleoside guanosine to replenish the nucleotide pools through the salvage pathway (**Figure I-19**). The results show that addition of guanosine to the medium rescued nucleotide levels in those cells treated with MPA (**Figures R-1B, R-1C, R-1D**), arguing that despite the inhibition of *de novo* synthesis of guanine nucleotides, cells were capable of restoring normal nucleotide levels through the salvage pathway. Critically, p53 stabilization induced by 10 µM MPA was restored to basal levels when cells were supplemented with exogenous guanosine (**Figure R-2A**). Treatment with other nucleosides, including adenine, cytosine and uridine, did not rescue the p53

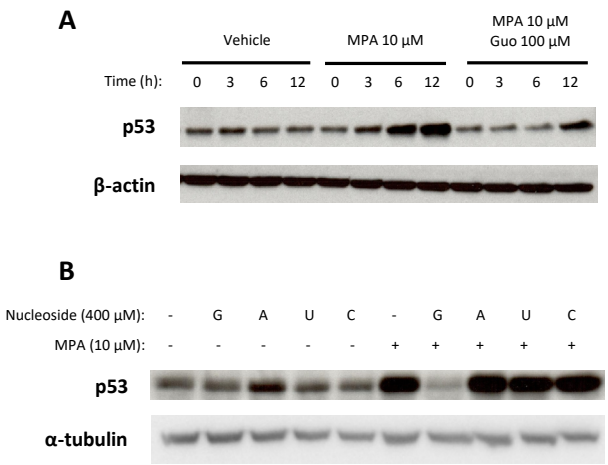

Figure R-2. Exogenous guanosine rescues p53 stabilization induced by MPA treatment. (A) Immunoblot showing protein levels of p53 and loading control β-actin after treatment with vehicle, 10 µM MPA or 10 µM MPA in combination with 100 µM guanosine at the indicated times. (B) Immunoblot showing protein levels of p53 and loading control α-tubulin after 24 hours of MPA 10 µM treatment alone or in combination with indicated nucleosides: G (guanosine), A (adenine), U (uridine), C (cytosine).

activation (**Figure R-2B**), demonstrating that the rescue is specific for guanosine and confirming that p53 stabilization is due to the specific inhibition of IMPDH by MPA. Together these results demonstrate that inhibition of IMPDH by MPA treatment leads to a drop in nucleotide levels, which induces p53 stabilization.

2. Stabilization of p53 induced by MPA is partially rescued by IRBC knock-down

To determine whether the IRBC complex is involved in mediating p53 stabilization following the addition of MPA, we treated HCT116 cells with RPL11 or RPL5 siRNAs for 24 hours, followed by the addition of 10 μM MPA for increasing times. The results show that the rescue of p53 stabilization after MPA treatment is only partial after 6 hours, with p53 levels continuing to increase after 12 and 24 hours treatment despite reductions in the levels of RPL11 and RPL5 (**Figure R-3A**). Our group has previously demonstrated that IRBC-driven p53 stabilization after depleting cells of specific RPs is completely rescued by co-depletion of either RPL11 or RPL5 (Fumagalli et al. 2009; Fumagalli et al. 2012). Consistent with these earlier findings we were able to block p53 stabilization induced by either depletion of RPL7a, a 60S RP, or RPS6, a 40S RP, by co-depleting RPL11 for 24 or 72 hours (**Figure R-3B**). That RPL11 or RPL5 depletion completely rescued p53 stabilization after impairing ribosome biogenesis by RP depletion, but failed to completely prevent p53 induction after nucleotide synthesis inhibition, led us to speculate that more than one response was affecting p53 stability in the case of MPA treatment.

To determine whether an additional step was implicated in the stabilization of p53, we first co-depleted of RPL7a and either RPL11 or RPL5 for 24 hours, conditions where p53 stability is completely rescued (**Figure R-3B**), and then added 10 μM MPA for an additional 6 hours. Although induction of p53 caused by RPL7a was completely rescued by co-depletion of either RPL11 or RPL5, a portion of p53 was still stabilized following MPA treatment in cells first co-depleted of RPL7a and RPL11 or RPL5 (**Figure R-3C**). In addition, it should be noted that MPA had only minor impact on the

induction of p21, whereas loss of RPL7a had a strong effect, which was not reversed by MPA treatment. Together the results suggest that IRBC complex is involved in p53 stabilization after MPA treatment, but a second response is also implicated in regulating p53 protein levels following nucleotide imbalance.

3. MPA treatment leads to activation of Chk1 but not Chk2

As previously shown, MPA induces decrease in all guanine nucleotides including the deoxynucleotide, dGTP (**Figure R-1B**). A major insult which triggers p53 stabilization is DDR (Reinhardt & Schumacher 2012) and MPA has been reported to inhibit DNA synthesis, eventually leading to DNA damage (Liu et al. 2008). Therefore MPA treatment could be altering DNA synthesis by potentially decreasing dGTP availability and creating a potential deoxynucleotide imbalance. ATM and ATR kinases mediate Chk1, Chk2 and p53 phosphorylation after replicative stress and/or DDR

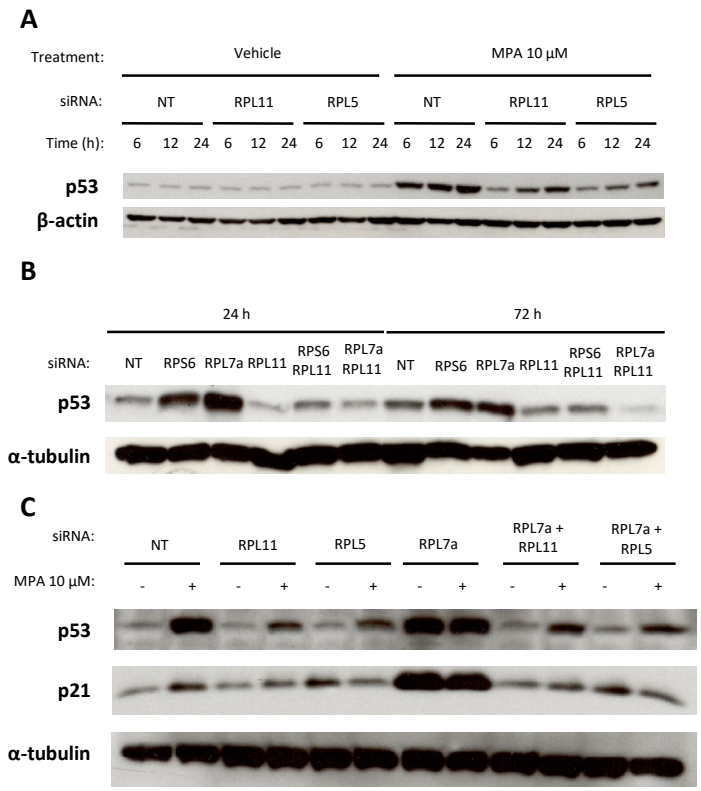

Figure R-3. p53 stabilization is partially rescued by RPL11 and RPL5 knock-down. (A) HCT116 cells were transfected with indicated siRNAs for 24 hours and then treated with either vehicle (methanol) or MPA 10 µM. The immunoblot shows p53 and loading control β-actin protein levels at indicated time-points after treatment. (B) Immunoblot showing p53 and loading control α-tubulin protein levels after 24 hours of transfection with the specified siRNAs. (C) HCT116 cells were transfected for 24 hours with the indicated siRNAs and then treated either vehicle or MPA 10 µM for 6 additional hours. The immunoblot shows p53, p21 and loading control α-tubulin levels after treatment.

(Meek 2004). To elucidate whether cells treated with MPA undergo replicative stress and/or DDR, we measured levels of p53 serine 15 phosphorylation as a markers of ATM and ATR activation. As controls we treated HCT116 cells with etoposide, a DNA damaging agent, or ActD, a chemotherapeutic drug, which at low doses (5 nM) disrupts ribosome biogenesis by selectively inhibiting RNA Pol I transcription without significantly affecting general guanine nucleotide levels, except for GMP (**Figure R-4B**). The results showed that both MPA and etoposide induced increased levels of serine 15 phosphorylation, whereas ActD had little to no effect (**Figure R-4A**). The results are consistent with MPA inducing replicative stress and/or DNA damage.

Since p53 can be phosphorylated at serine 15 by ATM and ATR, which also phosphorylate Chk2 and Chk1 respectively, we measured the levels of phosphorylated Chk1 and Chk2 by Western blot analysis. As compared to control cells or cells treated with 5 nM ActD, we observed increased Chk1 phosphorylation after 6 hours of MPA treatment, though not to the levels induced by etoposide (**Figure R-4C**). In contrast to Chk1, we saw no phosphorylation of Chk2 by either MPA or ActD, though etoposide led to strong activation of the kinase (**Figure R-4C**). Consistent with the absence of Chk2 phosphorylation, there was no effect of MPA treatment on γ-H2AX phosphorylation, a marker of DDR, whereas etoposide induced a strong response, as measured by Western blot analysis or immunofluorescence (**Figures R-4C and R-4D**). Chk1 phosphorylation together with concomitant absence of Chk2 and γ-H2AX phosphorylation suggests that MPA treatment for 24 hours, in addition to inducing the IRBC, leads to the activation of replicative stress pathway, but not DDR (Zeman & Cimprich 2013; Zannini et al. 2014).

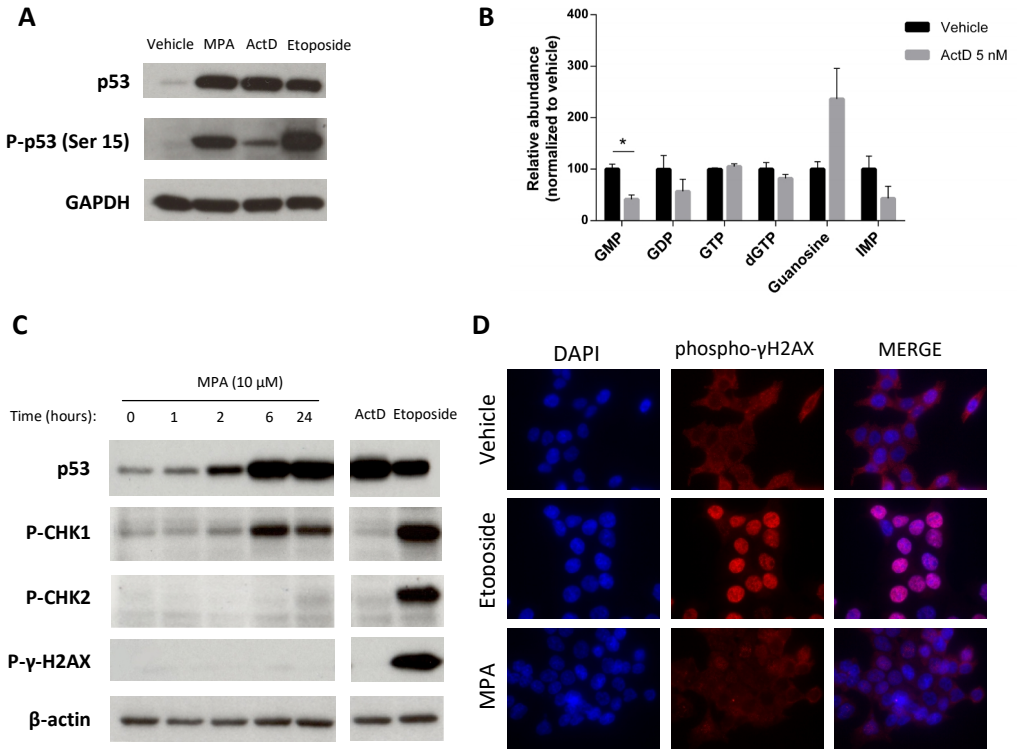

Figure R-4. MPA treatment leads to Chk1 phosphorylation but not Chk2. (A) Immunoblot showing protein levels of total p53, phospho-p53(ser15) and loading control GAPDH after 24 hours of vehicle, MPA (10 µM), ActD (5 nM) or Etoposide (50 µM) treatment. (B) Histogram showing guanine nucleotide levels after ActD treatment as measured by LC-MS. (C) HCT116 cells were treated with 10 µM MPA for indicated times or ActD (5nM) and Etoposide (50 µM) for 24 hours. Immunoblot shows levels of p53, phospho-Chk1 (P-Chk1), phospho-Chk2 (P-Chk2), phospho-γ-H2AX (P-γ-H2AX) and loading control β-actin proteins. (D) Immunofluorescence of HCT116 cells treated with vehicle, 50 µM etoposide or MPA for 24h and stained with an antibody against phoshorylated γ-H2AX and the nuclear marker DAPI.

4. MPA treatment leads to activation of S phase and replicative stress

To determine whether MPA induced replicative stress, we analysed the speed of incorporation of labelled nucleotides into DNA. Briefly, cells are pulse-labelled with 5'-cIoro-2'-deoxyuridine (CldU) and then the incorporation of the nucleotide analogue is evaluated by binding of a specific antibody conjugated with a fluorophore. This labeling system allows us to compare replication speed by comparing fiber lengths

between different treatments. The results show that DNA synthesis was strongly impeded in cells treated with 10 µM MPA for 24 hours (**Figure R-5A**), consistent with replicative stress and the induction of Chk1 phosphorylation (**Figure R-4C**). The observation of Chk1 phosphorylation and reduced speed of DNA replication in cells treated with MPA would require progression into S phase. However, others have shown that MPA treated cells arrest in G_0/G_1 (Sun et al. 2008), as they do in the case of general insults to ribosome biogenesis, such as ActD treatment (Choong et al. 2009; Fumagalli et al. 2012) or depletion of RPs (Fumagalli et al. 2009; Fumagalli et al. 2012; Teng, Mercer, et al. 2013). In agreement with a reduced speed of DNA replication and

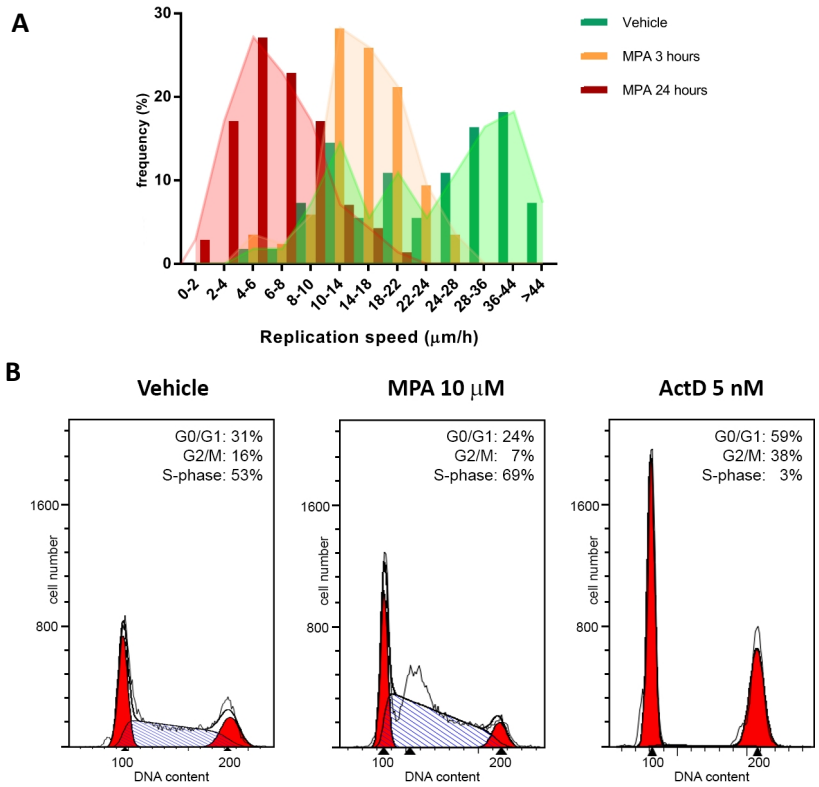

Figure R5. MPA treatment leads S phase accumulation and causes DNA synthesis slow down. (A) Histogram showing frequency of replication forks with the indicated speed range (calculated from: CldU tracks measurement/time of analog incorporation) after indicated vehicle or MPA 10µM treatments for the specified time in HCT116 cells. At least two-hundred fibres were counted per condition. (B) Cell cycle profile showing distribution of HCT116 cells treated for 24 hours with the indicated treatments.

Chk1 phosphorylation, cell cycle analysis clearly showed that unlike ActD-treated cells, which are arrested in G_1/G_2, MPA-treated cells tend to accumulate in S phase (**Figure R-5B**). Taken together these results suggest that MPA is not arresting cell cycle progression in G_0/G_1, but that cells are progressing into S phase.

5. MPA and Actinomycin D disrupt ribosome biogenesis and trigger the IRBC

Despite the apparent induction of the IRBC following MPA treatment (**Figure R-3A**), the findings above demonstrated that cells are not arresting in G_0/G_1 phase of the cell cycle, but progressing into S phase, where they could encounter replicative stress, as suggested by Chk1 phosphorylation and the reduced speed of DNA replication (**Figures R-4C and R-5A**). To elucidate the role of the IRBC in MPA-induced p53 stabilization, we immunoprecipitated RPL5 from HCT116 cells after 6 hours treatment with either ActD or MPA and then determined the extent to which HDM2 and RPL11 co-immunoprecipitated with RPL5. In both situations, the amounts of RPL11 and HDM2 bound to RPL5 were similar, as measured by Western blot analysis (**Figure R-6A**). The binding of IRBC complex to HDM2 together with p53 activation implies that both drugs impair ribosome biogenesis to a similar extent and elicit an IRBC response. That MPA treatment would lead to impaired ribosome biogenesis, as has been previously reported by others (Huang et al. 2008; Lo et al. 2012), would be consistent with the apparent degree to which the IRBC complex is bound to HDM2 (**Figure R-6A**), but is inconsistent with the cell cycle profiles (**Figure R-5B**).

Given the finding above, it was important to establish the effect of ActD and MPA on nascent ribosome biogenesis, as we have previously described (Fumagalli et al. 2009; Donati et al. 2013). To measure the extent to which either drug affected rRNA synthesis, we analyzed on Northern blots steady-state levels of rRNA by ethidium bromide (EB) staining and nascent rRNA levels by pulse labeling with ^{3}H-uridine. The results of such an experiment of EB stained agarose gels shows that all species of rRNA were equally represented under all three conditions. However, the

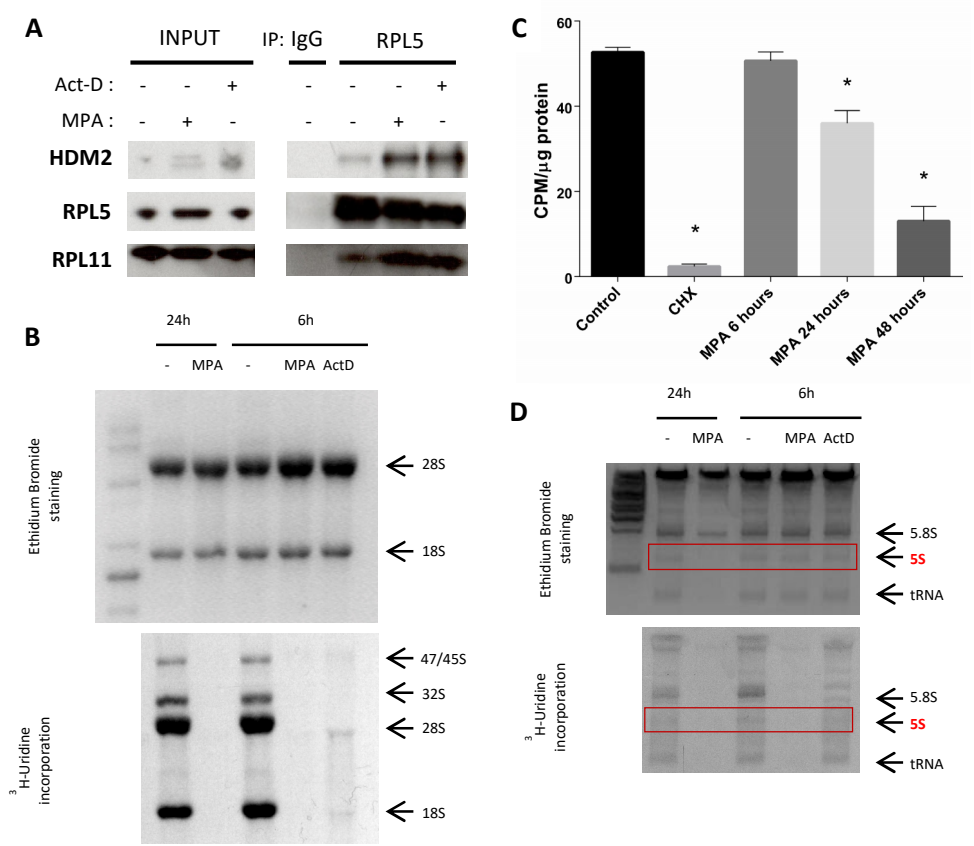

Figure R-6. Nucleotide imbalance induced by MPA inhibits rRNA synthesis. (A) HCT116 cells were treated for 6 hours with the indicated treatments. Immunoblot shows levels of HDM2 and RPL11 co-immunoprecipitated with RPL5. (B) Histogram showing levels of protein synthesis in 10 µM MPA-treated HCT116 cells for the indicated times as measured by ^{3}H-leucine incorporation. (C) EB-stained (up) and autoradiogram (down) of agarose gel loaded with total cellular RNA from HCT116 cells labelled with ^{3}H-uridine treated with the indicated treatments and times. (D) EB-stained (up) and autoradiogram (down) of TBE-urea polyacrylamide gel loaded with samples from (C).

incorporation of ^{3}H-uridine into nascent rRNA showed that ActD and MPA caused a dramatic decrease in the amounts of 47S precursor rRNA and the newly synthesized 18S and 28S rRNA (**Figure R-6B**). Consistent with these findings MPA reduced protein synthesis as measured by the incorporation of ^{3}H-leucine into nascent protein (**Figure R-6C**). However, the results also revealed that the incorporation ^{3}H-uridine into nascent 5S rRNA was also affected by MPA treatment, but not by ActD (**Figure R-6D**). This is consistent with the fact that low doses of ActD selectively inhibit RNA Pol I, but not RNA Pol III, the enzyme which mediates the synthesis of 5S rRNA. Given that 5S

rRNA is an essential component of the IRBC complex, its inhibition would be expected to impede the generation of nascent RPL5/RPL11/5S rRNA pre-ribosomal complexes and thus the induction of the IRBC. This would potentially explain why at 24 hours of MPA treatment cells accumulate in S phase, instead of arresting at G_1/G_2, as with ActD (**Figure R-5B**).

To test the hypothesis that MPA leads to a reduction in the IRBC complex we immunoprecipitated HDM2 after 24 hours of treatment, instead of 6 hours, to determine whether the IRBC complex was still bound to HDM2 at later time-points, when the 5S rRNA becomes limiting. To do so, we ectopically expressed a myc epitope-tagged HDM2 in HCT116 cells in order to avoid HDM2 induction elicited by MPA and ActD treatment, as we have previously described (Donati et al. 2013). The results show that when we immunoprecipitate the myc-tagged HDM2 after 24 hours of treatment with either ActD or MPA, we co-immunoprecipitate less RPL5, RPL11 and 5S rRNA with HDM2 following MPA treatment as compared to that of ActD, consistent

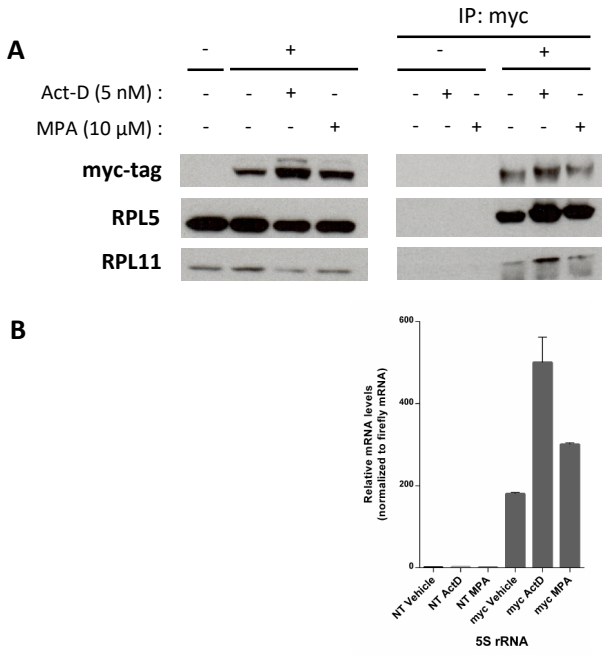

Figure R-7. Less IRBC complex is bound to HDM2 after MPA treatment when compared to ActD. (A) HCT116 cells were transfected with a plasmid expressing Myc-tagged HDM2 for 24 hours and then treated with specified treatments for additional 24 hours. Immunoblot shows levels of RPL5 and RPL11 co-immuno-precipitated with Myc-tagged HDM2 after 24 hours of indicated treatments. (B) 5S rRNA levels co-immunoprecipitated with Myc-tagged HDM2 as measured by RT-qPCR.

with a reduction in the amount of IRBC complex bound to HDM2 over time (**Figures R-7A and R-7B**). These findings suggest that the differences observed in terms of cell cycle progression in the presence of MPA could be related to a lack of nascent 5S rRNA in MPA-treated cells, which would eventually lead to an insufficient synthesis of the IRBC complex, allowing cells to escape the G_1 arrest and enter to S phase.

6. MPA treatment affects p53 activity

In order to determine whether the inhibition of 5S rRNA synthesis by MPA treatment is responsible for cells escaping the G_1 phase of the cell cycle and entering S phase, we first asked whether the addition of MPA together with ActD, would hamper the ability of ActD to block cells in G_1 phase of the cell cycle. Our prediction would be that adding MPA to ActD would inhibit nascent 5S rRNA synthesis allowing cells to escape G_1 arrest even in the presence of ActD. The results of such an experiment show cells accumulating in S phase when treated with ActD and MPA, whereas they arrest in G_1/G_2 phase when treated with ActD alone (**Figure R-8A**). Importantly,

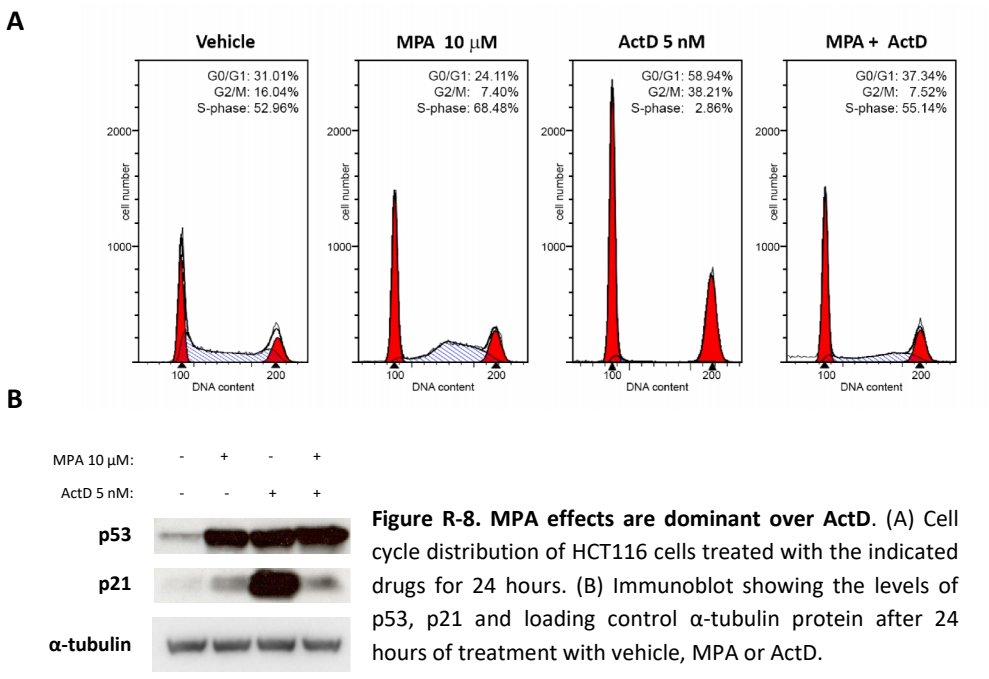

Figure R-8. MPA effects are dominant over ActD. (A) Cell cycle distribution of HCT116 cells treated with the indicated drugs for 24 hours. (B) Immunoblot showing the levels of p53, p21 and loading control α-tubulin protein after 24 hours of treatment with vehicle, MPA or ActD.

although under these conditions p53 levels were similar between both treatments, p21 levels were severely reduced in cells treated with MPA alone or in combination with ActD (**Figure R-8B**). These findings suggest that MPA treatment affects p53 activity, but not p53 stability, potentially due to inhibition of 5S rRNA synthesis.

To measure the transcriptional activity of p53 stabilized by MPA treatment we transfected cells with a plasmid expressing luciferase gene under the control of a promoter containing 13 copies of p53 binding site derived from the p21 gene promoter. We observed that luciferase activity was lower in those cells treated with MPA alone or in combination with ActD (**Figure R-9A**). Furthermore, when the endogenous mRNA levels of p53 transcriptional targets p21 and Hdm2 were measured, the same pattern was observed (**Figure R-9B**), with lower levels of p53 target genes mRNAs in MPA treated cells. The outcome of these experiments was compatible with the hypothesis that loss of newly synthesized IRBC complex was due to MPA inhibition of nascent 5S rRNA synthesis.

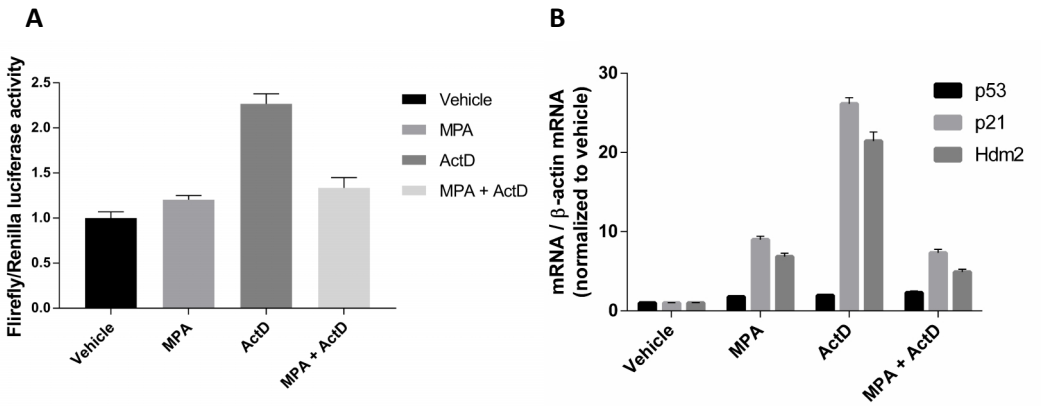

Figure R-9. Nucleotide imbalance affects p53 transcriptional activity with respect to ActD treatment. (A) HCT116 cells were transfected for 24 hours with a luciferase-expressing plasmid and then treated for additional 24 hours. Histogram showing luciferase activity with respect to the control.after 24 hours of indicated treatments (vehicle, MPA 10 μM, ActD 5 nM or combination). (B) Relative mRNA levels of p53, p21 and HDM2 after 24 hours of treatment (vehicle, MPA 10 μM, ActD 5 nM or combination) as measured by RT-qPCR.

7. Lower doses of MPA enhance IRBC

If MPA impairs the IRBC complex formation by inhibiting 5S rRNA synthesis, we rationalized that perhaps by lowering the MPA dose we could establish a dose at which the formation of the IRBC complex is not affected, but we still impair ribosome biogenesis leading to p53 activation and cell cycle arrest. To test this possibility we treated HCT116 cells with increasing concentrations of MPA and observed that p21 levels decreased as we increased the concentration of MPA (**Figure R-10A**). In parallel,

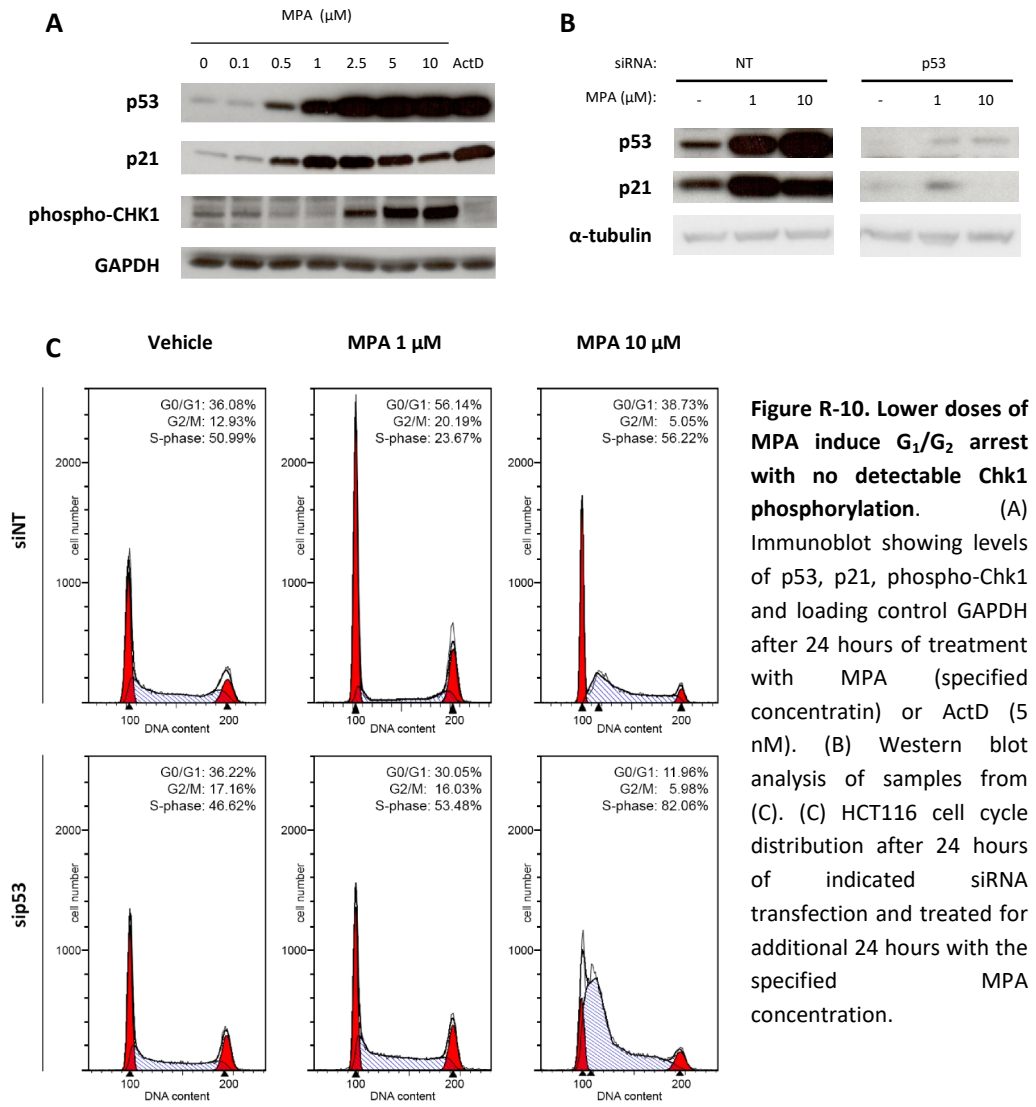

Figure R-10. Lower doses of MPA induce G_1/G_2 arrest with no detectable Chk1 phosphorylation. (A) Immunoblot showing levels of p53, p21, phospho-Chk1 and loading control GAPDH after 24 hours of treatment with MPA (specified concentratin) or ActD (5 nM). (B) Western blot analysis of samples from (C). (C) HCT116 cell cycle distribution after 24 hours of indicated siRNA transfection and treated for additional 24 hours with the specified MPA concentration.

at 1 µM MPA we observed the highest induction of p21, with no detectable Chk1 phosphorylation, suggesting no induction of the replicative stress response. Consistent with these findings, when cell cycle analyses were conducted on cells treated with 1 µM versus 10 µM MPA, we observed a strong G_1/G_2 arrest at the lower concentration, which was largely absent at the higher dose of MPA (**Figure R-10C**). This effect is p53-dependent, as cells depleted of p53 showed more cells accumulating in S phase when compared to the controls (**Figures R-10B and R-10C**). In order to elucidate whether this effect was specific to HCT116 cell line, we performed the equivalent experiment in a number of other CRC cell lines and found that the effect of 1 and 10 µM MPA was almost identical in all cases (**Figure R-11A**).

As we expected, 1 µM MPA treatment of HCT116 does not affect guanine nucleotide levels to the same extent as 10 µM MPA does (**Figures R-11C and R-11D**), arguing at this concentration we are effectively producing 5S rRNA. To test this possibility, the levels of newly synthesized 5S rRNA were measured by ^{3}H-Uridine incorporation into nascent rRNA. At 1 µM and 10 µM doses of MPA, that after 2 hours of treatment, 5S rRNA synthesis was inhibited to a much higher extent at 10 µM MPA as compared with 1 µM MPA or as compared with ActD (**Figure R-11B**). Next we determined if the reduction in nascent 5S rRNA synthesis was paralleled by a decrease in the amount IRBC complex which co-immunoprecipitated with the myc-tagged HDM2. We observed higher amounts of RPL11, RPL5 and 5S rRNA bound to HDM2 at 1 µM versus10 µM MPA (**Figures R-12A and R-12B**). These results support our hypothesis that inhibition of 5S rRNA synthesis is impairing the formation of the IRBC complex at higher doses of MPA.

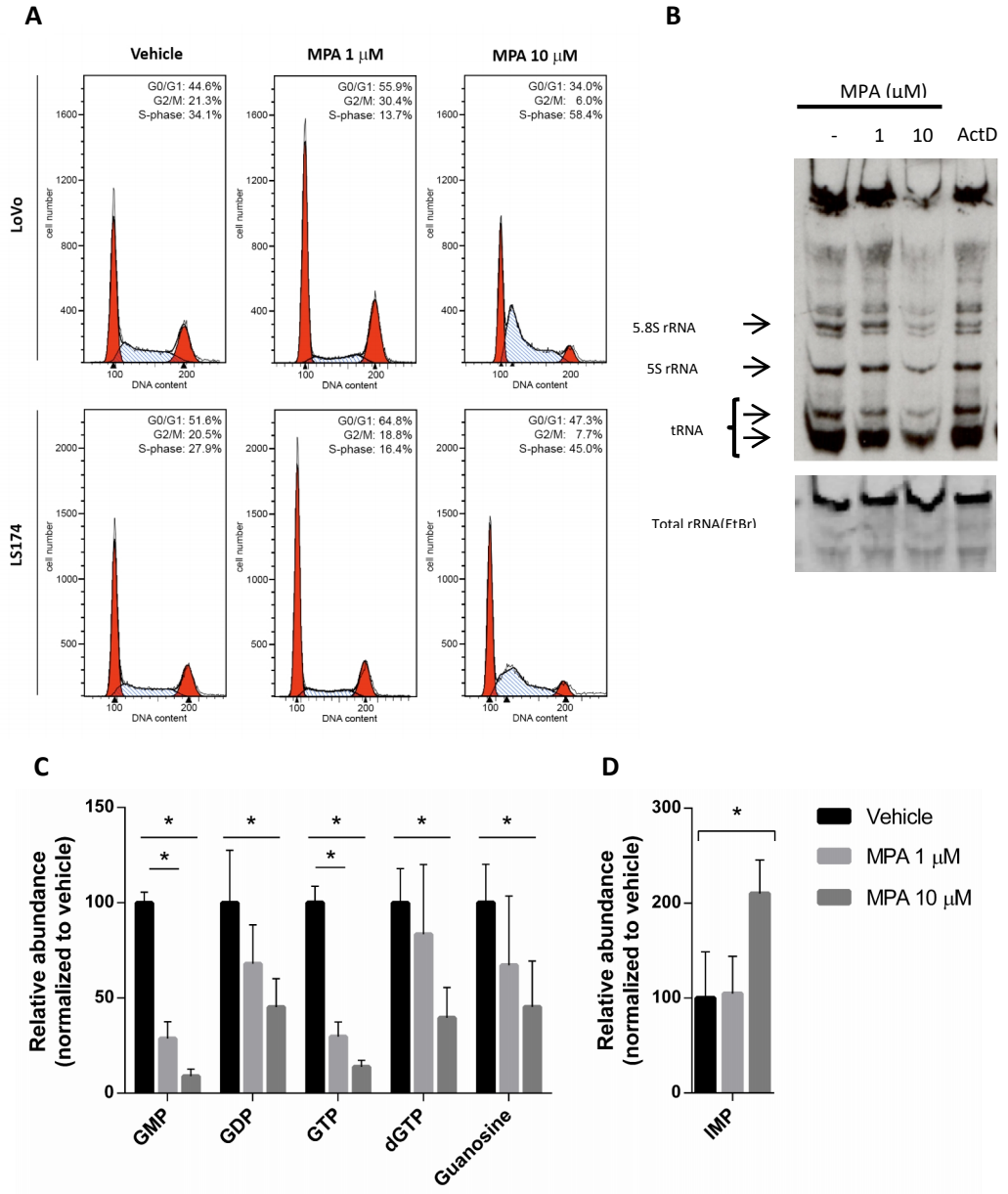

Figure R-11. MPA 1 µM effects on nucleotide pools and 5S rRNA synthesis. (A) Cell cycle profile of CRC cell lines after 24 hours treatment with either vehicle, MPA 1 µM or MPA 10 µM. Three upper pannels correspond to LoVo cell line and three bottom pannels to LS174 cell line. (B) EB-stained (down) and autoradiogram (up) of TBE-urea polyacrylamide gel loaded with HCT116 cell lysates after ^{3}H-uridine labeling and 2 hours of specified treatments. (C and D) Relative abundance of specified nucleotides with respect to vehicle-treated cells after treatment with wither MPA 1 µM or MPA 10 µM, as measured by LC-MS.

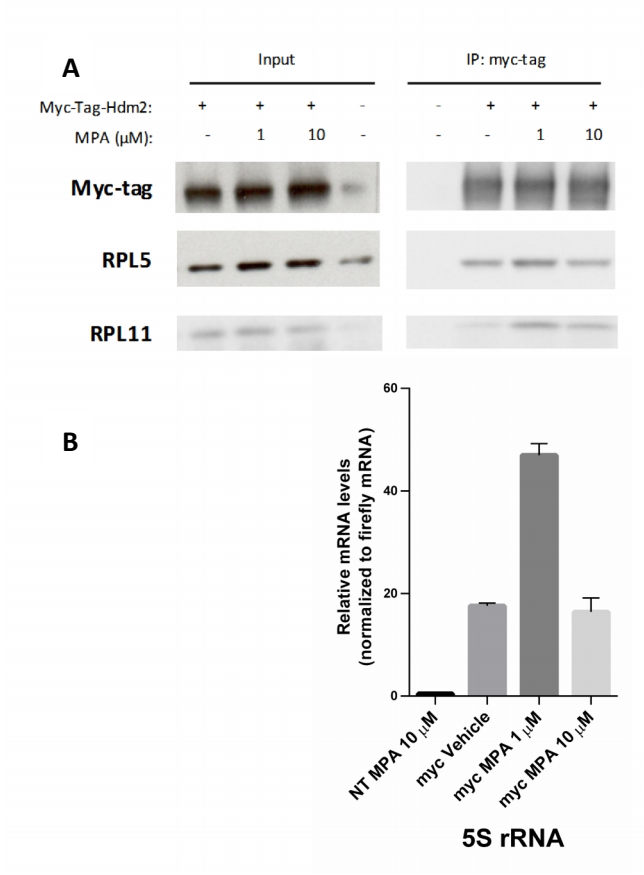

Figure R-12. Lower doses of MPA induce more IRBC complex binding to HDM2. (A) HCT116 cells were transfected with a plasmid expressing Myc-tagged HDM2 for 24 hours and then treated with different doses of MPA. Immunoblot shows levels of RPL5 and RPL11 co-immuno-precipitated with Myc-tagged HDM2 after 24 hours of indicated treatments. (B) 5S rRNA levels co-immunoprecipitated with Myc-tagged HDM2 as measured by RT-qPCR.

8. 5S rRNA complementation increases the amount of IRBC complex bound to HDM2 in 10 μM MPA-treated cells

If reduction in 5S rRNA is limiting IRBC complex formation at higher doses of MPA, we reasoned that ectopic introduction of 5S rRNA could potentially rescue complex formation. To test this we first amplified the 638 nucleotide-long sequence containing the putative transcriptional unit of human 5S rRNA gene from HCT116 cells by PCR (Sorensen et al. 1990) and then cloned the fragment containing the 5S rDNA into an expression plasmid. As expected, HCT116 cells transfected for 24 hours with increasing amounts of the 5S rRNA expressing plasmid showed increased levels of nascent 5S rRNA as measured by ^{3}H-leucine incorporation into rRNA (**Figure R-13A**). Next we asked if we could increase the amount of IRBC complex bound to HDM2 by

transfecting the 5S rRNA expressing plasmid. To do so we used a HCT116 isogenic cell line where one copy of RPL11 was fused at the N-terminus with the Venus tag. HCT116 RPL11-Venus cells were treated with vehicle, ActD 5 nM or MPA 10 µM for 24 hours. Transfection of either empty vector or 5S rRNA expressing plasmid was performed 6 hours after initiation of the treatment, with a total time of transfection of 18 hours. When comparing MPA treatments, Venus immunoprecipitation showed increased amounts of RPL5, HDM2 and 5S rRNA bound to RPL11-Venus in those cells transfected with 5S rRNA-expressing plasmid (**Figures R-13B and R-13C**). Moreover,

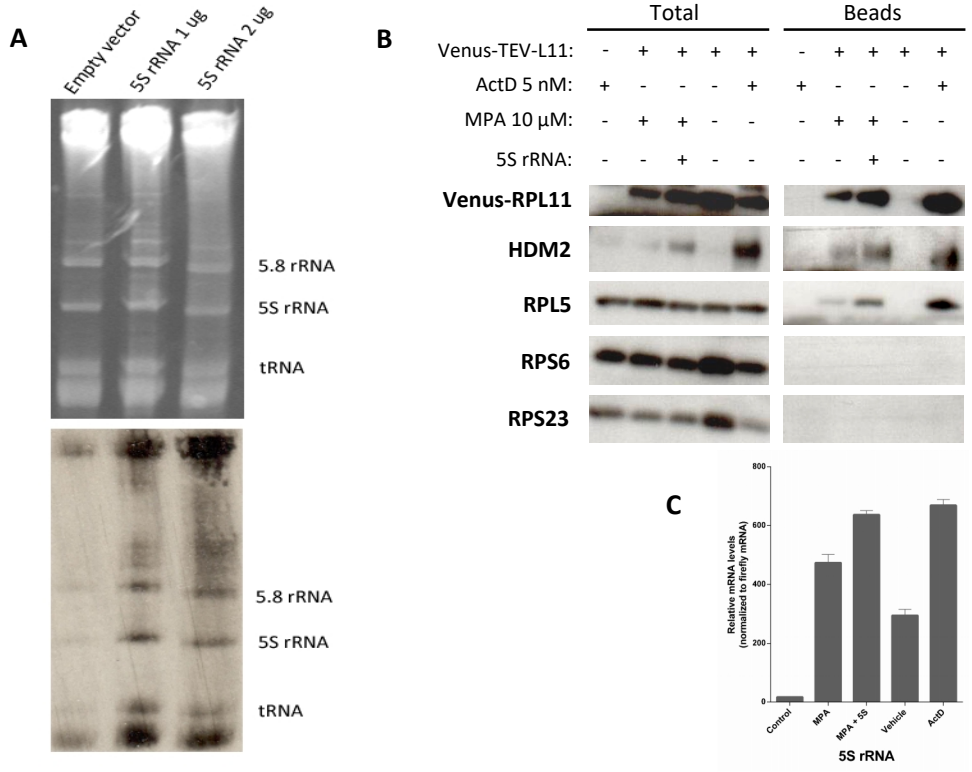

Figure R-13. 5S rRNA complementation increases levels of IRBC complex bound to HDM2. (A) EB-stained (up) and autoradiogram (down) of TBE-urea polyacrylamide gel loaded with total cellular RNA from HCT116 cells labelled with ^{3}H-uridine transfected with 5S rRNA expressing plasmid or empty vector for 24 hours (B) HCT116 RPL11-Venus (Venus-TEV-L11 +) or WT (Venus-TEV-L11 -) cells were transfected either with empty vector (5S rRNA -) or with a plasmid expressing 5S rRNA gene (5S rRNA +) 6 hours after starting treatment with indicated drugs for 24 hours. Immunoblot shows levels of RPL5, RPS6, RPS23 and HDM2 co-immuno-precipitated with RPL11-Venus. (C) 5S rRNA levels co-immunoprecipitated with Venus-RPL11 as measured by RT-qPCR.

we detected no RPS6 or RPS23, indicating that only the IRBC complex components co-immuncoprecipitated with RPL11-Venus. This result demonstrates that complementation of 10 µM MPA-treated cells with 5S rRNA increases the levels of IRBC complex bound to HDM2. Therefore, disruption of IRBC complex observed at 10 µM MPA-treated cells is due to inhibition of 5S rRNA synthesis.

9. Lack of p21 induction upon MPA treatment leads to escape from G_1 arrest

As previously shown, treatment of HCT116 cells with 10 µM MPA induced p21 at lower levels when compared to MPA 1 µM or ActD (**Figure R-10B**). Since p21 has an essential role in regulating cell cycle progression (el-Deiry et al. 1993), we hypothesized that the decreased p21 expression observed upon 10 MPA µM treatment was responsible for the escape of cells from G_1 arrest, leading to S phase entry and the replicative stress response. To determine if this was the case we took advantage of established isogenic HCT116 cell lines with disruption of p53 or p21 genes (Waldman et al. 1995; Bunz et al. 1998). Those cell lines with disrupted p53 or p21 do not arrest cell cycle at G_1/G_2 upon ActD treatment when compared to parental cells (**Figure R-14**). In the case of MPA, the S phase accumulation is even stronger when compared to parental cells (**Figure R-14**). This experiment supports the notion that lower levels of p21 induction observed at 10 µM MPA, compared to those observed with 1 µM MPA or ActD, is allowing cells to escape G_1 arrest dictated by IRBC. Since both p53 and p21 disrupted isogenic HCT116 cell lines showed similar results in terms of cell cycle distribution, the results argue that disruption of the IRBC complex formation by nucleotide imbalance is affecting p53-p21 axis, thus altering G_1 arrest induced by ribosome biogenesis impairment.

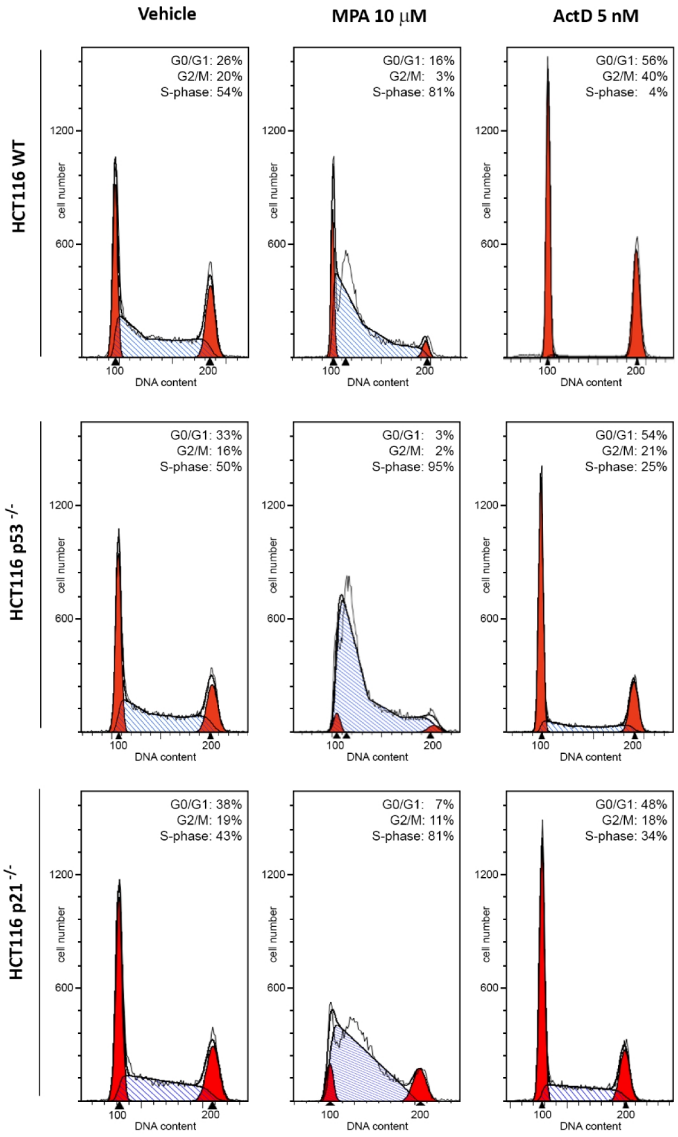

Figure R-14. p53 and p21 are key players of cell cycle arrest in MPA-treated cells. Cell cycle profiles of HCT116 parental, p53-/- or p21-/- cell lines treated for 24 hours with the indicated drugs and concentrations.

10. IRBC is a protective mechanism against replicative stress after nucleotide imbalance

MPA treatment inhibits the synthesis of 5S rRNA and this leads to disruption of IRBC complex formation, which correlates with altered p53 activity and escape of G_1 arrest and S phase entry. Eventually, this leads to the induction of the replicative stress response. According to this hypothesis, disruption of the IRBC complex should recapitulate the depletion of p53 or p21, thus allowing cells to escape G_1 arrest and enter S phase. To test this possibility we treated cells with a non-silencing siRNA (siNS) or one against RPL11, the latter to disrupt the IRBC. We then serum starved both siRNA treated cells for 16 hours to synchronize them in G_1 and then followed their progression through the cell cycle following re-addition of serum for 24 hours in the absence or presence of 10 μM MPA. Following 24 hours serum deprivation the cells in both treatment regimens were largely arrested in G_1 (**Figure R-15**). After re-addition of serum both control cells and RPL11 siRNA treated cells had moved into S phase (**Figure R-15**). The larger number of RPL11 siRNA treated cells in S phase probably reflects their slower passage through the cell cycle as a reflection of a decrease in protein synthesis rates, as we have recently reported (Teng, Mercer, et al. 2013). However, as compared to control cells RPL11 loss allowed the majority of MPA treated the cells to escape G_1 arrest and enter S phase, where they accumulated (**Figure R15**), similar to the response observed in the case of p53 or p21 loss (**Figures R-10B and R-14**). Together, these results argue the role of the IRBC acting through p53-p21 axis as a protective mechanism against S phase entry, preventing replicative stress and potential genomic instability.

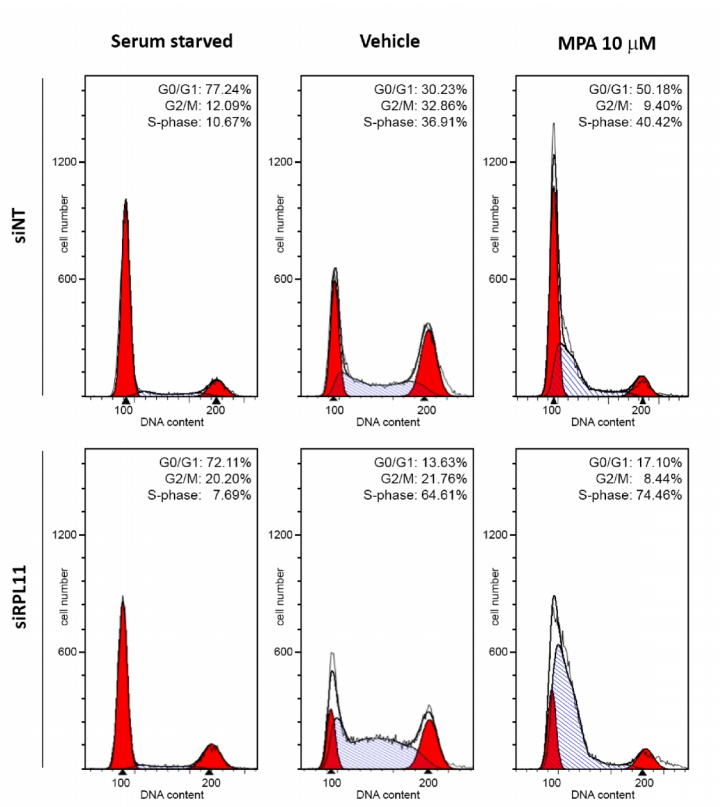

Figure R-15. IRBC complex acts as a preventive mechanism against genomic instability. Cell cycle profiles of HCT116 cells transfected with either siNT or siRPL11, then synchronized by serum starvation and re-fed with serum in presencer or absence of 10 μM MPA.

DISCUSSION

1. Nucleotide metabolism inhibition effects on p53 stabilization

One of the major hallmarks of cancer cells is the metabolic reprogramming required to sustain elevated rates of growth and proliferation. In order to fulfill high proliferation demands, cancer cells need to increase energy production as well as macromolecule biosynthesis: carbohydrates, proteins, lipids and nucleotides (Cairns et al. 2011; Heiden Vander et al. 2011). Exacerbated proliferative requirements entail increased synthesis of ribonucleotides and deoxyribonucleotides to cover the augmented proliferative demands derived from RNA and DNA synthesis (Tong et al. 2009). Cancer cells exhibit higher concentrations of nucleotides as well as of nucleotide biosynthesis (Traut 1994; Lane & W-M Fan 2015). For example, it has been shown that rather than being an energy source, glutamine in proliferating cells is used for protein and nucleotide biosynthesis as a nitrogen donor during both purine and pyrimidine synthesis (Hosios et al. 2016). In some cancers like neuroblastoma, a shunt from glycolysis and glutaminolysis to pentose phosphate pathway and nucleotide synthesis has been reported (DeBerardinis et al. 2007). Importantly, under certain biological contexts such as persistent oncogenic activation, some transcription factors have been reported to be involved in redirecting glucose and glutamine metabolism to increase flux through the pentose phosphate pathway and nucleotide biosynthesis in cancer cells (Mitsuishi et al. 2012). These studies clearly illustrate the metabolic adaptation that cancer cells undergo with the objective of reaching high rates of growth and proliferation.

The fact that cancer cells rely on high rates of purine and pyrimidine production as well as increased DNA replication rates makes them more sensitive to the inhibition of nucleotide biosynthetic pathways and DNA-damaging agents (Cheung-Ong et al. 2013). In this regard, the anti-cancer drugs hydroxyurea, methotrexate and 5-FU, commonly used in the clinic, are known to interfere with nucleotide synthesis (Madaan et al. 2012; Longley, Harkin & Johnston 2003; Gorlick et al. 1996). Nucleotide depletion usually leads to replicative stress and DDR by creating

an imbalance in the nucleotide pools that induce genetic instability, favoring errors in DNA replication (Zeman & Cimprich 2013). For instance, imbalances in the deoxynucleotide pools caused by mutations in DNA polymerase δ in CRC have been proposed as a source of infidelity during DNA replication, thus leading to potential mutations (Mertz et al. 2015). DDR induce cellular checkpoints that arrest cell cycle mainly by phosphorylation and stabilization of p53 through the action of the ATR/ATM and Chk1/Chk2 kinases (Gaillard et al. 2015). Some of the recent strategies in cancer therapy have proposed to suppress these checkpoints in order to force the cell to progress through the cell cycle to induce replicative stress and DNA damage, which would eventually lead to mitotic catastrophe and cell death (Dobbelstein & Sørensen 2015).

On the other hand, interfering with nucleotide synthesis not only would impair DNA replication by depleting deoxyribonucleotides, but also RNA synthesis by lowering the levels of ribonucleotides. In fact, in a growing cell, ribonucleotides are much more abundant than deoxyribonucleotides. Moreover, it is estimated that the energetic requirements in terms of ATP expenditure for RNA synthesis are 10-fold higher than those for DNA (Traut 1994; Lane & W-M Fan 2015). In fact, it is argued that cellular deoxyribonucleotides pools are too small to support DNA synthesis; instead, their chief role is in DNA repair. During DNA synthesis, it is reported that ribonucleotides are the source of deoxyribonucleotides without shuttling through the cellular pool of deoxyribonucleotides (Murthy & Reddy 2006). Given the observations above and that rRNA is accounts for 85% of the total cellular RNA (Lane & W-M Fan 2015), it follows that nucleotide depletion, by impairing rRNA synthesis, affects ribosome biogenesis. Importantly, nucleotide biosynthesis inhibitors such as 5-FU and MPA have been shown to decrease rRNA synthesis and to apparently elicit the IRBC (Sun et al. 2007; Sun et al. 2008; Donati et al. 2013). Similar to replicative stress or DDR activation, the IRBC response also stabilizes p53 levels, although through a different sequence of events that culminate with the inhibition of HDM2 after the binding to the IRBC complex (Donati et al. 2013). This suggests that p53 stabilization

observed after treatment with nucleotide biosynthesis inhibitors might result from two signaling “avenues”, one involving the impairment of rRNA synthesis, the other DNA replication. Importantly, it should be noted that there is cross talk between these pathways, as recent reports demonstrate that during DNA repair rRNA transcription is silenced by inhibition of RNA Pol I through the recruitment to the nucleolus of Nijmegen Breakage Syndrome protein 1 (NBS1), involved in the ATM repair pathway by Treacle (Larsen et al. 2014; Ciccia et al. 2014).

Our data clearly demonstrate that MPA impinges on rRNA biogenesis, displaying similar effects to those induced by low doses of the RNA Pol I inhibitor ActD (**Figures R-6C and R-6D**). In addition, we have demonstrated the role of the IRBC in MPA-induced p53 stabilization by immunoprecipitating the IRBC complex upon MPA treatment and showing its increased association with HDM2 (**Figures R-7A and R-7B**). We have previously demonstrated that p53 stabilization induced by RP depletion is completely rescued by co-depletion of any of the components of the IRBC complex (Fumagalli et al. 2009; Fumagalli et al. 2012; Donati et al. 2013). However, depletion of protein components of the IRBC in MPA treated cells only partially restores p53 levels to basal levels (**Figure R-3A**). Addition of MPA to HCT116 cells previously co-depleted of one RP other than RPL5 or RPL11, and one component of the IRBC complex also fails to restore p53 to basal levels (**Figure R-3C**). Taken together these results suggested that in addition to IRBC, parallel response(s) might be involved in regulating p53 levels upon MPA treatment. We sought to better understand the replicative stress response and DDR following MPA administration, in light of the previous studies reporting activation of these pathways following nucleotide imbalance (Zeman & Cimprich 2013; Liu et al. 2008). Phosphorylation of both p53 serine 15 and Chk1 serine 345 in parallel to the slower rate of DNA synthesis observed after MPA treatment suggested the activation of replicative stress response as a potential parallel response regulating MPA-induced p53 stabilization (**Figures R-4A and R-5A**). In preliminary studies from our laboratory, inhibition of Chk1 and ATR by both pharmacological and genetic means

in MPA-treated cells did not completely rescue p53 protein levels (data not shown); however, this line of research will require further development.

Several mechanisms involved in regulating p53 stabilization following nucleotide imbalance have been reported in the literature. HCT116 displayed p53 stabilization following deprivation of the amino acids serine and glycine, essential precursors of the *de novo* nucleotide biosynthesis (Maddocks et al. 2013). In the report by Maddocks et al, p53 stabilization was argued to be AMPK dependent due to the imbalance in adenosine nucleotides caused by serine and glycine starvation (Maddocks et al. 2013). However, our data do not demonstrate significant effect of MPA on adenine nucleotides (**Figure R-1C**) or alteration of AMPK activity and Acetyl-CoA Carboxylase (ACC) phosphorylation (data not shown). On the other hand, GMPS, the enzyme that carries out the conversion from XMP to GMP, has been argued to translocate to the nucleus and bind to USP7, with the ensuing complex binding directly to p53 and inducing its stabilization in U2OS cells following DDR activation by etoposide or hydroxyurea (Reddy et al. 2014). Reddy et al also reported a similar response, though weaker, upon DDR caused by MPA (Reddy et al. 2014). However, depletion of GMPS was not effective in rescuing p53 stabilization induced by MPA treatment in HCT116 cells (data not shown), consistent with the fact that we do not observe a DDR following MPA treatment, as measured by the failure to Chk2 or γ-H2AX phosphorylation. It could be argued that the response is not as pronounced as that we observed for etoposide, we did not detect GMPS-USP7 or GMPS-p53 binding in MPA treated HCT116 ectopically transfected with HA-tagged USP7 and GMPS (data not shown). The results of these experiments suggest either a cell-line specific response or most likely the fact that we fail to induce a DDR in MPA-treated HCT116 cells.

Nucleotide depletion induced by MPA is due to IMPDH inhibition. There are two different isoforms of the enzyme, IMPDH1 and IMPDH2, which share 84% of the sequence identity and show no differences in catalytic activity, although their

expression differs amongst different tissue types. Moreover, IMPDH2 expression increases in non-differentiated proliferating tissues, decreases upon differentiation and is a direct target of c-Myc (Thomas et al. 2012). IMPDH has been described to have extra-catalytic functions. For instance, in *Drosophila melanogaster*, which contains one isoform of the enzyme, it has been reported that IMPDH acts as a transcription factor, which translocates to the nucleus under conditions of nucleotide depletion and binds to CT-rich regions, attenuating the expression of E2f genes thus acting as a repressor of cell proliferation (Kozhevnikova et al. 2012). It also has been demonstrated that IMPDH1 and IMPDH2 cluster into ring-shaped structures nearby the nucleus upon guanine nucleotide imbalance induced by MPA treatment (Ji et al. 2006). The function of IMPDH1/2 enzyme clustering upon nucleotide imbalance is not known. However, the fact that R224P mutation in the ATP-binding domain of IMPDH1 reduces its clustering capacity suggests that this aggregation might be involved in response to metabolic challenges. Although the R224P mutation does not affect catalytic activity of the enzyme, it has been shown to cause retinitis pigmentosa in humans (Thomas et al. 2012), suggesting a critical role of IMPDH clustering capacity in maintaining homeostasis in retina cells. Finally, it is noteworthy that IMPDH2 has been shown to immunoprecipitate together with GMPS, USP7 and p53 following etoposide treatment (Reddy et al. 2014), indicating a potential role of IMPDH2 in p53 stabilization upon DNA damage. These studies suggest extra-catalytic functions of IMPDH1 and IMPDH2. We have found IMPDH2 nuclear translocation and ring clustering upon MPA treatment in HCT116 cells (data not shown). Thus it is possible, by as yet unknown mechanisms, some of these IMPDH effects are implicated in regulation of p53 through a parallel response to that of the IRBC. Therefore these data may imply a dual function of nucleotide biosynthetic enzymes and a direct regulation of cellular processes following nucleotide depletion. We are currently developing stable cell lines expressing shRNAs against IMPDH1 and IMPDH2, which will be useful in order to directly assess the role of IMPDH1 and IMPDH2 in the MPA-induced p53 response.

Our studies describe the central role of IRBC in regulating p53 stabilization upon ribosome biogenesis impairment by MPA treatment. However, they also suggest, as stated above, that potential parallel mechanisms could be involved as well in p53 regulation when generation of new ribosomes is impeded by nucleotide depletion. Our data broaden the understanding of p53 stabilization after ribosome biogenesis impairment and nucleotide depletion. A better comprehension of the different checkpoints activated upon drug treatment could be beneficial to improve current treatment of p53-WT c-Myc-driven cancers and to develop new therapeutic strategies by activating or suppressing those checkpoints.

2. 5S rRNA has a central role in IRBC activation

The results of our studies demonstrate that nucleotide depletion induced by MPA affects ribosome biogenesis and elicits the IRBC. As stated before, we observed a comparable impact on ribosome biogenesis in ActD- and MPA-treated cells in terms of inhibition of protein synthesis (data not shown) and rRNA synthesis (**Figures R-6C and R-6D**). Immunoprecipitation experiments showed similar amounts of IRBC complex components bound to HDM2 after 6 hours treatment of either MPA or ActD (**Figure R-6A**), a time when we begin to detect the first increase in p53 levels (**Figure R-2A**). However, as compared to control cells, lower amounts of the IRBC complex were found to bind HDM2 after 24 hours treatment (**Figures R-7A and R-7B**), suggesting that sufficient amounts of new IRBC complex cannot be generated to silence the increasing levels of HDM2 driven by rise in p53. This observation would be consistent with earlier results from our laboratory and others, which showed it is the nascent IRBC complex which is critical in maintaining inhibition of HDM2 (Bursac et al. 2012; Donati et al. 2013). Bursac et al came to this conclusion by finding that the inhibition of the newly translated RPL5 and RPL11 by cycloheximide blocked the induction of p53 stabilization induced by ActD treatment (Bursac et al. 2012). In parallel, our laboratory set out to determine the role of 5S rRNA in mediating this response (Donati et al. 2013), given that in yeast a pre-ribosomal RPL5/RPL11/5S rRNA complex is incorpated

into the the nascent 60S ribosomes (Zhang et al. 2007) and the results from Levine and colleagues who had shown that ectopically expressed HDM2 interacted with 5S rRNA and RPL5 (Marechal et al. 1994). That it was the nascent complex was derived from two observations. First, the inhibition of nascent 5S rRNA synthesis by depletion of TFIIIA blocked the induction of p53, but had no impact on total 5S rRNA; and second, depletion of hRRS1 and BXDC1, required for assembly of the RPL5/RPL11/5S rRNA complex into the nascent 60S ribosome, induced p53 stabilization (Donati et al. 2013). Together, these two observations argued that it was the nascent RPL5/RPL11/5S rRNA complex that inhibited HDM2 and that the point of bifurication to the binding of HDM2 resided upstream of its assembly into the 60S ribosome.

Recently, the source of the pre-ribosomal RPL11-RPL5-5S rRNA complex that binds to HDM2 upon ribosome biogenesis impairment was challenged (Onofrillo et al. 2017). As stated above our results and those of Bursac et al (Bursac et al. 2012) support the hypothesis that it is the nascent IRBC complex, which upon ribosome biogenesis impairment is redirected to the binding and inhibition of HDM2, the one that maintains the IRBC response active after insults in ribosome biogenesis. Onofrillo et al argued instead it was a pre-existing pool of 5S rRNA essential for inducing p53 stabilization after ribosome biogenesis inhibition (Onofrillo et al. 2017). However, immunoprecipitation experiments of pulse-chase labeled rRNA showed the presence of nascent 5S rRNA in IRBC complex (Onofrillo et al. 2017), indicating that 5S rRNA was still produced and incorporated into the nascent complex. This was probably due to the incomplete 5S rRNA neosynthesis suppression as shown by ^{3}H-Uridine pulse-chase experiments (Onofrillo et al. 2017). Moreover, immunoprecipitation experiments were performed from total cell lysates (Onofrillo et al. 2017), thus potentially including contamination from mature ribosomes, which should have been tested by carrying out PCR analyses for the presence of other rRNA species. Although 5S rRNA and RPL5 are in 2-fold excess in the nucleoli with respect to the rest of RPs and rRNA (Knight & Darnell 1967; Phillips & McConkey 1976; Rinke et al. 1982), this is a minimal pool and would not account for the ability of cycloheximide or rapamycin, the latter which

blocks the translation of 5'TOP mRNAs, to inhibit the induction of the IRBC (Bursac et al. 2012). Our data demonstrates that new IRBC complex formation is necessary to bind presumably increasing amounts of HDM2 and sustain IRBC response over a 24 hour period. This is supported by two facts: (I) levels of IRBC complex co-immunoprecipitated with HDM2 are decreased after 24 hours of 10 µM MPA treatment with respect to ActD or 1 µM MPA treatments (**Figures R-7A, R-7B, R-12A, R-12B**); and (II) 5S rRNA complementation by ectopic expression increase the levels of IRBC complex in 10 µM MPA-treated HCT116 cells with respect to those cells transfected with the empty vector (**Figures R-13B and R-13 C**). Hence, the results of these experiments together support the concept that the nascent IRBC complex is essential for maintaining p53 response over time after disruption of ribosome biogenesis.

Unlike what we observed in ActD-treated cells, 10 µM MPA treatment induced lower levels of p21 and S phase accumulation (**Figures R-5B and R-8B**). Here we show that the incorporation of ^{3}H-uridine into nascent 5S rRNA is completely abolished after 6 hours of MPA treatment, whereas there is little impact with ActD (**Figure R-6D**). This observation is consistent with the fact that low doses of ActD inhibit RNA Pol I, but not RNA Pol III (Perry & Kelley 1970). We hypothesized that 5S rRNA depletion induced by MPA would impair IRBC complex formation. Combination of 10 µM MPA and ActD showed similar phenotypes in terms of p53 transcriptional activity, p21 induction and cell cycle profile to those induced by 10 µM MPA treatment alone (**Figures R-8A, R-8B, R-9A, R-9B**). This dominance of MPA treatment over ActD is consistent with a lack of 5S rRNA induced by nucleotide imbalance. It is also compatible with the data obtained at the lower dose of MPA, where we observed in HCT116 cells higher levels of p21 and increased proportion of cells arrested in G_1/G_2 (**Figures R-10A, R-10B, R-10C**). In addition, the amount of IRBC complex bound to HDM2 after 1 µM MPA treatment is higher when compared to 10 µM MPA (**Figure R-12A, R-12B**). This can be explained by the fact that at lower doses of MPA a nucleotide imbalance is created that leads to inhibition of rRNA synthesis and the induction of the IRBC. However, the insult in

nucleotide biosynthesis induced by 1 µM MPA is not severe enough to inhibit 5S rRNA synthesis. Importantly, pulse labeling experiments with ^{3}H-uridine incorporation in 10 µM MPA-treated HCT116 cells showed that 5S rRNA synthesis was strikingly inhibited, whereas there was little change at 1 µM MPA treatment conditions (**Figure R-11B**). Thus, differential response elicited by different doses of MPA might be explained by the availability of newly synthesized 5S rRNA required to generate new IRBC complex.

More importantly, the findings above support the hypothesis that one of the first insults sensed by the cell after nucleotide depletion is rRNA synthesis impairment. When this occurs, IRBC is elicited and IRBC complex inhibits HDM2 thus inducing p53 stabilization, which in turns arrests cell cycle at G_1 and prevents DNA replication. However, if the nucleotide depletion is severe enough to inhibit 5S rRNA synthesis, the IRBC cannot be executed properly and cells overcome this barrier by entering in S phase where they encounter replicative stress due to the nucleotide imbalance induced by 10 µM MPA. This is supported by the fact that no Chk1 phosphorylation is observed when cells are treated with 1 µM MPA (**Figure R-10A**). Importantly, our complementation experiments suggest that 5S rRNA is the limiting factor in IRBC complex formation upon nucleotide imbalance, as the levels of IRBC complex appear to be partially restored by ectopic expression of 5S rRNA in cells treated with 10 µM MPA (**Figures R-13B and R-13C**). In this regard, it will be critical to determine whether increasing the amount of IRBC complex by 5S rRNA complementation, would also increase p21 protein levels and rescues G_1/G_0 arrest after 10 µM MPA treatment.

Previous studies conducted in a variety of cell lines reported that the same dose of a given inhibitor of nucleotide biosynthesis induces either G_1 or S phase arrest in a cell line-dependent manner (Linke et al. 1996). Moreover, experiments conducted in U2OS cells showed that 12 hours of 10 µM MPA treatment induced G_1 arrest instead of S phase accumulation (Sun et al. 2008). On the other hand, our experiments conducted in HCT116 and four additional CRC cell lines (data partially shown in **Figure R-11A**) show equivalent cell cycle profiles, such that they are not dependent on the

cell line but on the MPA dose (**Figures R-10B and R-11A**). This discrepancy among different cell lines in terms of cell cycle profile suggests that the cell cycle arrest induced by MPA treatment might be cell line or tissue-specific. However, it cannot be discarded that increasing the dose of nucleotide inhibitors could potentially induce S phase accumulation in those cell lines reported to be arrested at G_1. That would be consistent with 5S rRNA as the limiting factor in nucleotide depletion-induced IRBC. For instance, the cell proliferation rate and thus the rate of 5S rRNA synthesis might vary among different cell lines. Those cells with higher rates of cell proliferation, generating more ribosomes, would be consuming greater amounts of nucleotides, such that 5S rRNA becomes more rapidly limiting under nucleotide imbalance conditions. Therefore, each cell line might have a specific threshold above which the 5S rRNA synthesis would be impeded. Given the fact that guanine ribonucleotides account for more than 30% of the 5S rRNA sequence it can be argued that specific guanine nucleotide synthesis inhibitors such as MPA might suppress 5S rRNA synthesis more rapidly due to stoichiometric imbalance. In this regard, it would be interesting to elucidate whether nucleotide depletion induced by inhibition of other nucleotide synthesis pathways, such as pyrimidine synthesis, would lead to the same response in terms of IRBC response disruption induced by 5S rRNA depletion and dose-dependent G_1 arrest. Finally, the potential influence of cell type and/or proliferation rate on IRBC disruption by nucleotide imbalance might be taken into account also in non-oncogenic scenarios. A dysfunctional regulation of nucleotide pools could alter IRBC response and sensitize cells to genomic instability and potential mutation of the DNA. In fact, nucleotide deficiency has been shown to induce genomic instability at early stages of specific cancer development (Bester et al. 2011). This might be crucial in human disease like ribosomopathies or tumorigenesis.

In agreement with previous studies from our laboratory (Donati et al. 2013) and others (Sloan et al. 2013), 5S rRNA complementation experiments have confirmed that it is an essential component of the IRBC complex and the limiting factor for a proper IRBC execution upon ribosome biogenesis impairment induced by nucleotide

depletion. With the aim of demonstrating that IRBC depletion induced by inhibition of 5S rRNA neosynthesis is the cause of decreased p21 induction and S phase accumulation observed upon nucleotide imbalance, we are currently complementing 10 µM MPA-treated HCT116 cells with 5S rRNA. We expect to (I) restore p53 transcriptional activity, (II) induce G_1 arrest and (III) higher p21 protein levels in those cells treated with 10 µM MPA and complemented with 5S rRNA.

3. IRBC as a preventive mechanism against genomic instability upon nucleotide imbalance

Genomic integrity preservation is essential for a cell to survive and proliferate. Several cellular mechanisms have evolved to prevent DNA replication under unfavorable conditions. The tumour suppressor p53, also known as the guardian of the genome, acts as one of the main barriers against potential DNA damage. To do so, p53 is stabilized upon a variety of insults in order to initiate a cellular response that will lead to cell cycle arrest or apoptosis in case the damage is not reparable. Induction of cell cycle arrest at G_1 phase through p21 activation is one of the main mechanisms to prevent genomic instability and potential DNA damage by stopping cell cycle before DNA replication (Levine 1997; Vogelstein et al. 2000). Our results show that ribosome biogenesis disruption caused by nucleotide depletion or other means such as RNA Pol I inhibition by ActD induced G_1/G_2 arrest (**Figures R-5B and R-10C**). However, if the nucleotide depletion affects 5S rRNA synthesis, the IRBC complex cannot be properly formed and cells escape the G_1 arrest and leak into S phase (**Figure R-10C**), where they encounter replicative stress due to nucleotide imbalance (**Figure D-1**).

We have demonstrated that the G_1 arrest induced by ribosome biogenesis impairment is p53- and p21-dependent, since depletion of either gene leads to S phase accumulation in the presence of insults that induce G_1 arrest such as ActD treatment or 1 µM MPA treatment (**Figure R-14**). Moreover, and consistent with a p53- and p21-dependent response, depletion of p53 or p21 in the presence of 10 µM

MPA increases the proportion of cells that accumulate in S phase (**Figures R-10C and R-14**). We hypothesized that disruption of the IRBC response caused by 5S rRNA synthesis inhibition leads to altered p53 activity towards p21. Insufficient p21 induction after ribosome biogenesis impairment would lead to inefficient G_1 arrest, thus permitting cells to pass to S phase. The fact that IRBC complex depletion induced by 10 μM MPA treatment affects p53 activity but not stability suggest a potential role of the IRBC complex in regulating p53 transcriptional activity and not only stability. Critically, the IRBC complex has been shown essential for HDM2 sequestering to the nucleolus upon different types of insults, including ribosome biogenesis impairment (Bernardi et al. 2004; Bursac et al. 2012), suggesting a critical role of IRBC complex localization in p53 stabilization and activation. We have shown that some p53 targets like p21 or HDM2 present lower levels of induction after 10 μM MPA treatment with respect to ActD (**Figure R-9B**), which would be consistent with a defect in IRBC formation. However, unlike p21 or HDM2, other targets such as TP53I3 and BTG2 showed a similar increase after treatment with 10 μM MPA, ActD or combination of both (data not shown). This together with comparable levels of p53 stabilization between ActD and MPA treatments might be indicating that nucleotide imbalance leads to alterations in p53 transcriptional activity without significative effects on p53 stabilization. The differential transcriptional activity observed with different insults to ribosome biogenesis in IRBC-driven p53 stabilization might suggest that the repertoire of genes activated upon ribosome biogenesis lesion could be specifically tailored to specific types of stress. Therefore, it would be critical to characterize (I) the dynamics of the IRBC complex upon ribosome biogenesis impairment induced by nucleotide imbalance; and (II) the potential transcriptional activity of IRBC complex depending on the kind of insult. Addressing these questions would be essential to further understand the p53 stabilization upon ribosome biogenesis impairment.

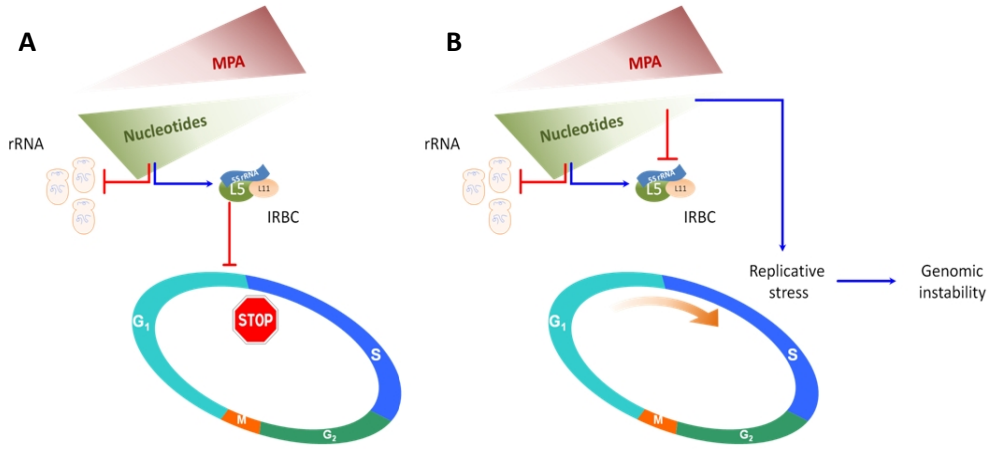

Figure D-1. The IRBC acts as a preventive mechanism against genomic instability. (A) Nucleotide depletion inhibits rRNA synthesis and elicits IRBC, which arrest cell cycle at G1 by activating p53-p21 axis. (B) Higher doses of MPA inhibit the synthesis of nascent 5S rRNA impeding the formation of nascent IRBC complex and causing G_1 arrest escape and S phase accumulation. DNA replication under conditions of imbalanced pools of nucleotides leads to replicative stress and potential genomic instability.

HCT116 cells treated with 10 µM MPA present defective p21 response when compared to cells treated with ActD despite similar levels of p53 induction (**Figures R-8B**). Given the fact that p21 is a major regulator of cell cycle, our hypothesis is that the differences observed in cell cycle profiles are due to p21 levels. Consistently, p21-disrupted HCT116 cells showed increased proportion of cells in S phase in all the treatments when compared to parental cells (**Figure R-14**). Previous studies had shown p21-deficient response after induction of p53 by hydroxyurea treatment in HCT116 cells (Gottifredi et al. 2001). Hydroxyurea decreases the levels of deoxynucleotides by inhibiting ribonucleotide reductase (RNR), suggesting that blocking DNA synthesis leads to decreased activity of p53 towards p21. Later studies demonstrated that the diminished p21 response induced by hydroxyurea is due to a defect in the elongation of p21 mRNA during transcription (Mattia et al. 2007). We cannot discard a p53-independent effect on p21 due to an impaired DNA replication.

Nevertheless, a potential mechanism regulating p21 after DNA replication would be elicited during S phase, which is compatible with a G_1 arrest escape triggered by depletion of 5S rRNA.

Previous experiments from our laboratory demonstrate that cells depleted of RPL11 or RPL5 proliferate slower than controls due to a decreased protein synthesis. Unlike RPL7a-depleted cells, which arrest in G_1/G_2 due to IRBC triggering, they do not elicit any obvious cell cycle checkpoint (Teng, Mercer, et al. 2013). Importantly, our data demonstrates that in conditions of disrupted ribosome biogenesis, depletion of IRBC complex increases the proportion of cells in S phase. RPL11-depleted HCT116 cells showed increased S phase accumulation when treated with both 1 and 10 µM MPA compared to parental controls (**Figure R-15**), similarly to p53- and p21-deficient cells (**Figure R-14**). The result of this experiment suggests that IRBC acts as a preventive mechanism against potential genomic instability by regulating p53. Consistent with a potential role as a barrier against genomic instability, the IRBC has been reported to play a role in tumorigenesis. For instance, *Eμ-Myc* mice carrying the mutation C305F in MDM2, which is characterized by the inability to bind to RPL11, were shown to succumb earlier to lymphoma (Macias et al. 2010). Similarly, the same mutation has been related to early appearance of tumours in the small intestine of *Apc$^{+/min}$ mice* (Liu et al. 2016). The role of IRBC in preventing tumorigenesis in an oncogene-driven scenario like c-Myc amplification suggests that deregulated ribosome biogenesis could act as a source of genomic instability.

Some ribosomopathies such as DBA are characterized by bone marrow failure and an increased susceptibility to cancer development later in life. Zebrafish with heterozygous mutations in RPs were shown to develop a rare type of tumours, malignant peripheral nerve sheath tumours (MPNST) (Amsterdam et al. 2004). Other studies have reported activation of ATR/ATM-Chk1/Chk2 pathway and upregulation of nucleotide biosynthesis pathway in hematopoietic cells from heterozygous RPS19 and RPL11 mutant embryos of zebrafish. The anemic phenotype was ameliorated by

exogenous supply of nucleotides, suggesting nucleotide imbalance and genomic instability induced by ribosome biogenesis impairment (Danilova et al. 2014). Accordingly, unpublished data from our laboratory showed that hematopoietic cells from heterozygous knock-out mice for *Rps6* have increased phosphorylation of γ-H2AX. Since ribosome biogenesis and nucleotide synthesis are coupled by PRPS2 enzyme (Cunningham et al. 2014), it is not unexpected that deregulation of one of the two processes would affect the other one. Chronic impairment of ribosome biogenesis might lead to compensatory overexpression of ribosome biosynthesis-related factors or potential loss of stoichiometry among ribosomal components including nucleotides, which will induce nucleotide imbalance and genomic instability.

4. Ribosome biogenesis disruption in cancer therapy

Many drugs used as chemotherapeutic treatment in cancer patients are known to interfere with ribosome biogenesis (Burger et al. 2010). Drugs like 5-FU or oxaliplatin, which have been described to impede ribosome biogenesis (Sun et al. 2007; Bruno et al. 2017), are widely used to treat different types of tumours. Importance of ribosome biogenesis as a clinical target is underscored by the fact that new drugs specifically designed to attack ribosome biogenesis are currently in clinical trials to test its efficacy on cancer patients (Bywater et al. 2012; Drygin et al. 2009). In fact, ribosome biogenesis impairment might be a good strategy in the treatment of p53 WT tumours with high rates of ribosome biogenesis, such as c-Myc-driven tumours.

We have identified 5S rRNA as a central molecule in driving cell cycle arrest and how nucleotide depletion can impede IRBC complex formation by hampering 5S rRNA *de novo* synthesis. Importantly, our data also suggest an essential role of IRBC in preventing genomic instability by regulating p53-p21 axis. A better understanding of the cross-talk between cellular checkpoints elicited upon ribosome biogenesis impairment and/or nucleotide synthesis depletion might be useful in the development

of therapeutic strategies in tumours with high rates of ribosome biogenesis such as c-Myc-driven cancers. For instance, some authors propose inhibition of Chk1, which drives replicative stress response, in order to lose the checkpoint and increase DNA replication initiation and potential DNA damage (Zhou & Bartek 2004; Toledo et al. 2011; Dobbelstein & Sørensen 2015). Similarly, IRBC complex depletion would induce the loss of IRBC upon ribosome biogenesis impairment, which could potentially lead to increased genomic instability and DNA damage. Therefore, gaining knowledge in how different cellular checkpoints are elicited could give us the possibility to either enhance or suppress them in order to develop new clinical strategies and improve the efficacy of anti-cancer chemotherapy.

Regarding cancer therapy, a better understanding of the mechanism of action of nucleotide biosynthesis inhibition in terms of ribosome biogenesis impairment, p53 stabilization and cell cycle control could be useful in the treatment of p53 WT c-Myc-driven tumours. An *in vivo* characterization of our data would be essential to find new cancer strategies for ribosome biogenesis and nucleotide synthesis inhibitors. Genetic depletion models of different nucleotide synthesis enzymes or proteins related to ribosome biogenesis would be very useful in this sense. The genetic approach would be particularly interesting to study the effect of inhibition of other nucleotide biosynthetic pathways like pyrimidine synthesis pathway. Elucidating whether the IRBC response disruption observed in MPA-treated cells is something specific of purine biosynthesis inhibition or, on the contrary, it is a response elicited by nucleotide imbalance in general, might have significant implications in cancer therapy. Finally, exploring the potential modulation of IRBC *in vivo* as a tool to control cell cycle distribution in order to sensitize cells to specific drugs could have potential applications as a clinical strategy.

CONCLUSIONS

1. Nucleotide depletion elicits the IRBC by inhibiting rRNA synthesis and induces p53 stabilization, although our data suggest that parallel responses might be activated as well.

2. Nascent IRBC complex is necessary to maintain p53 activity upon ribosome biogenesis impairment.

3. High doses of MPA inhibit 5S rRNA *de novo* synthesis and disrupt IRBC complex formation.

4. 5S rRNA complementation of MPA-treated cells restores the formation of the IRBC complex.

5. 5S rRNA is an essential component of the IRBC complex like RPL11 and RPL5 and it is the limiting factor in IRBC complex formation upon nucleotide imbalance.

6. IRBC inhibition induced by nucleotide imbalance alters p53 activity without affecting p53 stabilization.

7. Defective IRBC response caused by nucleotide imbalance leads to S phase accumulation instead of G_1 arrest, which leads to replicative stress response activation.

8. IRBC prevents potential genomic instability under nucleotide depletion conditions.

MATERIALS AND METHODS

Cell Culture and solutions

HCT116 human colorectal carcinoma cell line was obtained from the American Type Culture Collection and maintained in Dulbecco's modified Eagle medium (DMEM) supplemented with 10% heat-inactivated fetal bovine serum (Sigma-Aldrich, St Louis, MO, USA). Isogenic HCT116 cells disrupted for p53 or p21 expression were kindly provided by Dr Vogelstein's lab (The Johns Hopkins University of Medicine, Baltimore, MD, USA) and maintained under the same conditions described above for parental line. The rest of the cell lines used in our studies (LoVo and LS174) were obtained from the American Type Culture Collection and maintained under the same conditions explained above. Venus-RPL11 HCT116 isogenic cell line was prepared by CRISPR-Cas9 targeting technology by Drs Sandra Menoyo and Antonio Gentilella. Briefly one allele of RPL11 was modified with a targeting construct that generated a knocked-in allele encoding a fusion protein constituted by a Venus moiety fused to the N-terminus of RPL11. The targeting event was confirmed at the genomic level and cells were subsequently biologically characterized for Venus-RPL11 expression, incorporation into the 60S subunit and in polysomes, nucleolar localization upon IRBC-activating stimuli (ActD, MPA, RP depletion, 5-FU).

Reagents and plasmids

MPA was purchased from Sigma (Sigma-Aldrich, St Louis, MO, USA) and was dissolved in methanol. Both actinomycin D and etoposide were purchased from Sigma (Sigma-Aldrich, St Louis, MO, USA) and were dissolved in DMSO. Cycloheximide was purchased from Sigma (Sigma-Aldrich, St Louis, MO, USA) and dissolved in methanol. Transfection reagents lipofectamine RNAimax (for siRNA transfection) and lipofectamine 2000 (for plasmid transfection) and TRIzol RNA extraction reagent were purchased from Invitrogen (Carlsbad, CA, USA). Transfection was performed according to manufacturer's instructions. EN^{3}HANCE autoradiography enhancer and ^{3}H-Uridine were purchased from Perkin-Elmer. The protein assay kit was purchased from Pierce

(Rockford, IL, USA). The antibodies used are listed in table M-1. MagnaCHIP Protein A/G magnetic beads mix was from Millipore (Billerica, MA, USA). GFP-Trap beads were from ChromoTek GmbH (Planneg-Martinsried, Germany). Random hexamers and M-MLV Reverse transcriptase were from Invitrogen (Carlsbad, CA, USA). The SYBR Green kit was purchased from Roche (Basel, Switzerland). The Dual Luciferase kit was purchased from Promega (Madison, WI, USA). BamHI and BglII restriction enzymes and T4-DNA Ligase were purchased from New England Biolabs (Ipswich, MA, USA). Taq DNA Polymerase was purchased from Invitrogen (Carlsbad, CA, USA). The sequences of siRNAs used in the experiments, siRPL5, siRPL11, siRPL7a, sip53, and siNS are reported in **Table M-2**. For each treatment the amount of siRNA transfected was maintained constant between samples, by using siNS where required. pcDNA 3.1 (Addgene plasmid V790-20) and PG13-luc plasmids (wt p53 binding sites) (Addgene plasmid #16442) for luciferase activity assay were was obtained from Addgene (Cambridge, MA, USA).

Protein analysis

Cell protein extracts for western blot analysis were prepared by using a RIPA buffer (1% SDS lysis buffer (Tris pH7.4 50mM, SDS 1%) supplemented with the protease inhibitor cocktail (SIGMA), phosphatase inhibitor cocktail 3 (SIGMA) and Protease inhibitor (Roche). After lysis, cell lysates were incubated 30' on ice followed by centrifugation at 13,000 rpm for 10 minutes. Protein concentrations were determined for supernatants by the BCA assay (Pierce). 30 µg of total protein extracts were resuspended in protein loading buffer (Tris.HCl 375 mM, SDS 9%, glycerol 50% and bromophenol blue) and after treatment at 95 ^{o}C for 5 minutes, proteins were separated on 10% SDS–polyacrylamide gels by electrophoresis, and transferred to PVDF membranes. Blots were stained with amido black solution (0.1% Amido Black 10B dye, 10% acetic acid, 25% isopropanol) to confirm equal loading and transfer of proteins and then reacted with the western blots probed with the indicated antibodies (see **Table M-1**). Immunoblots were developed using secondary horseradish

peroxidase-coupled antibodies (Polyclonal swine anti-rabbit and polyclonal rabbit anti-mouse, Agilent, CA, USA) and an enhanced chemiluminescence kit (GE Healthcare).

Real-time PCR

Total cellular RNA was isolated using TRIzol reagent (Invitrogen) according to the manufacturer's instructions. cDNA was obtained from RNA by using random hexamers and M-MLV Reverse Transcriptase from Invitrogen following manufacturer's instructions. Quantitative PCR analysis was performed in triplicate on the Roche LightcCycler 96 detection system (Roche, Basel, Switzerland) using the SYBR Green kit (Roche, Basel, Switzerland). The sequences of primers utilized are reported in **Table M-2**. The PCR conditions were as follows: one incubation at 95 ^{o}C for 5 min followed by 45 cycles of 95 ^{o}C for 15 sec, 58 ^{o}C for 15 sec and a 72 ^{o}C for 20 sec followed by SYBR green signal acquisition at the end of each cycle. After amplification, dissociation curves were performed to ensure that a single PCR product was amplified. All the reactions were performed in triplicate, and the comparative Ct method was used for the quantification of the expression for each segment, by using *β-actin* as a normalization cDNA control. For 5S rRNA detection in anti-L5 or anti-Venus-L11 immunoomplexes, equal amount of starting lysates were subjected to immunoprecipitation, then purified immunoprecipitated material was spiked with 5 ng of Luciferase mRNA as normalization control among samples, before RNA purification with TRIzol reagent. A qPCR negative control was included to ensure that we had no contamination.

Cell-cycle analysis

After treatment with the indicated drugs for the indicated times, cells were trypsinized and washed twice with cold PBS. Same number of cells for each condition was fixed with cold 70% ethanol solution. After washing with FACS washing buffer (PBS, BSA 0.1%, EDTA 5nM) cells were re-suspended in a propidium iodide solution (PBS, 0.1% NP40, RNAse A 20 µg/mL, propidium iodide 40 µg/mL) and maintained at

room temperature for 30 minutes before FACS analysis, which was performed using FACSCanto II (BD biosciencies, CA, USA). Data were analyzed using ModFit LT versión 3.3 software (Verity Software House, ME, USA) for Windows.

Measurement of protein synthesis via [^{3}H]leucine incorporation

HCT116 cells treated with 10 µM MPA or cycloheximide (CHX) for the indicated times, grown in 12-well tissue culture plates, were pulse-labeled with [^{3}H]leucine for 30 min with 10 µCi/mL in DMEM/-Leucine. CHX was used as a control of protein synthesis inhibition at a concentration of 100 µg/mL for 2 hours. The incorporation of [^{3}H]leucine was stopped by adding 1 mL of 10% trichloroacetic acid (TCA) in which cells were lysed. After cell lysis, protein pellets were washed four times with 5% TCA, the TCA-insoluble proteins were solubilized in 250 µL of 0.1 M NaOH. A 200 µL aliquot of each specimen was transferred into a scintillation vial, 4 mL of aqueous scintillation liquid was added to each vial, and the samples were counted in a scintillation counter. The rest of the aliquot was used to quantify protein concentration as previously described. In each experiment, three wells were used per experimental point and data is represented as counts per minute (CPM) per µg of protein.

Autoradiographic Analysis of rRNA Synthesis

To evaluate rRNA synthesis, newly synthesized RNA was labeled by incubating the cells for 2 hours in medium containing 1.2 µCi [5,6-^{3}H]-uridine (Perkin Elmer) per mL. RNA was extracted by using TRIzol reagent (Invitrogen) according to manufacturer's instructions. Following extraction, 2 µg of total RNA was size-separated by electrophoresis on a 1% agarose-formaldehyde gel. To evaluate 5.8S rRNA, 5S rRNA and tRNA synthesis, 2 µg of each RNA sample was electrophoresed on a TBE-urea 10% polyacrylamide gel. Following electrophoresis, the RNA in both cases was transferred to Hybond N+ membrane (Amersham Biosciences), the blots were

sprayed with EN^{3}HANCE (Perkin Elmer) and exposed to Kodak BioMax MS film (Kodak) at -80 ^{o}C for autoradiography.

Immunoprecipitation

For immunoprecipitation, cells were lysed on ice in immunoprecipitation buffer (25 mM Tris HCl [pH 7.5], 150 mM KCl, 5 mM MgCl2, 1 mM EGTA, 1mM DTT, 10% glycerol, 0.8% Igepal/NP40, protease inhibitors cocktail [Roche] and RNaseOut [Invitrogen]). The lysates were cleared by centrifugation and quantified by BCA assay (Pierce). Ribosomes were pelleted by ultracentrifugation (32,000 rpm for 2 hr at 4 ^{o}C) to obtain post-ribosomal supernatants. Equivalent amounts of protein (1 mg for each sample) were incubated at 4 ^{o}C with rotation overnight in immunoprecipitation buffer with anti-RPL5, anti-Myc-TAG or IgG. MagnaCHIP Protein A/G magnetic beads (Millipore) were added to the extracts and mixed by rotation for an additional 2 hours at 4 ^{o}C. For immunoprecipitation of RPL11-Venus, the GFP-Trap beads (ChromoTek, GmbH) were resuspended in immunoprecipitation buffer together with post-ribosomal supernatants and incubated at 4 ^{o}C with rotation overnight, following manufacturer's instructions. The beads were washed four times with immunoprecipitation buffer, with each sample being divided into two aliquots before the fourth wash. Following final centrifugation, one aliquot was resuspended in protein loading buffer for western blot analysis; the other aliquot was resuspended in TRIzol reagent (Molecular Research Center) to recover immunoprecipitated RNA for 5S rRNA real time PCR analysis, as described above.

Luciferase assay

Transfection was performed according to the manufacturer's protocol with 2 µg of reporter plasmid (PG13-luc, see reagents and plasmids) and 250 ng of *Renilla* luciferase control plasmid (Promega, Madison, WI, USA) for 24 hours. Following this period, cells were treated for specified times and with the indicated drugs indicated in figures and figure legends. Cell extracts were subsequently prepared and assayed

using the Dual Luciferase kit (Promega) as per the manufacturer's instructions. Luciferase activities were normalized to the *Renilla* control plasmid, and values shown are the mean of three independent experiments.

Immunofluorescence

HCT116 cells were grown as monolayers on cover slips and treated for the specified times with the indicated drugs. Cells were fixed with 4% formaldehyde for 10 minutes at room temperature. After 5 minutes wash with PBS 1X, cells were permeabilized using 0.1% Triton X-100 in PBS 1x for 10 minutes on a shaker incubator at room temperature. Next, cells were incubated in blocking buffer (1% BSA/0.01% Triton X-100 in PBS 20mM glycine) for 30 minutes on a shaker at room temperature. Cells were incubated with primary antibody against phospho-γ-H2AX in (1/1000) blocking buffer for one hour at room temperature. Following a series of washes with PBS, cells were incubated with secondary antibodies (Alexa Fluor 546 goat anti-rabbit from Invitrogen, Carlsbad, CA, USA) in blocking buffer for 45 minutes at room temperature. After 2 PBS washes of 5 minutes, cover slips were mounted with Vectashield mounting solution containing 4',6-diamidino-2-phenylindole (DAPI). Images were taken with the Leica spectral confocal microscope TCS SP5 using a 63X N.A 1.4 objective and LAS AF software. Fluorophores were excited with DPSS 561 for 555 nm and Diode laser for 405 nm. Image analysis was performed using ImageJ software (NIH USA).

DNA Fibre Assays

HCT116 cells were pre-treated with 10 µM MPA for 1 hour (MPA 3 hours) or 22 hours (MPA 24 hours), pulse-labeled with 250µM CldU for 2 hours in presence (MPA 3 and24 hours) or absence of MPA (Vehicle). Labelled cells were harvested by trypsinization and resuspended in ice-cold PBS at 5×10^5 cells/ml. For DNA spreading, 2 µl of cells were spotted onto glass slides and lysed with 7 µl of spreading buffer (0.5% SDS, 200 mM Tris-HCl (pH 7.4), 50 mM EDTA). Slides were tilted (15° to

horizontal), allowing a stream of DNA to run slowly down the slide, air dried and then fixed in methanol/acetic acid (3:1) solution. CldU were detected by incubating acid-treated fibre spreads with anti-BrdU monoclonal antibody (Abcam, ab6326; 1/1000) diluted in blocking buffer (1% BSA in 0.1% Tween-20 -PBS) for 1.5 h at 37°C. After incubation with primary antibodies, fibre spreads were fixed with 4% PFA-PBS for 10 min at RT and finally incubated with secondary antibodies (Alexa 488-conjugated anti-mouse from Invitrogen, Carlsbad, CA, USA; 1/500) for 1.5 h at 37°C. Images were obtained using Leica TCS-SL confocal microscopy with a 63× oil immersion objective and then analysed using Fiji software. The length of at least 200 CldU tracks per condition was measured.

Liquid chromatography-mass spectrometry (LC-MS) analyses

HCT116 cells were treated for the indicated times with the specified drugs. Cells were then trypsinized and the same number of cells for each condition was washed twice with PBS. Metabolites were extracted from cell pellets adding 250 µL of methanol:H2O (1:1 v/v) solution and vortexing samples for 30 seconds. Samples were immersed in liquid N_2 to disrupt cell membranes followed by 30 seconds of ultrasonication. These two steps were repeated 3 times. Then samples were incubated at -20 oC for two hours. After that, samples were centrifuged at 17,000 g for 15 minutes and supernatant was collected into a LC-MS vial. Samples were injected in a UHPLC system (1290 Agilent) coupled to a triple quadrupole (QqQ) MS (6490 Agilent Technologies) operated in multiple reaction monitoring (MRM) and positive (POS) or negative (NEG) electrospray ionization (ESI) mode. Metabolites were separated using C18-RP (ACQUITY UPLC BEH C18 1.7 µM, Waters) chromatography at flow rate of 0.3 mL/min. The solvent system was A= 20 mM ammonium acetate + 15mM NH3 in water, and B=acetonitrile: water (95:5). The linear gradient elution started at 100% A (time 0-2 min), 65% A (time 2-5 min) and finished at 100% B (time 5.5 min). MRM transitions were: guanosine (NEG, 282 → 150, 133), IMP (NEG, 347 → 78.9, 96.9), dGMP (NEG, 346 → 150, 79), ATP (POS, 508→ 136, 410), dGTP (POS, 508→ 152.2, 81), GTP (POS,

524→152, 135), GMP (POS, 364→ 152,135), GDP (POS, 444→ 152,135), dATP (POS, 492→ 136, 81.1).

Molecular Cloning

The 638 nucleotide (nt) long sequence containing 5S rRNA gene (Sorensen et al. 1990) was amplified from HCT116 cells genomic DNA by using specific primers (5S rRNA_cloning Forward and Reverse, see **Table M-2**) and Taq DNA Polymerase from Invitrogen, following manufacturer's instructions. Both 638 nt-long PCR product and pcDNA3.1 plasmid were double-digested by using BglII and BamHI restriction enzymes (New England Biolabs, Ipswich, MA, USA) following manufacturer's instructions. The 4.5 kb fragment from plasmid digestion was used as acceptor vector for 638 nt PCR product. Ligation was performed by using T4-DNA Ligase (New England Biolabs, Ipswich, MA, USA) following manufacturer's instructions. The plasmid obtained from ligation was amplified by using competent *E. coli* cells and purified by maxiprep kit (Qiagen, Hilden, Germany).

Statistical analysis

Statistical analysis was performed using GraphPad Prism version 7.00 for Windows (GraphPad Software, San Diego, CA, USA). Data was analysed using t-test considering p values below 0.05 as significant.

Table M-1. List of Antibodies

Protein	Antibody	Brand	Reference
α-tubulin	α-Tubulin (mAb)	Sigma-Aldrich	T9026
β-actin	Actin Antibody (C-2)	Santa Cruz	sc-8432
GAPDH	GAPDH (14C10) Rabbit mAb	Cell signaling	2118
HDM2	Anti-MDM2 antibody [2A10]	Abcam	ab16895
Myc-Tag	Myc-Tag (9B11) Mouse mAb	Cell signaling	2276
p21	p21 Antibody (F-5)	Santa Cruz	sc-6246
p53	p53 Antibody (FL-393)	Santa Cruz	sc-6243
Phospho-γH2AX (Ser139)	Phospho-Histone H2A.X (Ser139) (20E3) Rabbit mAb	Cell signaling	9718
Phospho-Chk1 (Ser345)	Phospho-Chk1 (Ser345)(133D3)	Cell signaling	2348
Phospho-Chk2 (Thr68)	Phospho-Chk2 (Thr68) (C13C1) Rabbit mAb	Cell signaling	2197
Phospho-p53 (Ser15)	Phospho-p53 (Ser15) (16G8) Mouse mAb	Cell signaling	9286
RPL5	RPL5 Antibody	Bethyl	A303-933A
RPL11	Anti-RPL11 Monoclonal Antibody (3A4A7)	Invitrogen	37-3000
RPS6	RPS6 Antibody (C-8)	Santa Cruz	sc-74459
RPS23	RPS23 Antibody (SJ-K2)	Santa Cruz	sc-100837
GFP	GFP Antibody (FL)	Santa Cruz	sc-8334

Table M-2. List of siRNA and qPCR/PCR primer sequences

siRNA	**Sequence**
siNS	GCATCAGTGTCACGTAATA
siRPL7a	CACCACCTTGGTGGAGAACAA
siRPL5	GCTTGGTGATACAAGATAA
siRPL11	AAGGTGCGGGAGTATGAGTTA
sip53	GCATCTTATCCGAGTGGAA
qPCR Primer	**Sequence**
Firefly Luciferase forward	ACAGATGCACATATCGAGGTG
Firefly Luciferase reverse	GATTTGTATTCAGCCCATATTCG
5S rRNA forward	GGCCATACCACCCTGAACGC
5S rRNA reverse	CAGCACCCGGTATTCCCAGG
p53 forward	CTATGAGCCGCCTGAGGTTG
p53 reverse	CTGGAGTCTTCCAGTGTGATG
p21 forward	TCTCAGGGTCGAAAACGGC
p21 reverse	AGAAGATCAGCCGGCGTTTG
HDM2 forward	TCTCAAGCTCCGTGTTTGGTCAGT
HDM2 reverse	ACCTTGCAACAGCTGCAGATGAAC
β-actin forward	AATGTGGCCGAGGACTTTGATTGC
β-actin reverse	AGGATGGCAAGGGACTTCCTGTAA
PCR primers	**Sequence**
5S rRNA_cloning Forward	GGCCATACCACCCTGAACGC
5S rRNA_cloning Reverse	CAGCACCCGGTATTCCCAGG

REFERENCES

Abbas, T. & Dutta, A., 2009. P21 in Cancer: Intricate Networks and Multiple Activities. *Nature Reviews Cancer*, 9(6), pp.400–414.

Alberts B. et al, 5th edition 2007. *Molecular Biology of the Cell*, Garland Publishing.

Alt, J.R. et al., 2003. Mdm2 haplo-insufficiency profoundly inhibits Myc-induced lymphomagenesis. *The EMBO Journal*, 22(6), pp.1442–1450.

Allison, A.C.. & Eugui, E.M., 2000. Mycophenolate mofetil and its mechanisms of action. *Immunopharmacology*, 47, pp.85–118.

Ammons, D., Rampersad, J. & Fox, G.E., 1999. 5S rRNA gene deletions cause an unexpectedly high fitness loss in Escherichia coli. *Nucleic Acids Research*, 27(2), pp.637–642.

Amsterdam, A. et al., 2004. Many ribosomal protein genes are cancer genes in zebrafish Derek Stemple, ed. *PLoS Biology*, 2(5), p.e139.

Ananiev, J. et al., 2011. p53 - "The Guardian of Genome." *Acta Medica Bulgarica*, 38(2), pp.72–82.

Arabi, A. et al., 2005. c-Myc associates with ribosomal DNA and activates RNA polymerase I transcription. *Nature cell biology*, 7(3), pp.303–10.

Balagurumoorthy, P. et al., 1995. Four p53 DNA-binding domain peptides bind natural p53-response elements and bend the DNA (cooperative DNA binding/DNA bending/cyclization). *Biochemistry*, 92, pp.8591–8595.

Banin, S. et al., 1998. Enhanced phosphorylation of p53 by ATM in response to DNA damage. *Science (New York, N.Y.)*, 281(5383), pp.1674–7.

Baptiste, N. et al., 2002. The proline-rich domain of p53 is required for cooperation with anti-neoplastic agents to promote apoptosis of tumor cells. *Oncogene*, 21(1), pp.9–21.

Barak, Y. et al., 1993. mdm2 expression is induced by wild type p53 activity. *The EMBO journal*, 12(2), pp.461–8.

Barna, M. et al., 2008. Suppression of Myc oncogenic activity by ribosomal protein haploinsufficiency. *Nature*, 456.

Beckerman, R. & Prives, C., 2010. Transcriptional Regulation by p53. *Cold Spring Harbor perspectives in biology*, 2(8), pp.1–18.

Berg, J.M. (Jeremy M. et al., 2002. *Biochemistry*, W.H. Freeman.

Bernardi, R. et al., 2004. PML regulates p53 stability by sequestering Mdm2 to the nucleolus. *NATURE CELL BIOLOGY*, 6(7).

Berndsen, C.E. & Wolberger, C., 2014. New insights into ubiquitin E3 ligase mechanism. *Nature structural & molecular biology*, 21(4), pp.301–7.

Beroukhim, R. et al., 2010. The landscape of somatic copy-number alteration across human cancers. *Nature*, 463(7283), pp.899–905.

Bester, A.C. et al., 2011. Nucleotide deficiency promotes genomic instability in early stages of cancer development. *Cell*, 145(3), pp.435–446.

Bode, A.M. & Dong, Z., 2004. Post-translational modification of p53 in tumorigenesis. *Nature Reviews Cancer*, 4(10), pp.793–805.

Boisvert, F.-M. et al., 2007. The multifunctional nucleolus. *Nature Reviews Molecular Cell Biology*, 8(7), pp.574–585.

Boulon, S. et al., 2010. The nucleolus under stress. *Molecular cell*, 40(2), pp.216–27.

Bourdon, J.-C. et al., 1997. Further characterisation of the p53 responsive element – identification of new candidate genes for trans-activation by p53. *Oncogene*, 14(1), pp.85–94.

Brosh, R.M. et al., 2001. p53 Modulates the Exonuclease Activity of Werner Syndrome Protein. *Journal of Biological Chemistry*, 276(37), pp.35093–35102.

Brugarolas, J. et al., 1995. Radiation-induced cell cycle arrest compromised by p21 deficiency. *Nature*, 377(6549), pp.552–557.

Bruno, P.M. et al., 2017. A subset of platinum-containing chemotherapeutic agents kills cells by inducing ribosome biogenesis stress. *Nature Medicine*, (August 2016), pp.1–13.

Bunz, F. et al., 1998. Requirement for p53 and p21 to Sustain G2 Arrest After DNA Damage. *Science*, 282(5393).

Burger, K. et al., 2010. Chemotherapeutic drugs inhibit ribosome biogenesis at various levels. *Journal of Biological Chemistry*, 285(16), pp.12416–12425.

Bursac, S. et al., 2014. Activation of the tumor suppressor p53 upon impairment of ribosome biogenesis.

Biochimica et Biophysica Acta (BBA) - Molecular Basis of Disease, 1842(6), pp.817–830.

Bursac, S. et al., 2012. Mutual protection of ribosomal proteins L5 and L11 from degradation is essential for p53 activation upon ribosomal biogenesis stress. *Proceedings of the National Academy of Sciences*, 109(50), pp.20467–20472.

Bywater, M.J. et al., 2012. Inhibition of RNA polymerase I as a therapeutic strategy to promote cancer-specific activation of p53. *Cancer cell*, 22(1), pp.51–65.

Cairns, R.A., Harris, I.S. & Mak, T.W., 2011. Regulation of cancer cell metabolism. *Nature Reviews Cancer*, 11(2), pp.85–95.

Canman, C.E. et al., 1998. Activation of the ATM kinase by ionizing radiation and phosphorylation of p53. *Science (New York, N.Y.)*, 281(5383), pp.1677–9.

Ciccia, A. et al., 2014. Treacher Collins syndrome TCOF1 protein cooperates with NBS1 in the DNA damage response. *Proceedings of the National Academy of Sciences*, 111(52), pp.18631–18636.

Ciganda, M. & Williams, N., 2011. Eukaryotic 5S rRNA biogenesis. *Wiley Interdisciplinary Reviews: RNA*, 2(4), pp.523–533.

Coleman, M.L., Marshall, C.J. & Olson, M.F., 2004. RAS and RHO GTPases in G1-phase cell-cycle regulation. *Nature Reviews Molecular Cell Biology*, 5(5), pp.355–366.

Condon, C. et al., 1993. Depletion of functional ribosomal RNA operons in Escherichia coli causes increased expression of the remaining intact copies. *The EMBO journal*, 12(11), pp.4305–15.

Cunningham, J.T. et al., 2014. Protein and nucleotide biosynthesis are coupled by a single rate-limiting enzyme, PRPS2, to drive cancer. *Cell*, 157(5), pp.1088–1103.

Chabosseau, P. et al., 2011. Pyrimidine pool imbalance induced by BLM helicase deficiency contributes to genetic instability in Bloom syndrome. *Nature Communications*, 2, p.368.

Challagundla, K.B. et al., 2011. Ribosomal protein L11 recruits miR-24/miRISC to repress c-Myc expression in response to ribosomal stress. *Molecular and cellular biology*, 31(19), pp.4007–21.

Chao, C. et al., 2003. Cell Type- and Promoter-specific Roles of Ser18 Phosphorylation in Regulating p53 Responses. *Journal of Biological Chemistry*, 278(42), pp.41028–41033.

Chao, C. et al., 2006. Ser18 and 23 phosphorylation is required for p53-dependent apoptosis and tumor suppression. *The EMBO journal*, 25(11), pp.2615–2622.

Chen, D. et al., 2007. Ribosomal protein S7 as a novel modulator of p53–MDM2 interaction: binding to MDM2, stabilization of p53 protein, and activation of p53 function. *Oncogene*, 26(35), pp.5029–5037.

Cheung-Ong, K., Giaever, G. & Nislow, C., 2013. Chemistry & Biology Perspective DNA-Damaging Agents in Cancer Chemotherapy: Serendipity and Chemical Biology. *Chemistry & Biology*, 20, pp.648–659.

Cheung, T.H. & Rando, T.A., 2013. Molecular regulation of stem cell quiescence. *Nature reviews. Molecular cell biology*, 14(6), pp.329–40.

Choong, M.L. et al., 2009. Specific activation of the p53 pathway by low dose actinomycin D: A new route to p53 based cyclotherapy. *Cell Cycle*, 8(17), pp.2810–2818.

Daftuar, L. et al., 2013. Ribosomal proteins RPL37, RPS15 and RPS20 regulate the Mdm2-p53-MdmX network. *PloS one*, 8(7), p.e68667.

Dai, C. & Gu, W., 2010. P53 post-translational modification: Deregulated in tumorigenesis. *Trends in Molecular Medicine*, 16(11), pp.528–536.

Dai, M.-S. et al., 2004. Ribosomal protein L23 activates p53 by inhibiting MDM2 function in response to ribosomal perturbation but not to translation inhibition. *Molecular and cellular biology*, 24(17), pp.7654–68.

Dai, M.-S., Sun, X.-X. & Lu, H., 2010. Ribosomal protein L11 associates with c-Myc at 5 S rRNA and tRNA genes and regulates their expression. *The Journal of biological chemistry*, 285(17), pp.12587–94.

Dang, C. V. et al., 2006. The c-Myc target gene network. *Seminars in Cancer Biology*, 16(4), pp.253–264.

Dang, C.V. et al., 2012. MYC on the Path to Cancer. *Cell*, 149(1), pp.22–35.

Danilova, N. et al., 2014. The role of the DNA damage response in zebrafish and cellular models of Diamond Blackfan anemia. *Disease Models & Mechanisms*, 7(7), pp.895–905.

Danilova, N., Sakamoto, K.M. & Lin, S., 2008. Ribosomal protein S19 deficiency in zebrafish leads to developmental abnormalities and defective erythropoiesis through activation of p53 protein family. *Blood*, 112(13), pp.5228–5237.

DeBerardinis, R.J. et al., 2007. Beyond aerobic glycolysis: transformed cells can engage in glutamine metabolism that exceeds the requirement for protein and nucleotide synthesis. *Proceedings of the National Academy of Sciences of the United States of America*, 104(49), pp.19345–50.

Dechampesme, A.M. et al., 1999. Assembly of 5S ribosomal RNA is required at a specific step of the pre-rRNA processing pathway. *The Journal of cell biology*, 145(7), pp.1369–80.

DeLeo, A.B. et al., 1979. Detection of a transformation-related antigen in chemically induced sarcomas and other transformed cells of the mouse. *Proceedings of the National Academy of Sciences of the United States of America*, 76(5), pp.2420–4.

Deng, C. et al., 1995. Mice lacking p21CIP1/WAF1 undergo normal development, but are defective in G1 checkpoint control. *Cell*, 82(4), pp.675–684.

Deshmukh, M. et al., 1993. Yeast ribosomal protein L1 is required for the stability of newly synthesized 5S rRNA and the assembly of 60S ribosomal subunits. *Molecular and cellular biology*, 13(5), pp.2835–45.

Devlin, E.E. et al., 2010. A transgenic mouse model demonstrates a dominant negative effect of a point mutation in the RPS19 gene associated with Diamond-Blackfan anemia. *Blood*, 116(15), pp.2826–2835.

Devlin, J.R. et al., 2016. Combination therapy targeting ribosome biogenesis and mRNA translation synergistically extends survival in MYC-driven lymphoma. *Cancer Discovery*, 6(1), pp.59–70.

Dobbelstein, M. & Sørensen, C.S., 2015. Exploiting replicative stress to treat cancer. *Nature Reviews Drug Discovery*, 14(6), pp.405–423.

Dohme, F. & Nierhaus, K.H., 1976. Role of 5S RNA in assembly and function of the 50S subunit from Escherichia coli [in vitro assembly/peptidyltransferase (EC 2.3.2.12) center/A-site and P-site/elongation factor G dependent GTPasej. *Biochemistry*, 73(7), pp.2221–2225.

Donati, G. et al., 2013. 5S Ribosomal RNA Is an Essential Component of a Nascent Ribosomal Precursor Complex that Regulates the Hdm2-p53 Checkpoint. *Cell Reports*, 4(1), pp.87–98.

Drygin, D. et al., 2009. Anticancer Activity of CX-3543: A Direct Inhibitor of rRNA Biogenesis. *Cancer Research*, 69(19).

Dyson, N., 1998. The regulation of E2F by pRB-family proteins. *Genes and Development*, 12(15), pp.2245–2262.

Eilers, M. & Eisenman, R.N., 2008. Myc's broad reach. *Genes & development*, 22(20), pp.2755–66.

el-Deiry, W.S. et al., 1992. Definition of a consensus binding site for p53. *Nat Genet*, 1(1), pp.45–49.

el-Deiry, W.S. et al., 1993. WAF1, a potential mediator of p53 tumor suppression. *Cell*, 75(4), pp.817–25.

Eliyahu, D. et al., 1984. Participation of p53 cellular tumor antigen in transformation of normal embryonic cells. *Nature*, 312(5995), pp.646–649.

Erster, S. et al., 2004. In vivo mitochondrial p53 translocation triggers a rapid first wave of cell death in response to DNA damage that can precede p53 target gene activation. *Molecular and cellular biology*, 24(15), pp.6728–41.

Fasullo, M. & Endres, L., 2015. Nucleotide Salvage Deficiencies, DNA Damage and Neurodegeneration. *Int. J. Mol. Sci. Int. J. Mol. Sci*, 16, pp.9431–9449.

Fedoriw, A.M. et al., 2012. Nucleolar association and transcriptional inhibition through 5S rDNA in mammals M. Dundr, ed. *PLoS Genetics*, 8(1), p.e1002468.

Fernandez, P.C. et al., 2003. Genomic targets of the human c-Myc protein. *Genes & development*, 17(9), pp.1115–29.

Finlay, C.A., Hinds, P.W. & Levine, A.J., 1989. The p53 proto-oncogene can act as a suppressor of transformation. *Cell*, 57(7), pp.1083–1093.

Floryk, D. et al., 2006. Mycophenolic acid-induced replication arrest, differentiation markers and cell death of androgen-independent prostate cancer cells DU145. *Cancer letters*, 231(1), pp.20–9.

Fox, G.E. & Woese, C.R., 1975. The architecture of 5S rRNA and its relation to function. *Journal of molecular evolution*, 6(1), pp.61–76.

Fumagalli, S. et al., 2009. Absence of nucleolar disruption after impairment of 40S ribosome biogenesis reveals an rpL11-translation-dependent mechanism of p53 induction. *Nature cell biology*, 11(4), pp.501–508.

Fumagalli, S. et al., 2012. Suprainduction of p53 by disruption of 40S and 60S ribosome biogenesis leads to the activation of a novel G2/M checkpoint. *Genes & development*, 26(10), pp.1028–40.

Gaillard, H., García-Muse, T. & Aguilera, A., 2015. Replication stress and cancer. *Nature Reviews Cancer*, 15(5), pp.276–289.

Gentilella, A. et al., 2017. Autogenous Control Of 5'TOP mRNA Stability By 40S Ribosomes. *Molecular Cell*.

Gentilella, A., Kozma, S.C. & Thomas, G., 2015. A liaison between mTOR signaling, ribosome biogenesis and cancer. *Biochimica et Biophysica Acta - Gene Regulatory Mechanisms*, 1849(7), pp.812–820.

Giono, L.E. & Manfredi, J.J., 2006. The p53 tumor suppressor participates in multiple cell cycle checkpoints. *Journal of Cellular Physiology*, 209(1), pp.13–20.

Golomb, L. et al., 2012. Importin 7 and exportin 1 Link c-Myc and p53 to regulation of ribosomal Biogenesis. *Molecular Cell*, 45(2), pp.222–232.

Gomez-Roman, N. et al., 2003. Direct activation of RNA polymerase III transcription by c-Myc. *Nature*, 421(6920), pp.290–294.

Gorlick, R. et al., 1996. Intrinsic and Aquired Resistance to Methotrexate in Acute Leukemia. *New England Journal of Medicine*, 335(14), pp.1041–1048.

Gottifredi, V. et al., 2001. p53 accumulates but is functionally impaired when DNA synthesis is blocked. *Proceedings of the National Academy of Sciences of the United States of America*, 98, pp.1036–1041.

Grandori, C. et al., 2005. c-Myc binds to human ribosomal DNA and stimulates transcription of rRNA genes by RNA polymerase I. *Nature cell biology*, 7(3), pp.311–8.

Graña, X. & Reddy, E.P., 1995. Cell cycle control in mammalian cells: role of cyclins, cyclin dependent kinases (CDKs), growth suppressor genes and cyclin-dependent kinase inhibitors (CKIs). *Oncogene*, 11(2), pp.211–9.

Gresch, E.E., 1989. Genetic Alterations During Colorectal-Tumor Development. *Journal of Occupational and Environmental Medicine*, 31(10), p.815.

Grewal, S.S. et al., 2005. Myc-dependent regulation of ribosomal RNA synthesis during Drosophila development. *Nature Cell Biology*, 7(3), pp.295–302.

Gu, W., Shi, X.L. & Roeder, R.G., 1997. Synergistic activation of transcription by CBP and p53. *Nature*, 387(June), pp.819–823.

Guddat, U., Bakken, A.H. & Pieler, T., 1990. Protein-mediated nuclear export of RNA: 5S rRNA containing small RNPs in xenopus oocytes. *Cell*, 60(4), pp.619–628.

Harris, A. et al., 1988. The E mu-myc transgenic mouse. A model for high-incidence spontaneous lymphoma and leukemia of early B cells. *Journal of Experimental Medicine*, 167(2), pp.353–371.

Haupt, Y., 1995. Induction of apoptosis in HeLa cells by transcativation deficient p53. *Genes & Development*, 9(of 390), pp.2170–2183.

Haupt, Y. et al., 1997. Mdm2 promotes the rapid degradation of p53. *Nature*, 387(6630), pp.296–9.

He, T., 1998. Identification of c-MYC as a Target of the APC Pathway. *Science*, 281(5382), pp.1509–1512.

He, X. et al., 2016. Ribosomal protein L4 is a novel regulator of the MDM2-p53 loop. *Oncotarget*, 7(13), pp.16217–26.

Hedstrom, L., 2009. IMP dehydrogenase: Structure, mechanism, and inhibition. *Chemical Reviews*, 109(7), pp.2903–2928.

Heiden Vander, M.G. et al., 2011. Metabolic pathway alterations that support: Cell Proliferation. *Cold Spring Harbor Symposia on Quantitative Biology*, 76, pp.325–334.

Henras, A.K. et al., 2015. An overview of pre-ribosomal RNA processing in eukaryotes. *Wiley Interdisciplinary Reviews: RNA*, 6(2), pp.225–242.

Henras, A.K. et al., 2008. The post-transcriptional steps of eukaryotic ribosome biogenesis. *Cellular and Molecular Life Sciences*, 65(15), pp.2334–2359.

Hernandez-Verdun, D. et al., 2010. The nucleolus: Structure/function relationship in RNA metabolism. *Wiley Interdisciplinary Reviews: RNA*, 1(3), pp.415–431.

Honda, R., Tanaka, H. & Yasuda, H., 1997. Oncoprotein MDM2 is a ubiquitin ligase E3 for tumor suppressor p53. *FEBS Letters*, 420(1), pp.25–27.

Horn, H.F. & Vousden, K.H., 2007. Coping with stress: multiple ways to activate p53. *Oncogene*, 26(9), pp.1306–1316.

Hosios, A.M. et al., 2016. Amino Acids Rather than Glucose Account for the Majority of Cell Mass in Proliferating Mammalian Cells. *Developmental Cell*, 36, pp.540–549.

Huang, M. et al., 2008. Guanine nucleotide depletion inhibits pre-ribosomal RNA synthesis and causes nucleolar disruption. *Leukemia Research*, 32(1), pp.131–141.

Hunt, L.T. et al., 1984. Evolution of prokaryote and eukaryote lines inferred from sequence evidence. *Origins of Life*, 14(1–4), pp.657–664.

Iritani, B.M. & Eisenman, R.N., 1999. c-Myc enhances protein synthesis and cell size during B lymphocyte development. *Proceedings of the National Academy of Sciences of the United States of America*, 96(23), pp.13180–5.

Itahana, K. et al., 2007. Targeted Inactivation of Mdm2 RING Finger E3 Ubiquitin Ligase Activity in the Mouse Reveals Mechanistic Insights into p53 Regulation. *Cancer Cell*, 12(4), pp.355–366.

Jaako, P. et al., 2016. Induction of the 5S RNP-Mdm2-p53 ribosomal stress pathway delays the initiation but fails to eradicate established murine acute myeloid leukemia. *Leukemia*, 31, pp.213–221.

Jain, A.K. & Barton, M.C., 2010. Making sense of ubiquitin ligases that regulate p53. *Cancer Biology and Therapy*, 10(7), pp.665–672.

Jenkins, J.R., Rudge, K. & Currie, G.A., 1984. Cellular immortalization by a cDNA clone encoding the transformation-associated phosphoprotein p53. *Nature*, 312(5995), pp.651–4.

Ji, Y. et al., 2006. Regulation of the interaction of inosine monophosphate dehydrogenase with mycophenolic acid by GTP. *Journal of Biological Chemistry*, 281(1), pp.206–212.

Joerger, A.C. & Fersht, A.R., 2008. Structural biology of the tumor suppressor p53. *Annual review of biochemistry*, 77, pp.557–82.

Johnston, L.A. et al., 1999. Drosophila myc Regulates Celluar Growth during Development. *Cell*, 98, pp.779–790.

Jones, R.G. et al., 2005. AMP-activated protein kinase induces a p53-dependent metabolic checkpoint. *Molecular cell*, 18(3), pp.283–93.

Jones, S.N. et al., 1995. Rescue of embryonic lethality in Mdm2-deficient mice by absence of p53. *Nature*, 378(6553), pp.206–208.

Kakudo, Y. et al., 2005. Lack of correlation between p53-dependent transcriptional activity and the ability to induce apostosis among 179 mutant p53s. *Cancer Research*, 65(6), pp.2108–2114.

Kamada, R. et al., 2015. Tetramer formation of tumor suppressor protein p53: Structure, function, and applications. *Biopolymers*.

Kassavetis, G.A. et al., 1990. S. cerevisiae TFIIIB is the transcription initiation factor proper of RNA polymerase III, while TFIIIA and TFIIIC are assembly factors. *Cell*, 60(2), pp.235–245.

Kastan, M.B. et al., 1991. Participation of p53 Protein in the Cellular Response to DNA Damage. *Cancer Research*, 51(23 Pt 1), pp.6304–6311.

Keel, S.B. et al., 2012. Establishing Rps6 hemizygous mice as a model for studying how ribosomal protein haploinsufficiency impairs erythropoiesis. *Experimental Hematology*, 40(4), pp.290–294.

Kenzelmann Broz, D. et al., 2013. Global genomic profiling reveals an extensive p53-regulated autophagy program contributing to key p53 responses. *Genes and Development*, 27(9), pp.1016–1031.

Kern, S.E. et al., 1992. Oncogenic forms of p53 inhibit p53-regulated gene expression. *Science (New York, N.Y.)*, 256(5058), pp.827–30.

Kiparisov, S. et al., 2005. Structural and functional analysis of 5S rRNA in Saccharomyces cerevisiae. *Molecular Genetics and Genomics*, 274(3), pp.235–247.

Kitayner, M. et al., 2006. Structural Basis of DNA Recognition by p53 Tetramers. *Molecular Cell*, 22(6), pp.741–753.

Kleine-Kohlbrecher, D., Adhikary, S. & Eilers, M., 2006. Mechanisms of Transcriptional Repression by Myc. In *The Myc/Max/Mad Transcription Factor Network*. Berlin/Heidelberg: Springer-Verlag, pp. 51–62.

Knight, E. & Darnell, J.E., 1967. Distribution of 5 s RNA in HeLa cells. *Journal of Molecular Biology*, 28(3), pp.491–502.

Kozhevnikova, E.N. et al., 2012. Metabolic Enzyme IMPDH Is Also a Transcription Factor Regulated by Cellular State. *Molecular Cell*, 47, pp.133–139.

Kress, M. et al., 1979. Simian virus 40-transformed cells express new species of proteins precipitable by anti-simian virus 40 tumor serum. *Journal of Virology*, 31(2), pp.472–83.

Kressler, D., Hurt, E. & Baßler, J., 2010. Driving ribosome assembly. *Biochimica et Biophysica Acta - Molecular Cell Research*, 1803(6), pp.673–683.

Kruiswijk, F., Labuschagne, C.F. & Vousden, K.H., 2015. P53 in Survival, Death and Metabolic Health: a Lifeguard With a Licence To Kill. *Nat Rev Mol Cell Biol*, 16(7), pp.393–405.

Kruse, J.-P. et al., 2009. Modes of p53 regulation. *Cell*, 137(4), pp.609–22.

Kruse, J.P. & Gu, W., 2008. SnapShot: p53 Posttranslational Modifications. *Cell*, 133(5).

Kubbutat, M.H., Jones, S.N. & Vousden, K.H., 1997. Regulation of p53 stability by Mdm2. *Nature*, 387(6630), pp.299–303.

Kussie, P.H. et al., 1996. Structure of the MDM2 oncoprotein bound to the p53 tumor suppressor transactivation domain. *Science*, 274(5289), pp.948–953.

Lakin, N.D. & Jackson, S.P., 1999. Regulation of p53 in response to DNA damage. *Oncogene*, 18(53),

pp.7644–7655.

Land, H., Parada, L.F. & Weinberg, R.A., 1983. Tumorigenic conversion of primary embryo fibroblasts requires at least two cooperating oncogenes. *Nature*, 304(5927), pp.596–602.

Lane, A.N. & W-M Fan, T., 2015. SURVEY AND SUMMARY Regulation of mammalian nucleotide metabolism and biosynthesis. *Nucleic Acids Research*, 43(4), pp.2466–2485.

Lane, D.P. & Crawford, L. V, 1979. T antigen is bound to a host protein in SV40-transformed cells. *Nature*, 278(5701), pp.261–263.

Larsen, D.H. et al., 2014. The NBS1–Treacle complex controls ribosomal RNA transcription in response to DNA damage. *Nature Cell Biology*, 16(8), pp.792–803.

Lee, Y. & Nazar, R.N., 1997. Ribosomal 5S rRNA maturation in Saccharomyces cerevisiae. *Journal of Biological Chemistry*, 272, pp.15206–15212.

Leemans, C.R., Braakhuis, B.J. & Brakenhoff, R.H., 2011. The molecular biology of head and neck cancer. *Nat Rev Cancer*, 11(1), pp.9–22.

Lees-Miller, S.P. et al., 1992. Human DNA-activated protein kinase phosphorylates serines 15 and 37 in the amino-terminal transactivation domain of human p53. *Molecular and cellular biology*, 12(11), pp.5041–5049.

Di Lello, P. et al., 2006. Structure of the Tfb1/p53 Complex: Insights into the Interaction between the p62/Tfb1 Subunit of TFIIH and the Activation Domain of p53. *Molecular Cell*, 22(6), pp.731–740.

Lempiäinen, H. & Shore, D., 2009. Growth control and ribosome biogenesis. *Current Opinion in Cell Biology*, 21(6), pp.855–863.

Van Leuven, S.I. et al., 2006. Mycophenolate mofetil (MMF): Firing at the atherosclerotic plaque from different angles? *Cardiovascular Research*, 69(2), pp.341–347.

Levine, A.J., 1997. p53, the cellular gatekeeper for growth and division. *Cell*, 88(3), pp.323–331.

Li, M. et al., 2003. Mono- versus polyubiquitination: differential control of p53 fate by Mdm2. *Science (New York, N.Y.)*, 302(5652), pp.1972–1975.

Liao, J.-M. et al., 2013. Ribosomal proteins L5 and L11 co-operatively inactivate c-Myc via RNA-induced silencing complex. *Oncogene*, 33, pp.4916–4923.

Lin, C.Y. et al., 2012. Transcriptional amplification in tumor cells with elevated c-Myc. *Cell*, 151(1), pp.56–67.

Lin, D. et al., 1992. Growth arrest induced by wild-type p53 protein blocks cells prior to or near the restriction point in late G1 phase. *Proceedings of the National Academy of Sciences of the United States of America*, 89(19), pp.9210–4.

Lin, E., Lin, S.-W. & Lin, A., 2001. The participation of 5S rRNA in the co-translational formation of a eukaryotic 5S ribonucleoprotein complex. *Nucleic Acids Research*, 29(12), pp.2510–2516.

Lindstrom, M.S. et al., 2007. Cancer-Associated Mutations in the MDM2 Zinc Finger Domain Disrupt Ribosomal Protein Interaction and Attenuate MDM2-Induced p53 Degradation. *Molecular and Cellular Biology*, 27(3), pp.1056–1068.

Linke, S.P. et al., 1996. A reversible, p53-dependent G0/G1 cell cycle arrest induced by ribonucleotide depletion in the absence of detectable DNA damage. *Genes & development*, 10(8), pp.934–47.

Linzer, D.I.H. & Levine, A.J., 1979. Characterization of a 54K Dalton cellular SV40 tumor antigen present in SV40-transformed cells and uninfected embryonal carcinoma cells. *Cell*, 17(1), pp.43–52.

Liu, L. et al., 1993. Amplification and Overexpression of the MDM2 Gene in a Subset of Human Malignant Gliomas without p53 Mutations. *Cancer Research*, 53(12), pp.2736–2739.

Liu, S. et al., 2016. Disruption of the RP-MDM2-p53 pathway accelerates APC loss-induced colorectal tumorigenesis. *Oncogene*, 36(July), pp.1–10.

Liu, Y.C. et al., 2008. Global regulation of nucleotide biosynthetic genes by c-myc D.-Y. Jin, ed. *PLoS ONE*, 3(7), p.e2722.

Lo, D. et al., 2012. Ubiquitin- and MDM2 E3 ligase-independent proteasomal turnover of nucleostemin in response to GTP depletion. *The Journal of biological chemistry*, 287(13), pp.10013–20.

Longley, D.B., Harkin, D.P., Johnston, P.G., et al., 2003. 5-Fluorouracil: mechanisms of action and clinical strategies. *Nature Reviews Cancer*, 3(5), pp.330–338.

Longley, D.B., Harkin, D.P. & Johnston, P.G., 2003. 5-Fluorouracil: mechanisms of action and clinical strategies. *Nature.Com*, 3(May), pp.330–338.

Lowe, S.W. & Sherr, C.J., 2003. Tumor suppression by Ink4a–Arf: progress and puzzles. *Current Opinion in Genetics & Development*, 13(1), pp.77–83.

Lu, H. & Levine, A.J., 1995. Human TAFII31 protein is a transcriptional coactivator of the p53 protein. *Proceedings of the National Academy of Sciences of the United States of America*, 92(11), pp.5154–8.

Macias, E. et al., 2010. An ARF-Independent c-MYC-Activated Tumor Suppression Pathway Mediated by Ribosomal Protein-Mdm2 Interaction. *Cancer Cell*, 18, pp.231–243.

Madaan, K., Kaushik, D. & Verma, T., 2012. Hydroxyurea: a key player in cancer chemotherapy. *Expert Review of Anticancer Therapy*, 12(1), pp.19–29.

Maddocks, O.D.K. et al., 2013. Serine starvation induces stress and p53-dependent metabolic remodelling in cancer cells. *Nature*, 493(7433), pp.542–6.

Majd, N. et al., 2014. A Review of the Potential Utility of Mycophenolate Mofetil as a Cancer Therapeutic. *Journal of Cancer Research*, 2014, pp.1–12.

Mannava, S. et al., 2008. Direct role of nucleotide metabolism in C-MYC-dependent proliferation of melanoma cells. *Cell Cycle*, 7(15), pp.2392–2400.

Marechal, V. et al., 1994. The ribosomal L5 protein is associated with mdm-2 and mdm-2-p53 complexes. *Molecular and cellular biology*, 14(11), pp.7414–20.

Massagué, J., 2004. G1 cell-cycle control and cancer. *Nature*, 432(7015), pp.298–306.

Mateyak, M.K. et al., 1997. Phenotypes of c-Myc-deficient rat fibroblasts isolated by targeted homologous recombination. *Cell growth & differentiation : the molecular biology journal of the American Association for Cancer Research*, 8(10), pp.1039–48.

Mattia, M. et al., 2007. p53-Dependent p21 mRNA Elongation Is Impaired when DNA Replication Is Stalled . *MOLECULAR AND CELLULAR BIOLOGY*, 27(4), pp.1309–1320.

McGowan, K.A. et al., 2011. Reduced ribosomal protein gene dosage and p53 activation in low-risk myelodysplastic syndrome. *Blood*, 118(13), pp.3622–3633.

Mcmahon, S.B., 2011. Control of nucleotide biosynthesis by the MYC oncoprotein: Old friends get reacquainted. , 7(15), pp.2275–2276.

Meek, D.W., 2004. The p53 response to DNA damage. *DNA Repair*, 3(8), pp.1049–1056.

Meek, D.W., 2009. Tumour suppression by p53: a role for the DNA damage response? *Nature reviews. Cancer*, 9(10), pp.714–723.

Meek, D.W. & Anderson, C.W., 2009. Posttranslational modification of p53: cooperative integrators of function. *Cold Spring Harbor perspectives in biology*, 1(6), p.a000950.

Mélèse, T. & Xue, Z., 1995. The nucleolus: an organelle formed by the act of building a ribosome. *Current opinion in cell biology*, 7(3), pp.319–24.

Mendrysa, S.M. et al., 2006. Tumor suppression and normal aging in mice with constitutively high p53 activity. *Genes and Development*, 20(1), pp.16–21.

Mercer, W.E., Avignolo, C. & Baserga, R., 1984. Role of the p53 protein in cell proliferation as studied by microinjection of monoclonal antibodies. *Molecular and cellular biology*, 4(2), pp.276–81.

Mertz, T.M. et al., 2015. Colon cancer-associated mutator DNA polymerase δ variant causes expansion of dNTP pools increasing its own infidelity. *Proceedings of the National Academy of Sciences*, 112(19), pp.E2467–E2476.

Meuth, M., 1989. The molecular basis of mutations induced by deoxyribonucleoside triphosphate pool imbalances in mammalian cells. *Experimental cell research*, 181(2), pp.305–16.

Mihara, M. et al., 2003. p53 has a direct apoptogenic role at the mitochondria. *Molecular cell*, 11(3), pp.577–90.

Mitsuishi, Y. et al., 2012. Nrf2 Redirects Glucose and Glutamine into Anabolic Pathways in Metabolic Reprogramming. *Cancer Cell*, 22(1), pp.66–79.

Momand, J. et al., 1992. The mdm-2 oncogene product forms a complex with the p53 protein and inhibits p53-mediated transactivation. *Cell*, 69(7), pp.1237–1245.

Montanaro, L., Treré, D. & Derenzini, M., 2008. Nucleolus, Ribosomes, and Cancer. *The American Journal of Pathology*, 173, pp.301–310.

Montes de Oca Luna, R., Wagner, D.S. & Lozano, G., 1995. Rescue of early embryonic lethality in mdm2-deficient mice by deletion of p53. *Nature*, 378(6553), pp.203–206.

Moorhead, G., Trinkle-Mulcahy, L. & Ulke-Lemee, A., 2007. Emerging roles of nuclear protein phosphatases. *Nature Reviews Molecular Cell Biology*, 8(3), pp.234–244.

Morgado-Palacin, L. et al., 2015. Partial Loss of Rpl11 in Adult Mice Recapitulates Diamond-Blackfan Anemia and Promotes Lymphomagenesis. *Cell Reports*, 13, pp.712–722.

Morris, G.F., Bischofft, J.R. & Mathews, M.B., 1996. Transcriptional activation of the human proliferating-

cell nuclear antigen promoter by p53. , 93, pp.895–899.

Moser, A.R. et al., 1995. ApcMin: A mouse model for intestinal and mammary tumorigenesis. *European Journal of Cancer*, 31(7–8), pp.1061–1064.

Murdoch, K.J. & Allison, L.A., 1996. A Role for Ribosomal Protein L5 in the Nuclear Import of 5S rRNA in Xenopus Oocytes. *EXPERIMENTAL CELL RESEARCH*, 227, pp.332–343.

Murthy, S. & Reddy, G.P.-V., 2006. Replitase: Complete machinery for DNA synthesis. *Journal of Cellular Physiology*, 209(3), pp.711–717.

Narla, A. & Ebert, B.L., 2010. Ribosomopathies: Human disorders of ribosome dysfunction. *Blood*, 115(16), pp.3196–3205.

Nelson, D.L. (David L., Cox, M.M. & Lehninger, A.L., 2013. *Lehninger principles of biochemistry*, W.H. Freeman and Company.

Nesbit, C.E., Tersak, J.M. & Prochownik, E. V, 1999. MYC oncogenes and human neoplastic disease. *Oncogene*, 18(19), pp.3004–3016.

Nie, Z. et al., 2012. c-Myc is a universal amplifier of expressed genes in lymphocytes and embryonic stem cells. *Cell*, 151(1), pp.68–79.

Oliner, J.D. et al., 1992. Amplification of a gene encoding a p53-associated protein in human sarcomas. *Nature*, 358(6381), pp.80–83.

Onofrillo, C. et al., 2017. The pre-existing population of 5S rRNA effects p53 stabilization during ribosome biogenesis inhibition. *Oncotarget*, 8(3), pp.4257–4267.

Oren, M., Maltzman, W. & Levine, A.J., 1981. Post-translational regulation of the 54K cellular tumor antigen in normal and transformed cells. *Molecular and cellular biology*, 1(2), pp.101–10.

Orsolic, I. et al., 2016. The relationship between the nucleolus and cancer: Current evidence and emerging paradigms. *Seminars in Cancer Biology*, 37–38, pp.36–50.

Parada, L.F. et al., 1984. Cooperation between gene encoding p53 tumour antigen and ras in cellular transformation. *Nature*, 312(5995), pp.649–651.

Perry, M.E. et al., 1993. The mdm-2 gene is induced in response to UV light in a p53-dependent manner. *Proceedings of the National Academy of Sciences of the United States of America*, 90(24), pp.11623–7.

Perry, R.P. & Kelley, D.E., 1970. Inhibition of RNA synthesis by actinomycin D: Characteristic dose-response of different RNA species. *Journal of Cellular Physiology*, 76(2), pp.127–139.

Phillips, W.F. & McConkey, E.H., 1976. Relative stoichiometry in ribosomal proteins in HeLa cell nucleoli. *The Journal of biological chemistry*, 251(10), pp.2876–81.

Pomerantz, J. et al., 1998. The Ink4a tumor suppressor gene product, p19Arf, interacts with MDM2 and neutralizes MDM2's inhibition of p53. *Cell*, 92(6), pp.713–23.

Pourdehnad, M. et al., 2013. Myc and mTOR converge on a common node in protein synthesis control that confers synthetic lethality in Myc-driven cancers. *Proceedings of the National Academy of Sciences of the United States of America*, 110(29), pp.11988–93.

Qi, Z. & Voit, E.O., 2014. Identification of cancer mechanisms through computational systems modeling. *Transl Cancer Res*, 33(33).

Ravid, T. & Hochstrasser, M., 2008. Diversity of degradation signals in the ubiquitin-proteasome system. *Nature reviews. Molecular cell biology*, 9(9), pp.679–90.

Reddy, B.A. et al., 2014. Nucleotide Biosynthetic Enzyme GMP Synthase Is a TRIM21-Controlled Relay of p53 Stabilization. *Molecular Cell*, 53, pp.458–470.

Reich, Nancy; Levine, A.J., 1984. Growth regulation of a cellular tumour antigen, p53, in nontransformed cells. *Nature*, 308(5955), pp.199–201.

Reinhardt, H.C. & Schumacher, B., 2012. The p53 network: Cellular and systemic DNA damage responses in aging and cancer. *Trends in Genetics*, 28(3), pp.128–136.

Rentoft, M. et al., 2016. Heterozygous colon cancer-associated mutations of SAMHD1 have functional significance. *Proceedings of the National Academy of Sciences*, 113(17), pp.4723–4728.

van Riggelen, J., Yetil, A. & Felsher, D.W., 2010. MYC as a regulator of ribosome biogenesis and protein synthesis. *Nature reviews. Cancer*, 10(4), pp.301–9.

Riley, T. et al., 2008. Transcriptional control of human p53-regulated genes. *Nature reviews. Molecular cell biology*, 9(5), pp.402–412.

Ringshausen, I. et al., 2006. Mdm2 is critically and continuously required to suppress lethal p53 activity in vivo. *Cancer Cell*, 10(6), pp.501–514.

Rinke, J. et al., 1982. Precursor molecules of both human 5S ribosomal RNA and transfer RNAs are bound

by a cellular protein reactive with anti-La lupus antibodies. *Cell*, 29(1), pp.149–59.

Rodriguez, M.S. et al., 2000. Multiple C-terminal lysine residues target p53 for ubiquitin-proteasome-mediated degradation. *Molecular and cellular biology*, 20(22), pp.8458–8467.

Rousseau, D. et al., 1999. Growth inhibition by CDK-cyclin and PCNA binding domains of p21 occurs by distinct mechanisms and is regulated by ubiquitin-proteasome pathway. *Oncogene*, 18(30), pp.4313–4325.

de Rozieres, S. et al., 2000. The loss of mdm2 induces p53-mediated apoptosis. *Oncogene*, 19(13), pp.1691–1697.

Rudt, F. & Pieler, T., 1996. Cytoplasmic retention and nuclear import of 5S ribosomal RNA containing RNPs. *The EMBO journal*, 15(6), pp.1383–91.

Sainsbury, S., Bernecky, C. & Cramer, P., 2015. Structural basis of transcription initiation by RNA polymerase II. *Nature Publishing Group*, 16.

Sakamuro, D. et al., 1997. The polyproline region of p53 is required to activate apoptosis but not growth arrest. *Oncogene*, 15(8), pp.887–898.

Sarnow, P. et al., 1982. Adenovirus E1b-58kd tumor antigen and SV40 large tumor antigen are physically associated with the same 54 kd cellular protein in transformed cells. *Cell*, 28(2), pp.387–394.

Schmidt, E. V, 1999. The role of c-myc in cellular growth control. *Oncogene*, 18(19), pp.2988–2996.

Schneider, R.K. et al., 2016. Rps14 haploinsufficiency causes a block in erythroid differentiation mediated by S100A8 and S100A9. *Nature Medicine*, 22(3), pp.288–297.

Schon, O. et al., 2002. Molecular mechanism of the interaction between MDM2 and p53. *Journal of Molecular Biology*, 323(3), pp.491–501.

She, Q.B., Chen, N. & Dong, Z., 2000. ERKs and p38 kinase phosphorylate p53 protein at serine 15 in response to UV radiation. *Journal of Biological Chemistry*, 275(27), pp.20444–20449.

Sherr, C.J., 2006. Divorcing ARF and p53: an unsettled case. *Nature Reviews Cancer*, 6(9), pp.663–673.

Sherr, C.J., 1994. Growth factor-regulated G1 cyclins. *Stem Cells*, 12 Suppl 1, p.47.

Shieh, S.Y. et al., 1997. DNA damage-induced phosphorylation of p53 alleviates inhibition by MDM2. *Cell*, 91(3), pp.325–334.

Shieh, S.Y. et al., 2000. The human homologs of checkpoint kinases Chk1 and Cds1 (Chk2) phosphorylate, p53 at multiple DNA damage-inducible sites. *Genes and Development*, 14(3), pp.289–300.

Shvarts, A. et al., 1996. MDMX: a novel p53-binding protein with some functional properties of MDM2. *The EMBO journal*, 15(19), pp.5349–57.

Sloan, K.E., Bohnsack, M.T. & Watkins, N.J., 2013. The 5S RNP Couples p53 Homeostasis to Ribosome Biogenesis and Nucleolar Stress. *Cell Reports*, 5(1), pp.237–247.

Sluss, H.K. et al., 2004. Phosphorylation of serine 18 regulates distinct p53 functions in mice. *Molecular and cellular biology*, 24(3), pp.976–984.

Smirnov, A. V. et al., 2008. Specific features of 5S rRNA structure — Its interactions with macromolecules and possible functions. *Biochemistry (Moscow)*, 73(13), pp.1418–1437.

Sorensen, P.D., Simonsen, H. & Frederiksen, S., 1990. Nucleotide sequence of a human 5S rRNA gene. *Nucleic acids research*, 18(10), pp.4170–4174.

Steitz, J.A. et al., 1988. A 5S rRNA/L5 complex is a precursor to ribosome assembly in mammalian cells. *The Journal of cell biology*, 106(3), pp.545–56.

Sun, F.-J. & Caetano-Anollés, G., 2009. The Evolutionary History of the Structure of 5S Ribosomal RNA. *Journal of Molecular Evolution*, 69(5), pp.430–443.

Sun, X.-X., Dai, M.-S. & Lu, H., 2007. 5-fluorouracil activation of p53 involves an MDM2-ribosomal protein interaction. *The Journal of biological chemistry*, 282(11), pp.8052–9.

Sun, X.X., Dai, M.S. & Lu, H., 2008. Mycophenolic acid activation of p53 requires ribosomal proteins L5 and L11. *Journal of Biological Chemistry*, 283(18), pp.12387–12392.

Szymański, M. et al., 2003. 5 S rRNA: structure and interactions. *The Biochemical journal*, 371(Pt 3), pp.641–651.

Takahashi, T. et al., 1989. P53: a Frequent Target for Genetic Abnormalities in Lung Cancer. *Science (New York, N.Y.)*, 246(4929), pp.491–494.

Takebe, N. et al., 2006. IMP dehydrogenase inhibitor mycophenolate mofetil induces caspase-dependent apoptosis and cell cycle inhibition in multiple myeloma cells. *Molecular Cancer Therapeutics*, 5(2).

Tanaka, H. et al., 2000. A ribonucleotide reductase gene involved in a p53-dependent cell-cycle checkpoint for DNA damage. *Nature*, 404(6773), pp.42–9.

Tasdemir, E. et al., 2008. Regulation of autophagy by cytoplasmic p53. *Nature cell biology*, 10(6), pp.676–687.

Teng, T., Mercer, C.A., et al., 2013. Loss of Tumor Suppressor RPL5/RPL11 Does Not Induce Cell Cycle Arrest but Impedes Proliferation Due to Reduced Ribosome Content and Translation Capacity. *Molecular and Cellular Biology*, 33(23), pp.4660–4671.

Teng, T., Thomas, G. & Mercer, C.A., 2013. Growth control and ribosomopathies. *Current Opinion in Genetics and Development*, 23(1), pp.63–71.

Teufel, D.P. et al., 2007. Four domains of p300 each bind tightly to a sequence spanning both transactivation subdomains of p53. *Proceedings of the National Academy of Sciences of the United States of America*, 104(17), pp.7009–7014.

The Cancer Genome Network Atlas, 2012. Comprehensive molecular characterization of human colon and rectal cancer. *Nature*, 487(7407), pp.330–337.

Thomas, E.C. et al., 2012. Different Characteristics and Nucleotide Binding Properties of Inosine Monophosphate Dehydrogenase (IMPDH) Isoforms. *PLoS ONE*, 7(12).

Thut, C.J. et al., 1995. p53 transcriptional activation mediated by coactivators TAFII40 and TAFII60. *Science (New York, N.Y.)*, 267(5194), pp.100–4.

Tibbetts, R.S. et al., 1999. A role for ATR in the DNA damage-induced phosphorylation of p53. *Genes and Development*, 13(2), pp.152–157.

Toledo, F. & Wahl, G.M., 2006. Regulating the p53 pathway: in vitro hypotheses, in vivo veritas. *Nature reviews. Cancer*, 6(12), pp.909–923.

Toledo, L.I., Murga, M. & Fernandez-Capetillo, O., 2011. Targeting ATR and Chk1 kinases for cancer treatment: A new model for new (and old) drugs. *Molecular Oncology*, 5(4), pp.368–373.

Tong, X., Zhao, F. & Thompson, C.B., 2009. The molecular determinants of de novo nucleotide biosynthesis in cancer cells. *Current Opinion in Genetics and Development*, 19(1), pp.32–37.

Traut, T.W., 1994. Physiological concentrations of purines and pyrimidines. *Molecular and Cellular BiochemistryMol Cell Biochem*, 140(140), pp.1–22.

Tressler, R.J., Garvin, L.J. & Slate, D.L., 1994. Anti-tumor activity of mycophenolate mofetil against human and mouse tumorsin vivo. *International Journal of Cancer*, 57(4), pp.568–573.

Tschochner, H. & Hurt, E., 2003. Pre-ribosomes on the road from the nucleolus to the cytoplasm. *Trends in Cell Biology*, 13(5), pp.255–263.

Venema, J. & Tollervey, D., 1999. Ribosome Synthesis in *Saccharomyces cerevisiae*. *Annual Review of Genetics*, 33(1), pp.261–311.

Venot, C. et al., 1998. The requirement for the p53 proline-rich functional domain for mediation of apoptosis is correlated with specific PIG3 gene transactivation and with transcriptional repression. *EMBO Journal*, 17(16), pp.4668–4679.

Vogelstein, B., Lane, D. & Levine, a J., 2000. Surfing the p53 network. *Nature*, 408(6810), pp.307–310.

Volarevic, S. et al., 2000. Proliferation, But Not Growth, Blocked by Conditional Deletion of 40S Ribosomal Protein S6. *Science*, 288(5473), pp.2045–2047.

Vousden, K.H. & Lu, X., 2002. Live or let die: the cell's response to p53. *Nature reviews. Cancer*, 2(8), pp.594–604.

Wade, M., Li, Y.-C. & Wahl, G.M., 2013. MDM2, MDMX and p53 in oncogenesis and cancer therapy. *Nature Reviews: Cancer*, 13(2), pp.83–96.

Wagner, A.J., Kokontis, J.M. & Hay, N., 1994. Myc-mediated apoptosis requires wild-type p53 in a manner independent of cell cycle arrest and the ability of p53 to induce p21waf1/cip1. *Genes and Development*, 8(23), pp.2817–2830.

Waldman, T., Kinzler, K.W. & Vogelstein, B., 1995. p21 is necessary for the p53-mediated G1 arrest in human cancer cells. *Cancer research*, 55(22), pp.5187–90.

Walker, K.K. & Levine, A.J., 1996. Identification of a novel p53 functional domain that is necessary for efficient growth suppression. *Proceedings of the National Academy of Sciences of the United States of America*, 93(26), pp.15335–40.

Warner, J.R., 1999. The economics of ribosome biosynthesis in yeast. *Trends in Biochemical Sciences*, 24(11), pp.437–440.

Watson, I.R. & Irwin, M.S., 2006. Ubiquitin and ubiquitin-like modifications of the p53 family. *Neoplasia (New York, N.Y.)*, 8(8), pp.655–66.

Weinberg, R.L. et al., 2005. Comparative binding of p53 to its promoter and DNA recognition elements. *Journal of Molecular Biology*, 348(3), pp.589–596.

Williams, R.H. et al., 1968. Mycophenolic acid: antiviral and antitumor properties. *The Journal of antibiotics*, 21(7), pp.463–4.

Wolin, S.L. & Cedervall, T., 2002. The La Protein. *Annual Review of Biochemistry*, 71(1), pp.375–403.

Xiong, X. et al., 2011. Ribosomal protein S27-like and S27 interplay with p53-MDM2 axis as a target, a substrate and a regulator. *Oncogene*, 30(15), pp.1798–811.

Xue, S. & Barna, M., 2012. Specialized ribosomes: a new frontier in gene regulation and organismal biology. *Nature Reviews Molecular Cell Biology*, 13(6), pp.355–369.

Yadavilli, S. et al., 2009. Ribosomal protein S3: A multi-functional protein that interacts with both p53 and MDM2 through its KH domain. *DNA repair*, 8(10), pp.1215–24.

Yang, V.W., 2009. Krüppel-like factors in cancers. In *The Biology of Krüppel-like Factors*. pp. 205–219.

Yoo, C.J. et al., 1997. The yeast La protein is required for the 3' endonucleolytic cleavage that matures tRNA precursors. *Cell*, 89(3), pp.393–402.

Zannini, L., Delia, D. & Buscemi, G., 2014. CHK2 kinase in the DNA damage response and beyond. *Journal of Molecular Cell Biology*, 6(6), pp.442–457.

Zeman, M.K. & Cimprich, K.A., 2013. Causes and consequences of replication stress. *Nature Cell Biology*, 16(1), pp.2–9.

Zhang, J. et al., 2007. Assembly factors Rpf2 and Rrs1 recruit 5S rRNA and ribosomal proteins rpL5 and rpL11 into nascent ribosomes. *Genes & development*, 21(20), pp.2580–92.

Zhou, B.-B.S. & Bartek, J., 2004. Targeting the checkpoint kinases: chemosensitization versus chemoprotection. *Nature Reviews Cancer*, 4(3), pp.216–225.

Zhou, X. et al., 2013. Ribosomal protein S14 unties the MDM2-p53 loop upon ribosomal stress. *Oncogene*, 32(3), pp.388–96.

Zwerner, J. & Fiorentino, D., 2007. Mycophenolate mofetil. *Dermatologic Therapy*, 20(4), pp.229–238.